DOI:10.14753/SE.2020.2408

SEMMELWEIS EGYETEM

DOKTORI ISKOLA

Ph.D. értekezések

2408.

CZIMBALMOS CSILLA

Szív- és érrendszeri betegségek élettana és klinikuma

című program

Programvezető: Dr. Merkely Béla, egyetemi tanár

Témavezető: Dr. Merkely Béla, egyetemi tanár és

Dr. Vágó Hajnalka, egyetemi docens

DOI:10.14753/SE.2020.2408

ASSESSMENT OF PHYSIOLOGICAL AND PATHOLOGICAL REMODELLING IN ATHLETE'S HEART AND CARDIOMYOPATHIES USING CARDIAC MAGNETIC RESONANCE IMAGING

Doctoral Dissertation

Csilla Czimbalmos MD

Doctoral School of Basic and Translational Medicine
Semmelweis University

Supervisors: Hajnalka Vágó MD, PhD
Béla Merkely MD, DSc

Official reviewers:
Gergely Ágoston MD, PhD
Gergely Szabó MD, PhD

Head of the Final Examination Committee:
Zoltán Benyó MD, DSc

Members of the Final Examination Committee:
András Zsáry MD, PhD
Réka Faludi MD, PhD

Budapest
2020

DOI:10.14753/SE.2020.2408

Table of contents

DOI:10.14753/SE.2020.2408

DOI:10.14753/SE.2020.2408

DOI:10.14753/SE.2020.2408

Abbreviations

ACEI	angiotensin-converting-enzyme inhibitor
AHA	American Heart Association
ARB	angiotensin receptor blockers
ARVC	arrhythmogenic right ventricular cardiomyopathy
AUC	area under curve
AOO	asynchronous atrial pacing
BPM	beats per minute
BSA	body surface area
bSSFP	balanced steady-state free precession
CMR	cardiac magnetic resonance
CQ	conventional quantification method
CRT	cardiac resynchronization therapy
CRT-D	cardiac resynchronization therapy defibrillator
CRT-P	cardiac resynchronization therapy pacemaker
DCM	dilated cardiomyopathy
DOO	dual chambered asynchronous pacing
EAM	electroanatomic mapping
ECG	electrocardiogram (also electrocardiography, electrocardiographic)
EDWT	maximal end-diastolic wall thickness
EF	ejection fraction
ESC	European Society of Cardiology
FWHM	full-width half maximum
GCS	global circumferential strain
GLS	global longitudinal strain
GRS	global radial strain
HCM	hypertrophic cardiomyopathy
HR	heart rate

ICD	implantable cardioverter defibrillator
IVS	intraventricular septum
LV	left ventricle
LVA	low voltage areas
LBBB	left bundle branch block
LGE	late gadolinium enhancement
LVEDD	left ventricular end-diastolic diameter
LVEDV	left ventricular end-diastolic volume
LVEDVi	left ventricular end-diastolic volume index (standardized to BSA)
LVEF	left ventricular ejection fraction
LVESV	left ventricular end-systolic volume
LVESVi	left ventricular end-systolic volume index (standardized to BSA)
LVH	left ventricular hypertrophy
LVM	left ventricular mass
LVMi	left ventricular mass index (standardized to BSA)
LVNC	left ventricular noncompaction
LVOT	left ventricular outflow tract
LVSV	left ventricular stroke volume
LVSVi	left ventricular stroke volume index (standardized to BSA)
NPV	negative predictive value
nsVT	non-sustained ventricular tachycardia
PAV	paced atrioventricular delay
PPV	positive predictive value
PLAX	parasternal long-axis view
PSAX	parasternal short-axis view
PW	posterior wall
ROC	receiver operating characteristic
RFCA	radiofrequency catheter ablation

RV	right ventricular
RVEDV	right ventricular end-diastolic volume
RVEDVi	right ventricular end-diastolic volume index (standardized to BSA)
RVEF	right ventricular ejection fraction
RVOT	right ventricular outflow tract
RVESV	right ventricular end-systolic volume
RVESVi	right ventricular end-systolic volume index (standardized to BSA)
RVM	right ventricular mass
RVMi	right ventricular mass index (standardized to BSA)
RVSV	right ventricular stroke volume
RVSVi	right ventricular stroke volume index (standardized to BSA)
SAR	specific absorbtion rate
SCD	sudden cardiac death
SD	standard deviation
SGE	spoiled gradient echo
TFC	Task Force Criteria
TPM	trabeculae and papillary muscles
TPMi	trabeculae and papillary muscles index (standardized to BSA)
TPM%	trabeculae and papillary muscles as the percentage of total LV myocardial mass
TQ	threshold-based quantification method
TTP	time to peak
TWI	T-wave inversion
VF	ventricular fibrillation
VPB	ventricular premature beats
VT	ventricular tachycardia
2D	two-dimensional
3D	three-dimensional

DOI:10.14753/SE.2020.2408

2-CH two-chamber view

3-CH three-chamber view

4-CH four-chamber view

DOI:10.14753/SE.2020.2408

1. Introduction

1.1 Cardiac remodelling

The life saving capacity of appropriate diagnostic imaging in cardiovascular diseases has inspired intensive research into cardiac remodelling. While cardiac remodelling has been well characterized using our traditional diagnostic tools, suprisingly little attention has been given to assessing these conditions with cardiac magnetic resonance (CMR) imaging. Hereby our task is to characterize systematically cardiac remodelling in an effort to create the bedrock to receive our contextualized results.

Cardiac remodelling is a compensatory process caused by mechanical, neurohormonal and genetic factors leading to functional and structural changes of the heart (1, 2). The term cardiac remodelling was first used to describe maladaptive changes after myocardial infarction including scar formation, left ventricular dilation and geometrical changes with increasing spherical geometry (3). Similar changes in left and also right ventricular geometry may be present in cardiomyopathies. Moreover, certain geometrical and structural alterations observed in pathological cardiac remodelling may be also caused by physiological factors such as intensive and regular exercise (4).

In case of pathological remodelling many molecular and cellular mechanisms are contributing to ventricular remodelling including increased oxidative stress, inflammation, vascular changes, myocyte loss and hypertrophy, fibrosis and alterations in ion transport processes leading to electrophysiological changes **(Figure 1)** (5).

DOI:10.14753/SE.2020.2408

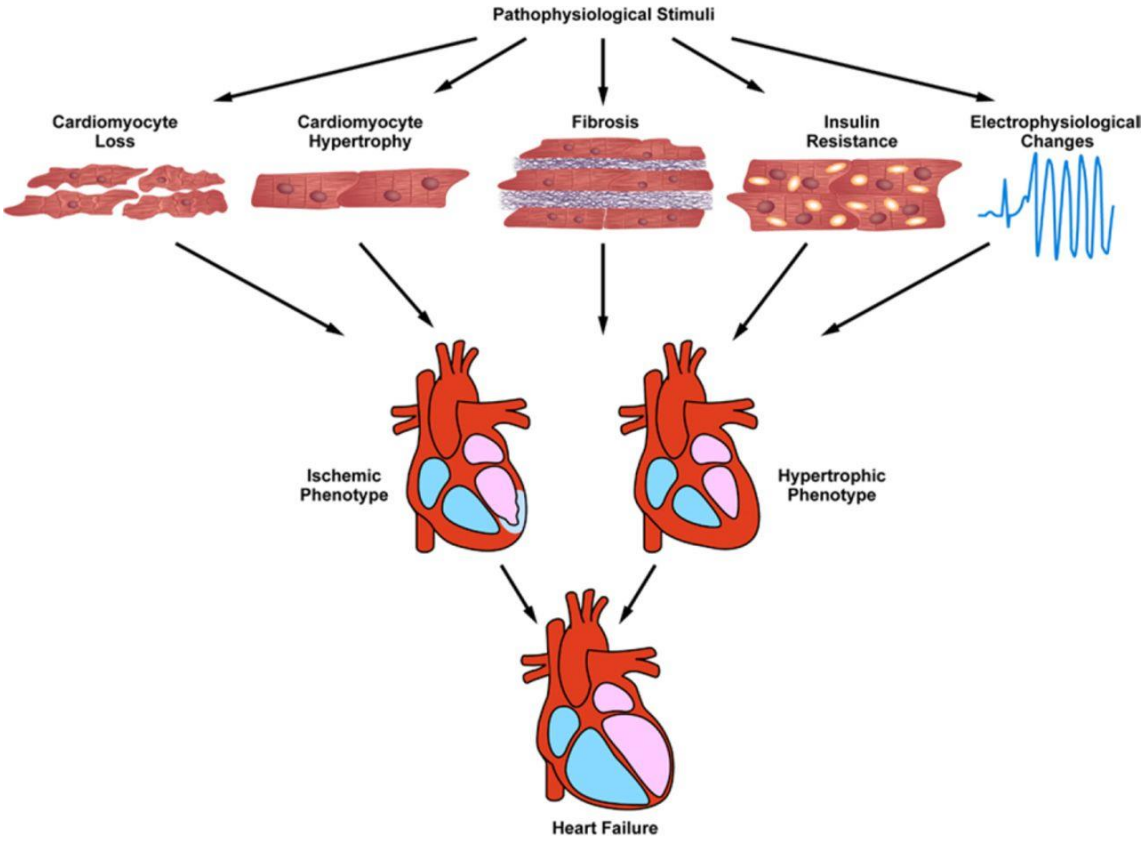

Figure 1: Potential pathological stimuli contributing to cardiac remodelling (5).

Although cardiac remodelling represents a compensatory process, if persist, may lead to continuous progressive changes affecting cardiomyocytes, smooth muscle cells, endothelium and interstitial matrix. Left ventricular parameters representing cardiac remodelling (left ventricular end-diastolic, end-systolic volume, ejection fraction) are closely related to cardiovascular outcomes, and are feasible endpoints to evaluate the efficacy of pharmacological and non-pharmacological therapeutic options (6).

1.2 Physiological remodelling in athletes

The term remodelling originally reflected a maladaptation to an underlying pathology. As pathological volume and pressure overload leads to dilation and hypertrophy of the left ventricle, haemodynamic changes observed in highly trained athletes may lead to similar changes including both enlarged ventricles and increased wall thickness. Physiological cardiac remodelling as a response to regular and intensive physical training, is a well-known phenomenon. Physiological cardiac remodelling in athletes

was described first in the 19th century by a physician using auscultation and percussion (7, 8). Modern imaging technologies enable a more detailed structural and functional characterization of the athlete's heart **(Figure 2)**.

Physical training can be divided into two main categories based on its metabolic characteristics. According to Morganroth's work on the differentiation between endurance and power athletes, dynamic or endurance training causes volume overload, while static or strength training leads to pressure overload resulting in chamber dilation and hypertrophy, respectively (9-11). As the majority of sports contain various degree of endurance and power training, more detailed classifications were established based on the static and dynamic components of sports (12). Literature data imply that many other factors may influence the degree and nature of the cardiac adaptation including gender, training intensity and duration, age, ethnicity and currently unknown factors (4, 13-18). Therefore to establish the physiological upper limit of cardiac adaptation in an athlete may often cause difficulties in the clinical routine. The importance of this question arises from the fact that false positive diagnosis of cardiomyopathies may lead to unnecessary interruption of a professional's sports career. On the other hand, unrecognized pathologies may cause sudden unexpected cardiac death in young competitive athletes. The annual incidence rate of sudden cardiac death (SCD) in athletes is about 0.7-3.0 per 100 000 young athletes under 35 years (19-24). The incidence of sudden cardiac death in athletes is higher than in non-athletes. Competitive sports activity enhances the risk of SCD by 2- to 3-fold, and a clear male predominance was observed with a 2.3-10-fold risk compared to women (19, 20). Beside male gender, older age and Afro-Caribbean origin are all associated with an increased SCD risk (23-28). The aetiology of SCD in young athletes varies in different studies depending mainly on geographical and ethnical differences. Based on North American data the leading cause of SCD is hypertrophic cardiomyopathy (HCM) (22, 25), while European data suggests a higher prevalence of arrhythmogenic right ventricular cardiomyopathy (ARVC), especially in the Veneto region of Italy (29). The limited existing data regarding the aetiology of SCD in Hungarian athletes suggest, that although the most common cardiomyopathy in this population is HCM, in athletes with aborted sudden cardiac death the underlying cause is most commonly ARVC highlighting the extremely arrhythmogenic nature of the disease (30).

DOI:10.14753/SE.2020.2408

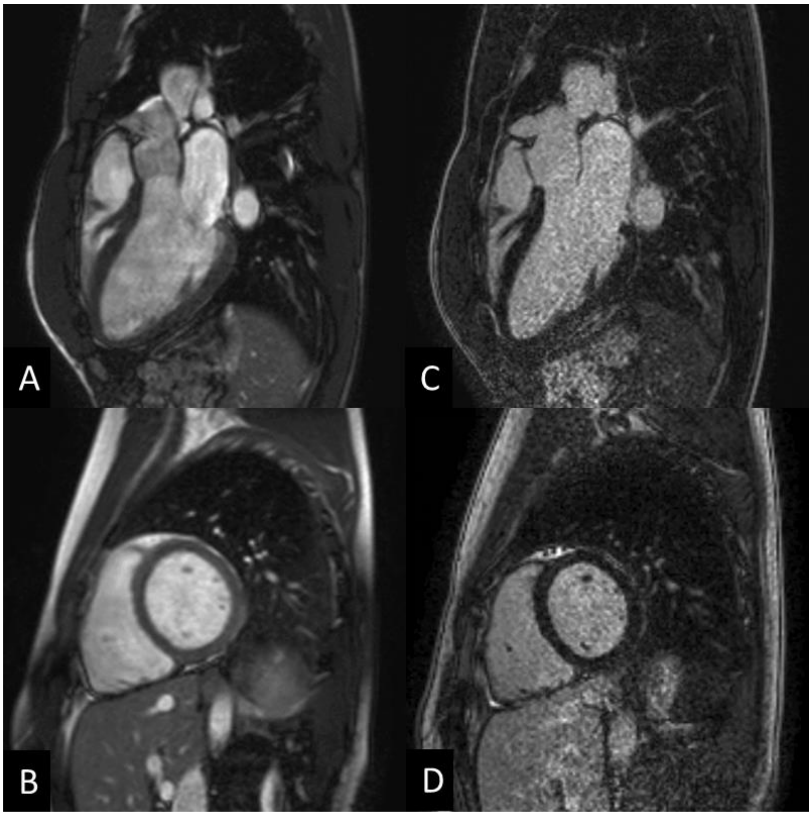

Figure 2: Cardiac magnetic resonance images of an athlete: cine balanced steady-state free precession (bSSFP) images (A,B) and late gadolinium enhancement images (C, D) in long- and short-axis views. Heart and Vascular Center, Semmelweis University.

As cardiomyopathies – mostly HCM and ARVC – represent a significant proportion of SCD cases in young athletes, attention has been focused on differentiation of these conditions from physiological cardiac remodelling. Diagnostic dilemmas may arise mainly in highly trained athletes where cardiac adaptation may reach a level, which can mimic cardiomyopathies **(Figure 3)**. Structural and functional alterations including ventricular dilation, slightly decreased ejection function, and electrical alterations (such as potentially abnormal electrocardiogram (ECG) findings and variety of arrhythmias) can be a part of the healthy, highly trained athlete's heart spectrum (31).

DOI:10.14753/SE.2020.2408

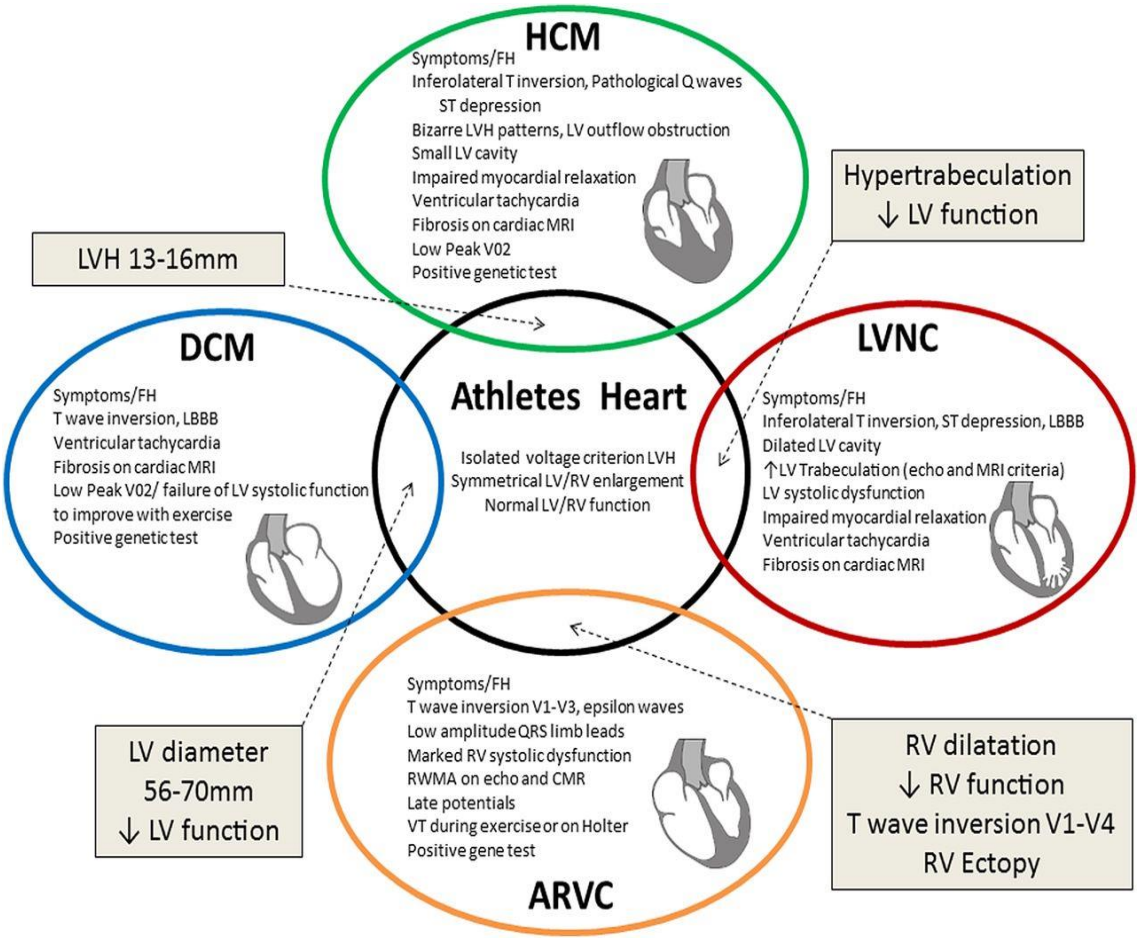

Figure 3: The Grey zone of overlap between physiological and pathological remodelling causing diagnostic dilemmas (32). ARVC, arrhythmogenic right ventricular cardiomyopathy; DCM, dilated cardiomyopathy; HCM, hypertrophic cardiomyopathy; LBBB, left bundle branch block; LV, left ventricular; LVH, left ventricular hypertrophy; LVNC, left ventricular noncompaction; MRI, magnetic resonance imaging; RV, right ventricular.

1.3 Pathological remodelling in cardiomyopathies

1.3.1 Hypertrophic cardiomyopathy

Hypertrophic cardiomyopathy is a genetic disorder manifesting in left ventricular hypertrophy in the absence of secondary causes with an estimated prevalence of 0.16-0.29% (33-37). The hypertrophy is frequently asymmetrical. It predominantly involves the basal interventricular septum, but midventricular, apical, inferolateral, right ventricular involvement and concentric forms may occur. HCM is a single gene disorder

with an autosomal dominant pattern of inheritance caused by mutations in genes encoding sarcomere-associated proteins. Autosomal recessive and X-linked mutations are extremely rare and should raise the suspicion of HCM phenocopies (38, 39). Histological features include myocyte hypertrophy, myocyte disarray and interstitial fibrosis. According to the current guideline of the European Society of Cardiology (ESC) the diagnostic criterion of HCM in adults is a maximal end-diastolic wall thickness ≥15 mm in one or more left ventricular myocardial segments that is not explained solely by loading conditions (40). Other conditions such as aortic stenosis, arterial hypertension, athlete's heart and different phenocopies including amyloidosis, Anderson-Fabry, Pompe disease, Danon disease or endomyocardial fibrosis may mimic HCM and can cause diagnostic difficulties **(Figure 4)**.

Patients may stay asymptomatic for decades despite the presence of severe hypertrophy. The most frequent symptoms are heart failure with preserved ejection fraction, chest pain, palpitations, presyncope, syncope and sudden cardiac death. The symptoms develop mainly due to diastolic dysfunction, left ventricular outflow tract (LVOT) obstruction, imbalance between myocardial oxygen supply and demand and arrhythmias related to cardiac remodelling with myocardial hypertrophy, myocyte disarray and fibrosis (41).

The estimated annual SCD risk is approximately 0.5-2%. Patients after aborted sudden cardiac arrest caused by ventricular fibrillation (VF) or sustained ventricular tachycardia (VT), implantation of an implantable cardioverter defibrillator (ICD) as secondary prevention is strongly indicated (40, 42). ICD implantation for primary prevention is recommended in patients with at least one risk factor including unexplained syncope, an abnormal blood pressure response to exercise (hypotension), massive (≥30 mm) thickening of the interventricular septum or ventricular wall, a positive family history of HCM and SCD, multiple episodes of documented nonsustained VT using an extended (30-day) period of cardiac rhythm monitoring, and extensive (≥15% of left ventricular mass) late gadolinium enhancement (LGE) determined by CMR imaging. To simplify risk assessment, the European Society of Cardiology established the HCM Risk Calculator (40), baseline and periodic re-evaluation is recommended because of the progressive nature of the disease. Besides SCD prevention, therapeutic options represent symptomatic treatment including pharmacological or interventional therapy; current therapies do not target the underlying genetic defect (41).

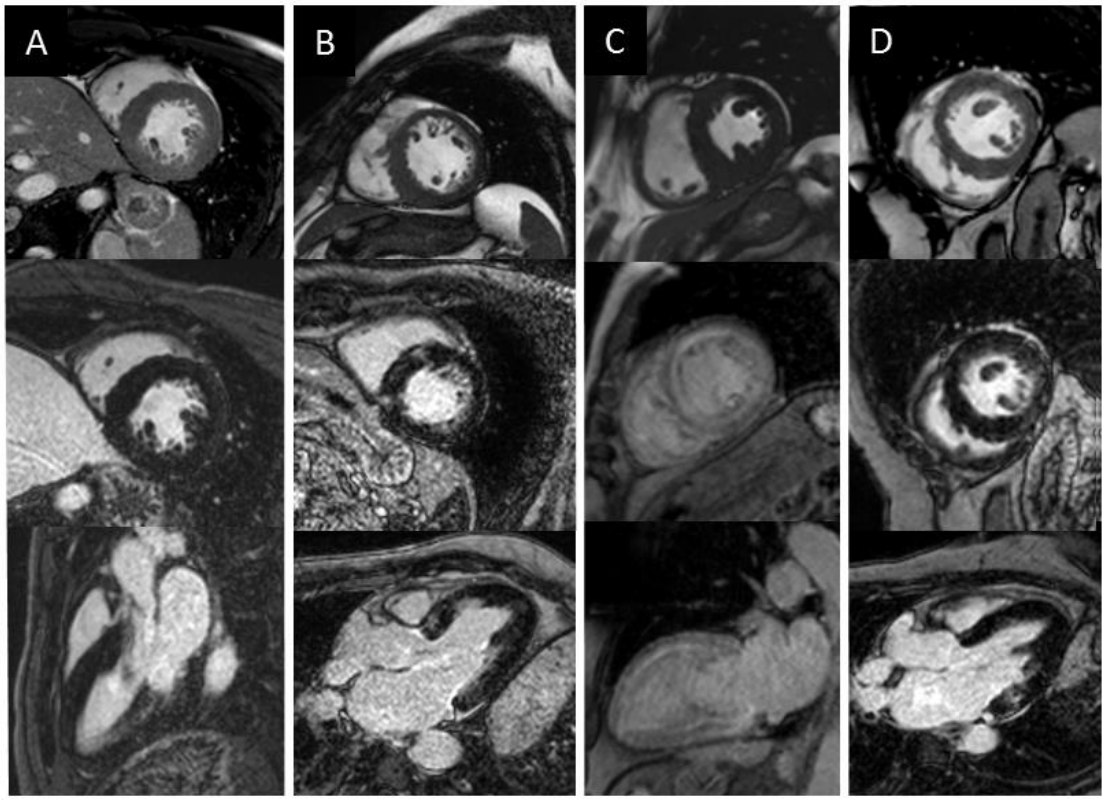

Figure 4: Cine bSSFP and late gadolinium enhancement images of HCM and HCM phenocopies: aortic stenosis (A), HCM (B), amyloidosis (C), Anderson-Fabry disease (D). Heart and Vascular Center, Semmelweis University.

HCM patients participating in competitive sport are representing a high risk population (42, 43). Present guidelines recommend the disqualification of HCM patients from any competitive sports regardless of the presence or absence of major risk factors (44, 45)**.** Pelliccia and his colleagues recently published a paper about athletes with HCM. In this small, mainly low risk HCM population, although cardiac symptoms and cardiac arrest occurred, the incidence of symptoms and events were not different between patients, who were dismissed and who continued their exercise programs (46). These controversial data suggest that only additional larger scaled studies with massive population of athletes diagnosed with HCM could accurately evaluate the characteristics of this unique population, and clarify the role of regular exercise in disease progression and clinical outcomes.

Diagnosing HCM in athletes is challenging in the everyday clinical routine. The overlap between mild HCM phenotypes and pronounced left ventricular hypertrophy of an athlete offered a challenge in the process of identifying the accurate diagnosis in the

grey zone of hypertrophy many years ago. The algorithm aiming to resolve this problem is presented in **Figure 5** (47). Although it may be helpful in some cases in athletes with possible HCM, however, some of the patterns (e.g. LV cavity, atrial enlargement) may not be useful. Recent literature implies that the clinical characteristics of athletes with HCM significantly differ from sedentary HCM patients (48), therefore it is crucial to establish new parameters and cut-off values which could help to diagnose athletes with HCM.

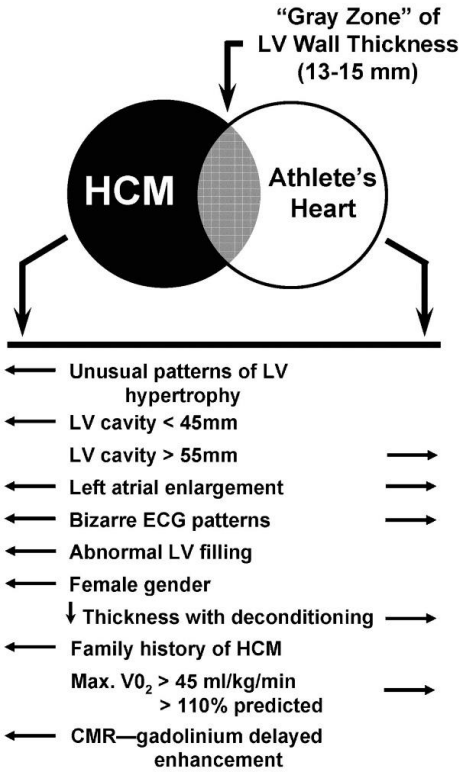

Figure 5: Criteria to distinguish HCM and athlete's heart in patients in the grey zone of hypertrophy. (47) CMR, cardiac magnetic resonance; ECG, electrocardiogram; HCM, hypertrophic cardiomyopathy; LV, left ventricular.

1.3.2 Arrhythmogenic right ventricular cardiomyopathy

Arrhythmogenic right ventricular cardiomyopathy is a genetic disorder resulting in fibrofatty infiltration of the myocardium (49). Although most commonly it affects the right ventricle, based on literature data the left ventricle is involved in more than 50% of the cases (50-52). The estimated prevalence of the disease (0.02-0.05%) displays relevant geographic differences (49). The diagnosis is based on the current Task Force

criteria (TFC) including global or regional right ventricular dysfunction, structural changes, tissue characterization, repolarization and depolarization abnormalities, arrhythmias and family history **(Table 1)** (53).

Table 1: Revised Task Force Criteria for the diagnosis of ARVC, adapted from Marcus et al. (53) The diagnosis is fulfilled by the presence of 2 major, or 1 major plus 2 minor criteria or 4 minor criteria from different groups. Diagnostic terminology for revised criteria: definite diagnosis: 2 major or 1 major and 2 minor criteria or 4 minor from different categories; borderline: 1 major and 1 minor or 3 minor criteria from different categories; possible: 1 major or 2 minor criteria from different categories. PLAX, parasternal long-axis view; RVOT, right ventricular outflow tract; BSA, body surface area; PSAX, parasternal short-axis view; aVF, augmented voltage unipolar left foot lead; and aVL, augmented voltage unipolar left arm lead, SAECG, signal-averaged electrocardiogram.

Category	Major criteria	Minor criteria
I. Global or regional dysfunction and structural alterations	By 2D echo: ● Regional RV akinesia, dyskinesia, or aneurysm ● and 1 of the following (end diastole): — PLAX RVOT ≥32 mm (corrected for body size [PLAX/BSA] ≥19 mm/m2) — PSAX RVOT ≥36 mm (corrected for body size [PSAX/BSA] ≥21 mm/m2) — or fractional area change ≤33% By MRI: ● Regional RV akinesia or dyskinesia or dyssynchronous RV contraction ● and 1 of the following: — Ratio of RV end-diastolic volume to BSA ≥110 mL/m2 (male) or ≥100 mL/m2 (female) — or RV ejection fraction ≤40% By RV angiography: ● Regional RV akinesia, dyskinesia, or aneurysm	By 2D echo: ● Regional RV akinesia or dyskinesia ● and 1 of the following (end diastole): — PLAX RVOT ≥29 to <32 mm (corrected for body size [PLAX/BSA] ≥16 to <19 mm/m2) — PSAX RVOT ≥32 to <36 mm (corrected for body size [PSAX/BSA] ≥18 to <21 mm/m2) — or fractional area change >33% to ≤40% By MRI: ● Regional RV akinesia or dyskinesia or dyssynchronous RV contraction ● and 1 of the following: — Ratio of RV end-diastolic volume to BSA ≥100 to <110 mL/m2 (male) or ≥90 to <100 mL/m2 (female) — or RV ejection fraction >40% to ≤45%

II. Tissue characterization of wall	● Residual myocytes <60% by morphometric analysis (or <50% if estimated), with fibrous replacement of the RV free wall myocardium in ≥1 sample, with or without fatty replacement of tissue on endomyocardial biopsy	● Residual myocytes 60% to 75% by morphometric analysis (or 50% to 65% if estimated), with fibrous replacement of the RV free wall myocardium in ≥1 sample, with or without fatty replacement of tissue on endomyocardial biopsy
III. Repolarization abnormalities	● Inverted T waves in right precordial leads (V1, V2, and V3) or beyond in individuals >14 years of age (in the absence of complete right bundle-branch block QRS ≥120 ms)	● Inverted T waves in leads V1 and V2 in individuals >14 years of age (in the absence of complete right bundle-branch block) or in V4, V5, or V6 ● Inverted T waves in leads V1, V2, V3, and V4 in individuals >14 years of age in the presence of complete right bundle-branch block
IV. Depolarization/conduction abnormalities	● Epsilon wave (reproducible low-amplitude signals between end of QRS complex to onset of the T wave) in the right precordial leads (V1 to V3)	● Late potentials by SAECG in ≥1 of 3 parameters in the absence of a QRS duration of ≥110 ms on the standard ECG ● Filtered QRS duration (fQRS) ≥114 ms ● Duration of terminal QRS <40 μV (low amplitude signal duration) ≥38 ms ● Root-mean-square voltage of terminal 40 ms ≥20 μV ● Terminal activation duration of QRS ≥55 ms measured from the nadir of the S wave to the end of the QRS, including R', in V1, V2, or V3, in the absence of complete right bundle-branch block
V. Arrhythmias	● Nonsustained or sustained ventricular tachycardia of left bundle-branch morphology with superior axis (negative or indeterminate QRS in leads II, III, and aVF and positive in lead aVL)	● Nonsustained or sustained ventricular tachycardia of RV outflow configuration, left bundle-branch block morphology with inferior axis (positive QRS in leads II, III, and aVF and negative in lead aVL) or of unknown axis ● >500 ventricular extrasystoles per 24 hours (Holter)
VI. Family history	● ARVC confirmed in a first-degree relative who meets current Task Force criteria ● ARVC confirmed pathologically at autopsy or surgery in a first-degree relative ● Identification of a pathogenic mutation categorized as associated or probably associated with ARVC in the patient under evaluation	● History of ARVC in a first-degree relative in whom it is not possible or practical to determine whether the family member meets current Task Force criteria ● Premature sudden death (<35 years of age) due to suspected ARVC in a first-degree relative ● ARVC confirmed pathologically or by current Task Force Criteria in second-degree relative

As a progressive disease, ARVC is categorized into different phases: the early concealed phase, overt or electrical phase, and phase of right ventricular (RV) and biventricular failure. As one of the most arrhythmogenic cardiomyopathies, it often manifests as ventricular tachycardia or ventricular fibrillation. Heart failure may occur mainly in the advanced stage of the disease. Morphological and ECG changes may lack in early phase making the diagnosis even more difficult. Moreover, certain pathologies can mimic ARVC such as idiopathic right ventricular outflow tract (RVOT) tachycardia, sarcoidosis, myocarditis or even physiological cardiac remodelling called athlete's heart.

As approximately 50% of the patients with ICD experience appropriate therapy (54, 55), the extremely arrhythmogenic nature of the disease is not questionable. Numerous risk factors have been proposed for stratifying SCD risk and indication for ICD implantation as risk stratification represents a crucial point in the management of ARVC. The international Task Force consensus statement distinguishes between the following categoriws: high risk patients with aborted SCD due to VF, sustained VT, severe ventricular dysfunction (>10% annual mortality rate), intermediate risk patients with at least one major risk factor including syncope, nonsustained ventricular tachycardia (nsVT), moderate ventricular dysfunction, or at least one minor risk factor including mild ventricular dysfunction, heart, failure, young age, male gender, complex genotype, proband status, inducible VT/VF, extent of electroanatomic scar, or fragmented electrocardiograms on right ventricular (RV) endocardial voltage mapping (1-10% annual mortality rate) and low risk patients without risk factors (<1% annual mortality rate) (56). Antiarrhythmic drug therapy including sotalol, beta blockers and amiodarone are frequently used in ARVC patients to reduce VT burden, although the efficacy is still debated because of the controversies introduced in medical literature (57-59).

In ARVC patients, intensive training is associated with higher risk of life-threatening arrhythmias and heart failure (60-63). Competitive sport activity was associated with a 5-fold SCD risk in young adults with ARVC (19). Therefore, athletes with definite diagnosis of ARVC should not participate in competitive sports with the exception of low-intensity class 1A sports (45). As recent literature data imply, recreational sport activity shows no association with earlier onset of symptoms or increased risk of life-threatening arrhythmias. Restriction in patients performing only recreational sport activity has not been established as of yet (64, 65).

Although researchers initially mainly focused on the left ventricle in the athletic cardiac adaptation, in the last decade healthcare professionals have turned their attention to understand the structural and functional changes in the right ventricle as well (66-69). La Gerche and his colleagues found a lower rate of desmosomal gene mutations in athletes with RV arrhythmias compared to non-athletes. They hypothesized that regular intensive exercise alone may lead to proarrhythmogenic RV remodelling identifyied as "exercise-induced ARVC" (70).

Early diagnosis of ARVC is a difficult clinical scenario in highly trained athletes. Dilated right and left ventricles and decreased ejection fraction may be a consequence of regular high intensity training, and precordial T-wave inversions in both leads v1 and v2 are present in more than half of the athletes **(Figure 6)** (71). Therefore, further diagnostic criteria are warranted to be discovered to solve this critical clinical dilemma.

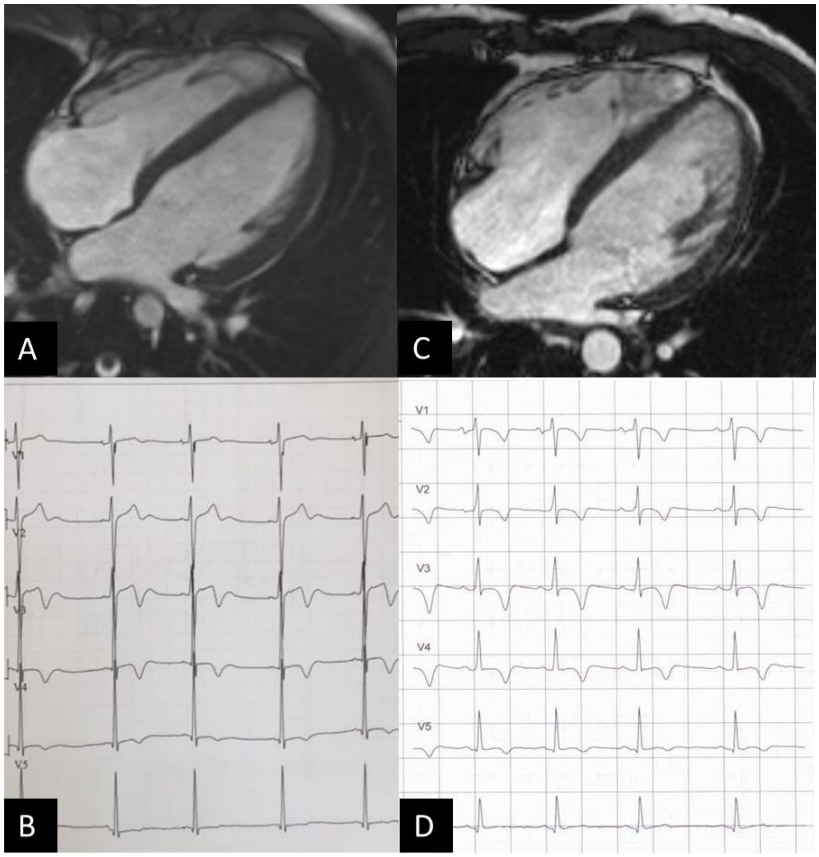

Figure 6: CMR images and 12-lead ECG of a highly trained athlete (A, B) and an ARVC patient (C,D) representing the overlapping features such as right ventricular dilation and T-wave inversions in the precordial leads. Heart and Vascular Center, Semmelweis University.

DOI:10.14753/SE.2020.2408

1.3.3 Dilated cardiomyopathy

Dilated cardiomyopathy (DCM) is a condition characterized by left ventricular or biventricular dilation and impaired systolic function, where pressure overload or coronary artery disease alone does not explain the myocardial dysfunction (72, 73). The estimated prevalence is 0.04-0.4% showing significant race-related and geographical differences (74, 75). Approximately 30-40% of the cases are genetic, affecting genes encoding cytoskeletal, sarcomere and nuclear envelope proteins. Non-genetic causes include alcohol abuse, toxins, drugs, inflammation, tachyarrhythmias, metabolic or endocrine disturbances. Symptoms most commonly are related to heart failure, arrhythmias and thromboembolic events (76).

The clinical diagnosis of DCM relies on non-invasive imaging. It has been defined by the presence of reduced systolic function (fractional shortening <25% or left ventricular ejection fraction (LVEF) <45%) and left ventricular dilation (LVEDD >117% of the predicted value corrected for age and body surface area) after excluding any known causes of myocardial dysfunction (77). Advanced imaging modalities may play a role in the early detection of the disease by more precise function and volume assessment, the detection of strain abnormalities or the presence of LGE (78).

The management mainly focuses on the change in LV size and function, arrhythmias and congestive symptoms. Main cornerstones of the pharmacological therapy of heart failure with reduced ejection fractions are angiotensin-converting enzyme inhibitors, β-blockers, aldosterone antagonists, angiotensin receptor-neprilysin inhibitor and ivabradine in patient with sinus rhythm above 70/min. Symptomatic patients besides optimal medical therapy with wide QRS and left bundle branch block (LBBB) morphology may benefit from cardiac resynchronization therapy (CRT) (79). ICD for primary prevention is indicated in patients with reduced ejection fraction (EF <35%) despite optimal medical treatment (80). However, literature implies that arrhythmia burden is unrelated to LV dysfunction (81) and a subset of patient may present ventricular arrhythmia in the early phase of the disease. These patients are classified as “arrhythmogenic DCM” patients. Halliday and his colleagues have proven that the presence of midwall LGE identifies patients with high SCD risk even in the subgroup of DCM patients with LVEF≥40% suggesting that DCM patients with only mildly reduced

or preserved LVEF but with midwall LGE may also benefit from ICD implantation (82).

Physiological cardiac remodelling caused by regular intensive training may mimic DCM. Up to 15% of the athletes have increased cardiac dimensions. Moreover LVEF may be reduced in 45% of highly trained elite athletes (15, 83). As competitive sport activity may increase the risk of SCD, symptomatic patients with DCM should not participate in most competitive sports with the exception of low-intensity sports (class 1A sports such as billiards, bowling, cricket, golf) in selected cases (45). The precise evaluation of cardiac dimensions and ventricular function are crucial in these clinical scenarios **(Figure 7)**.

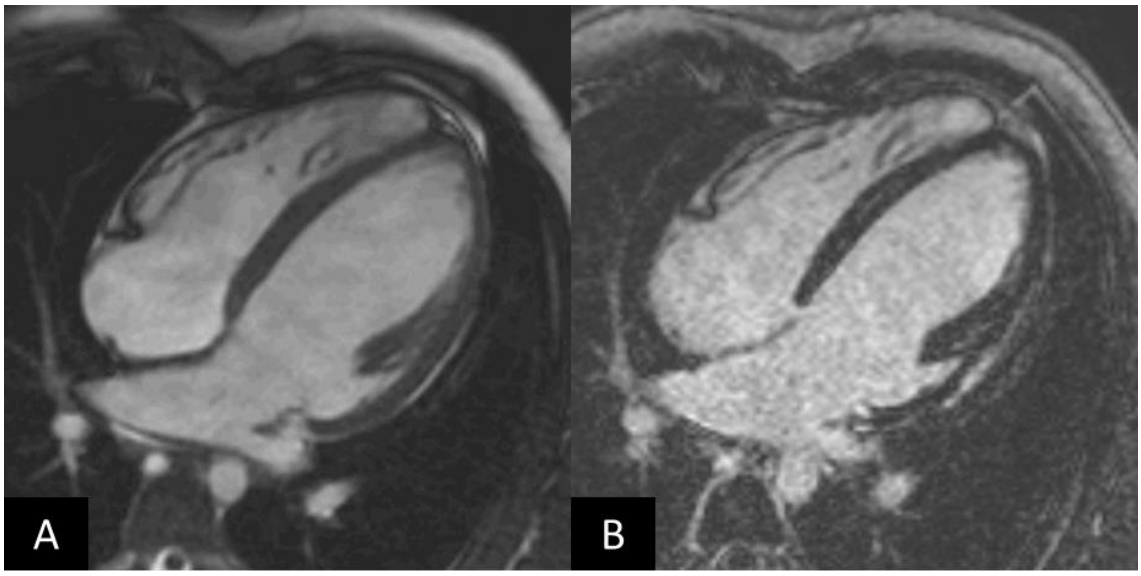

Figure 7: CMR images of a young water-polo player with preserved LVEF (50%). Four chamber cine image shows marked left ventricular dilatation (LVEDVi: 154 ml/m2, RVEDVi: 122 ml/m2), where the presence of mild midmyocardial septal LGE confirmed the suspicion of DCM. Heart and Vascular Center, Semmelweis University.

1.4 Reverse remodelling

1.4.1 Reverse remodelling in athletes – cardiac deconditioning

The physiological cardiac adaptation to vigorous exercise, in normal conditions is a reversible process **(Figure 8)**. In athletes with structural heart disease the ventricular dilation and/or hypertrophy may decrease, but will not completely return to normal.

Based on this observation, deconditioning may have an important role in the differential diagnosis between healthy athletes and cardiomyopathies (84-86).

However, extreme forms of cardiac adaptation in athletes raised the suspicion that exercise-related adaptations in healthy athletes are not always completely reversible. The study by Pelliccia et al. reported incomplete reversal of pronounced LV dilatation after deconditioning and chamber enlargement persisted in 20% of the retired athletes after five years (84).

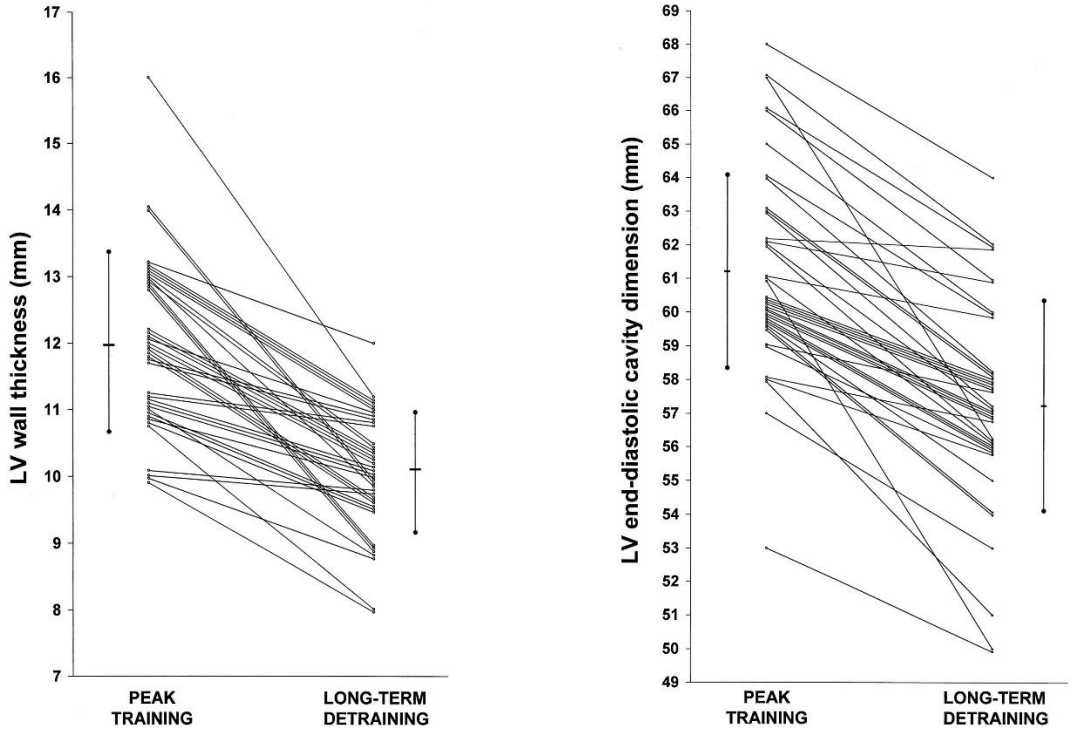

Figure 8: LV wall thickness and LV end-diastolic cavity dimensions in elite athletes after a long-term detraining. (84) LV, left ventricular.

Biffi et al. reported a significant decrease in the frequency and complexity of ventricular arrhythmias after deconditioning, suggesting that electrical remodelling is part of the athlete's heart spectrum **(Figure 9)** (87).

DOI:10.14753/SE.2020.2408

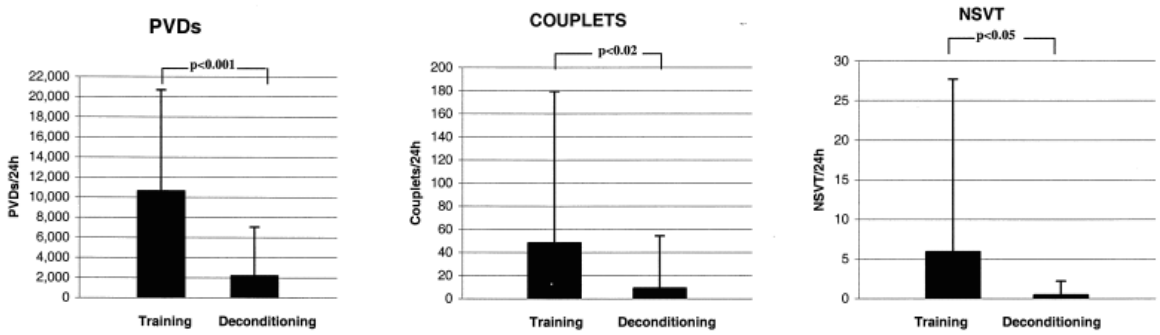

Figure 9: Number of premature beats, couplets and nsVTs at peak training and after deconditioning in 70 athletes based on 24-h Holter electrocardiogram. (87) PVDs, Premature ventricular beats; nsVT, nonsustained ventricular tachycardia.

Based on the fact, that reduction of the number of ventricular arrhythmias during detraining may be present in healthy athletes and athletes with cardiomyopathy, forced deconditioning in order to differentiate between pathology and physiological adaptation is not recommended (88).

1.4.2 Reverse remodelling due to pharmacological and non-pharmacological therapy

Patients with reduced ejection fraction (both with ischaemic and non-ischaemic aetiology) may undergo remarkable reverse remodelling after heart failure therapy or even spontaneously (89). In the absence of a universal definition for reverse remodelling, most studies define it as an increase in LVEF ≥10% with a decrease in left ventricular end-diastolic volume (LVEDV) and left ventricular end-systolic volume (LVESV). Many studies have proven that the improvement of LVEF and decrease in LVEDV and LVESV are associated with a better outcome (90-92) as shown in **Figure 10**.

DOI:10.14753/SE.2020.2408

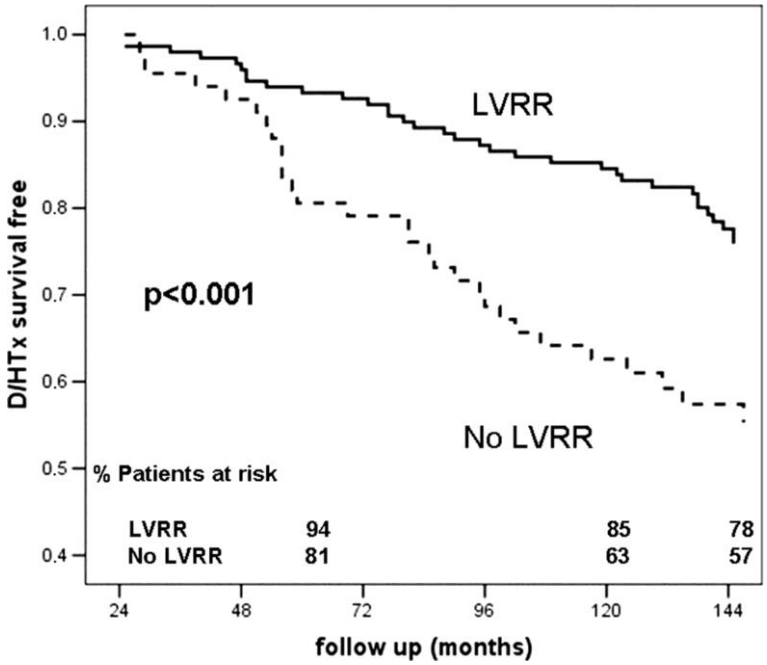

Figure 10: Survival curves of DCM patients show long-term prognostic impact of left ventricular reverse remodelling (93). LVRR, left ventricular reverse remodelling; D, death; HTx, heart transplantation.

Identifying patients who may remodel and who may not would be essential to optimize patient management. Therefore identifying predictors of reverse remodelling has a significant clinical importance. It has been proven that baseline end-diastolic volume, but not baseline LVEF predicts reverse remodelling (93-95). Baseline left atrial volume and right ventricular function might be also a predictor in specific patient populations (96, 97). Kubanek et al. showed that in DCM patients with recent onset of heart failure symptoms, the extent of LGE and higher myocardial oedema ratio is an independent predictor of reverse remodelling (98). Other CMR-based studies failed to prove the predictive nature of LGE suggesting that larger trials with more objective criteria for identification of mid-wall fibrosis are greatly demanded (94, 99).

Beside optimal medical therapy, cardiac resynchronization therapy (CRT) is an effective therapeutic option to achieve reverse remodelling in heart failure patients with reduced ejection fraction and wide QRS with LBBB morphology (79). **Figure 11.** represents remarkable reverse remodelling in a patient after CRT implantation.

DOI:10.14753/SE.2020.2408

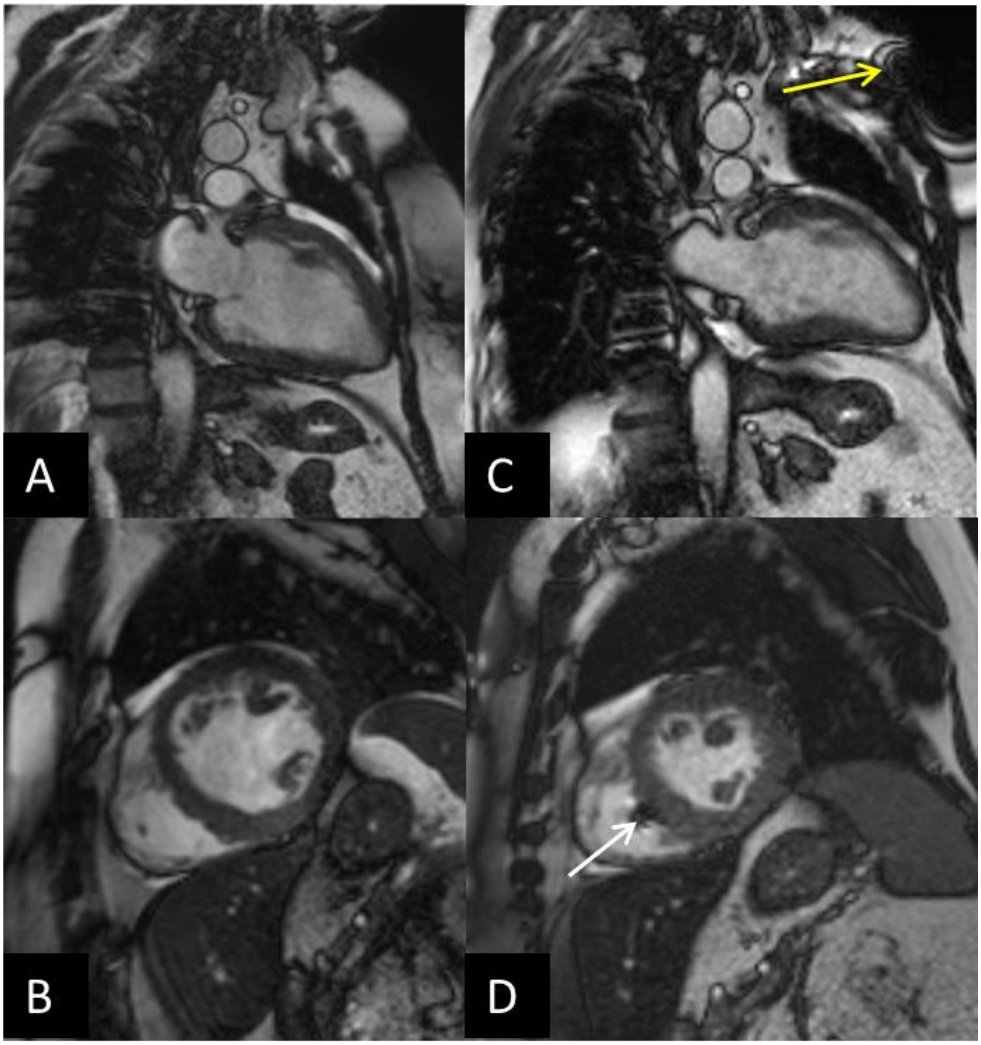

Figure 11: Long- (A,C) and short-axis (B, D) CMR cine images in end-diastolic phase at baseline (A-B) and six months after CRT implantation (C,D) represent apparent reverse remodelling. Sphericity index decreased (3D sphericity index: 0.34 vs 0.17); relative wall thickness increased (0.38 vs 0.51) and LV volumes also decreased (LVESVi 98 vs 33 ml/m2; LVEDVi 129 vs 74 ml/m2). Generator (yellow arrow) and lead related artifacts (white arrow) do not significantly affect image quality. Heart and Vascular Center, Semmelweis University.

While the rate of non-responders mainly depends on how CRT response is defined, approximately 30-40% of patients with guideline based CRT indication do not show a clear benefit after CRT implantation (100). Therefore, determining factors of outcome has a great importance. A native LBBB, non-ischaemic aetiology, female gender and a

wider QRS duration is associated with reverse remodelling and better outcome (101). Other factors such as mechanical dyssynchrony assessed using echocardiography have been intensively studied. Although several single-centre studies have proven the role of imaging in prediction of CRT response (102-105), in a large multicenter setting, no single echocardiographic parameter was able to predict CRT response (106). Combining advanced imaging techniques such as echocardiography-based strain imaging and CMR-based scar identification may have benefit in predicting CRT response. Hopefully, an ongoing large multicenter prospective study on multimodality-imaging may elucidate controversial issues in previous research (107).

Reverse remodelling represents a multilevel molecular, cellular and anatomic reversion towards a normal myocardial structure and function, and can manifest in myocardial recovery or remission. Further research may support our fundamental understanding of reverse remodelling's nature and the underlying mechanisms. (108).

1.5 Cardiac magnetic resonance imaging and its role in the assessment of cardiac remodelling

Cardiac magnetic resonance (CMR) imaging is the gold standard non-invasive method to evaluate left and right ventricular volumes, mass and ejection fraction. Furthermore, it enables identification and precise quantification of myocardial scar tissue.

Functional changes in cardiac remodelling can be characterized using CMR imaging for the assessment of left and right ventricular ejection fraction (LVEF, RVEF), and stroke volume (LVSV, RVSV). Quantification of the left and right ventricular volumes, mass and ejection fraction is based on manual delineation of the endocardium and epicardium on the short-axis cine images in end-systolic and end-diastolic phase. Using conventional quantification techniques the volume in between the endo- and epicardial contour is considered to be myocardial mass, and the volume within the endocardial line is considered to be blood. Novel threshold-based quantification techniques enable the quantification of the trabeculae and papillary muscles. The semi-automatic threshold-based algorithm allows us to estimate the spatially varying signal intensities of blood and muscle within an observer-provided epicardial contour. Voxels with signal

intensities above the specified threshold are considered to be blood, voxels with signal intensities below the threshold are considered to be myocardium. Quantification of papillary muscles and trabeculae may play an important role detailed volumetric assessment especially in conditions with hypertrophy such as in HCM or athlete's heart. Moreover, it may also contribute to a significant reduction in time required for post-processing (109).

CMR is an excellent modality for measuring strain, but the majority of the strain analysis techniques required additional sequences. CMR-based deformation imaging therefore has not been widely used till the development of feature tracking analysis. This novel quantification technique enables the assessment of myocardial strain using the conventional balanced steady-state free precession (bSSFP) cine images, no additional image acquisition is required. The optimal myocardium blood contrast provides optimal definition of the endocardial layer, therefore endocardial features can be tracked through the cardiac cylcle similar to the speckle tracking technique (110). Feature tracking enables measurement of global and regional left and right ventricular strain parameters, mechanical dispersion and intraventricular dyssynchrony as well.

Cardiac remodeling is not only characterized by functional, but also morphological changes. Changes in cavity size and mass can be measured as left and right ventricular end-diastolic volume (LVEDV, RVEDV), end-systolic volume (LVESV, RVESV) and myocardial mass (LVM, RVM). Alterations in ventricular geometry/shape can be described using geometric indices such as sphericity index, relative wall thickness or maximal end-diastolic wall thickness to left ventricular end-diastolic volume index ratio (EDWT/LVEDVi) and left ventricular mass to end-diastolic volume ratio.

CMR also enables to detect structural changes of the heart by detecting scar formation and replacement fibrosis with late gadolinium enhancement technique (111). Ten to twenty minutes after gadolinium-based contrast administration, applying T1-wheighted inversion recovery gradient-echo sequences and nulling the normal myocardium – supressing the signal from healthy myocardium –, enables to differentiate normal tissue (dark) and fibrotic tissue (bright) **(Figure 12)**. The localisation and pattern of the LGE allows us to differentiate between ischaemic and non-ischaemic aetiology as well as to distinguish between various non-ischaemic forms of cardiomyopathies **(Figure 12)**.

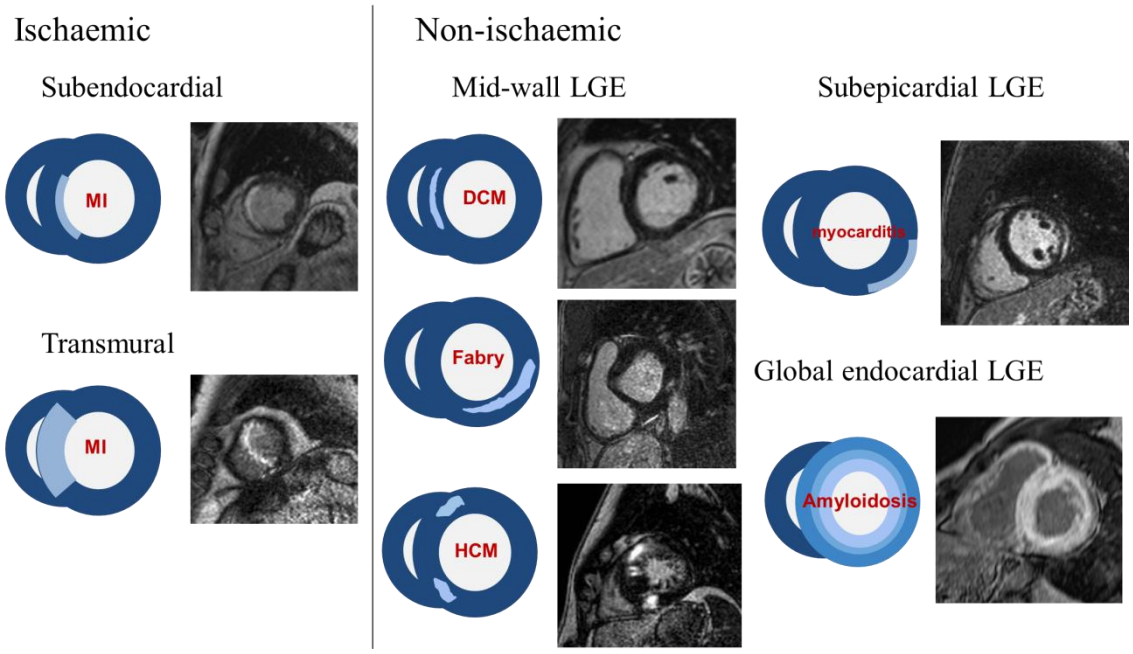

Figure 12: Representation of LGE patterns characteristic for ischaemic and non-ischaemic pathologies. Adapted by Karamitsos et al. (112). DCM, dilated cardiomyopathy; HCM, hypertrophic cardiomyopathy; LGE, late gadolinium enhancement; MI, myocardial infarction.

Beside the diagnostic role, the presence of LGE also has an added value in risk stratification. The extent and localisation of fibrosis in different cardiomyopathies are associated with adverse clinical outcomes including heart failure and ventricular arrhythmias (113-116). Patients with LGE have a higher incidence of ventricular arrhythmias and adverse cardiac outcomes (117-119). Ventricular scar may act as a substrate of life-threatening arrhythmias, and detecting fibrosis using CMR imaging is becoming a part of the clinical work-up also in the field of sports cardiology. Previously, it was understood that existing myocardial fibrotic tissue represents definite pathology, but recent literature suggests that focal LGE in the insertion points with unknown significance may be present in asymptomatic athletes. Potential mechanism behind aspecific myocardial fibrosis in athletes may be caused by pressure overload, exercise-induced repetitive microinjuries, genetic predisposition or silent myocarditis (120).

Advanced CMR techniques, such as native T1 mapping and calculation of extracellular volume, may also play an important role in the characterization of pathological and

physiological cardiac remodelling, especially in conditions with diffuse fibrosis (121, 122). Despite the many advantages of CMR techniques, implanted cardiac devices may carry some limitations. In the past, performing CMR examination in patients with pacemaker, ICD, CRT or implantable loop recorders has been contraindicated due to safety concerns. Recent data suggest that implanted cardiac devices represent no absolute contraindication. Manufacturers started to develop MRI conditional systems. A prospective, randomized multicenter study has proven no MRI-related contraindication, no MRI-attributed pacemaker sensing or threshold changes were observed (123). Moreover, large clinical studies have proven that applying prespecified safety protocol and careful programming, thoracic and non-thoracic MR examinations even in patients with non-conditional PM or ICD are safe. Addressing the concerns that MR examination may lead to decreased sensing, impedance or increased capture threshold, large clinical studies have proved that these changes on device parameters are non-significant. Cardiac events are very rare including power-on reset, especially in ICD devices with low battery life, but in case of appropriate programming and imaging, the CMR examination do not lead to serious adverse cardiac events (124, 125). As fractured or abandoned leads may increase the risk of heating, scanning in these cases is not recommended. In addition, it is recommended to avoid MR imaging within six weeks post device implantation.

The technical improvement regarding devices, improved image quality and positive safety results of large trials will lead to further improvement of scanning patients with implanted cardiac devices. In case of relative contraindications for CMR examination, the benefits and potential risks should be carefully assessed.

1.6 Electroanatomic mapping and its role in the assessment of cardiac remodelling

Besides functional and morphological changes, cardiac remodelling is characterized by structural alterations of the left ventricle including scar formation. As scar tissue is a potential substrate of ventricular arrhythmias, its identification and modification during

radiofrequency catheter ablation (RFCA) may play an important role in the treatment of malignant ventricular arrhythmias in patients with structural heart disease.

Electroanatomic mapping (EAM) using various mapping systems enables the detection of pathological fibrous, fatty, or inflammatory infiltrates inside the myocardium and the identification of low voltage or dense scar areas in three-dimensional electroanatomic maps. It may facilitate mapping and RFCA of cardiac arrhythmias including macro-reentrant VT (126). Accurate identification of the pathological substrate especially in DCM is difficult; literature is controversial regarding thresholds for abnormal bipolar and unipolar voltages. Several studies have suggested different cut-off levels for normal and abnormal bipolar and unipolar, endocardial and epicardial left ventricular voltage values obtained by EAM. Based on previously proposed cut-off values to detect pathological substrates, low voltage area is mainly defined as electrograms with a bipolar voltage <1.5 mV, while dense scar is usually defined as a bipolar voltage <0.5 mV for the LV endocardium (127, 128). These thresholds are well validated in patients with ischaemic aetiology and although they are adopted for patients with DCM, only limited data support the validity of these cut-offs in DCM (129). Glashan and his colleagues analysed EAM for pathological substrate identification in DCM, and validated their findings by histology. They have concluded that pathological substrates in DCM fundamentally differ from substrates in patients with ischaemic aetiologies. Therefore the currently applied EAM approaches need to be redefined and take the extent and localisation of fibrosis into account (130). Even though there are fixed thresholds for EAM, many clinical cardiac electrophysiologist change these cut-off values in order to better delineate pathological substrates.

As EAM provides a helpful tool in tissue characterization by reconstructing the VT circuits in structural heart diseases, it may contribute to improve outcomes of RFCA of ventricular tachycardia in patients with DCM.

DOI:10.14753/SE.2020.2408

2. Study aims

The main goal of our study was to analyse the functional, morphological and mechanical changes during physiological and pathological remodelling and reverse remodelling with the help of different CMR techniques.

2.1 Differentiation of pathological and physiological remodelling

The first aim of our studies was to describe then compare characteristics of physiological and pathological remodelling in athletes as well in cardiomyopathy patients, and to investigate the clinical and CMR characteristics of elite athletes with cardiomyopathies. We aimed to establish CMR parameters and cut-off values which may help to differentiate pathological and physiological remodelling.

2.2 Electro-anatomic and tissue characterization

Second aim was to investigate structural and electrophysiological remodelling in DCM patients by performing tissue characterization using CMR and electroanatomic characterization using electroanatomic mapping. We aimed to compare the distribution of late gadolinium enhancement and electroanatomical substrate. We proposed to assess VT ablation outcome and factors wich may influence the success.

2.3 Reverse remodelling assessment

Third goal was to investigate reverse remodelling as an effect of cardiac resynchronization therapy in symptomatic heart failure patients despite optimal medical therapy with broad QRS and LBBB morphology applying biventricular pacing during CMR examination. We also aimed to investigate the differences in the left ventricular function and mechanics between biventricular and asynchronous pacing modes.

DOI:10.14753/SE.2020.2408

3. Methods

3.1 Study design and study populations

3.1.1 Study design and study population of the Differentiation of pathological and physiological remodelling project

This retrospective study was conducted in the Semmelweis University Heart and Vascular Center. Healthy highly trained athletes, athletic and sedentary HCM and ARVC patients were examined using cardiac magnetic resonance imaging.

Non-athlete HCM patients (n=194, 50.2±13.6y, 108 male) with preserved ejection fraction (LVEF ≥50%) were consecutively enrolled. HCM was defined according to the current ESC guideline (40), as a maximal wall thickness ≥15 mm measured by CMR that is not explained solely by loading conditions. In 11% of our HCM patients who had wall thickness between 13–14 mm we evaluated other features including family history, electrocardiogram (ECG) and typical LGE pattern. Ten additional athletes (31±10y; 9 male, 14.4±6.5 training hours/week) were examined during training or competition period with the suspicion of HCM, and the comprehensive clinical investigation confirmed the diagnosis.

Non-athlete patients with definite diagnosis of ARVC (n=34, 40.5±13.4y, 22 male) were enrolled based on the revised Task Force Criteria (53). Eight additional highly trained athletes with ARVC (27.6±3.3y, 18.9±4.6 training hours/week, seven male) were enrolled, and the comprehensive investigation including resting ECG, ambulatory ECG monitoring, echocardiography, CMR and medical history confirmed the diagnosis.

Healthy athletes free of any cardiovascular diseases without ECG abnormality suggesting structural heart disease were recruited. The athletic cohort was comprised from canoe and kayak paddlers, water-polo players, rowers, handball players, speed skaters, swimmers, athletics, tennis players, cross country skiers, basketball players or cyclists.

Highly trained healthy athletes members of the National or Olympic Team (n = 150, 24.2±4.8y, 101 male) with a minimum of 18 hours of training per week for at least the last 18 months (male and female athletes with an average training per week: 22.1±5.1 h

and 21.2±3.5 h, respectively) performing highly dynamic, and at least, moderate static sports served as a control group of the sedentary HCM patient group.

Thirty-four highly trained healthy athletes with with a minimum of 15 hours of training per week for at least five years performing sports with high dynamic and static components (31.8 ± 6.1 years, 22 male, 18.6 ± 2.2 training h/week) served as a control group of the sedentary ARVC patient group.

Ethical approval was obtained from the Central Ethics Committee of Hungary (5012-0/2011-EKU (142/PI/11)). Informed consent was obtained from all individual participants included in the study.

3.1.2 Study design and study population of Electroanatomic and tissue characterization project

This retrospective study was conducted in the Heart Center University of Leipzig. DCM patients (n=50, 58±15y, 39 male) who underwent RFCA of sustained VT or ventricular premature beats (VPB) and CMR scan (<30 days prior the ablation) were enrolled. The inclusion of the patients was based on the morphological appearance of a dilated LV and reduced ejection fraction using separate LVEDVi and LVEF criteria for men and women (131). Patients with significant coronary artery disease were excluded, and in case of VPB only patients without improvement of the LVEF after ablation were included. The CMR and EAM data were analysed by two blinded investigators, a third investigator was responsible for the spatial alignment of the EAM and CMR. An interrogation of the implantable cardioverter-defibrillator (ICD) devices and Holter ECGs were used to follow-up.

3.1.3 Study design and study population of Reverse remodelling project

This prospective study was conducted in the Semmelweis University Heart and Vascular Center. Patients (n=13, 64±7y, five male) with CRT indication according to

the current guidelines (symptomatic heart failure, LVEF ≤35%, New York Heart Association functional class II-III on optimal medical therapy for at least 3 months), complete LBBB and broad QRS (>150 ms) were prospectively recruited. All patients were in sinus rhythm and normal atrioventricular conduction. Exclusion criteria were any contraindications of CMR examination or CRT implantation. Patients meeting all inclusion criteria and with no exclusion criteria underwent the implantation of a commercially available MRI conditional CRT-P (n=5) or CRT-D (n=8) device. Baseline CMR scan with contrast material was performed 1-14 days before CRT implantation, and follow-up non-contrast CMR scan was performed at six months ± 14 days after CRT implantation during biventricular pacing (DOO) and right atrial pacing (AOO). Changes of device parameters (e.g., impedance, thresholds, sensing and battery voltage) were recorded pre- and post CMR scan. ProBNP was measured and a 12-lead ECG was perormed at baseline and follow-up. CRT response was defined as the followings: 1) super-response: decrease in LVESVi >30%, 2) response: decrease in LVESVi >15%, 3) non-response: decrease in LVESVi <15%.

All patients provided written informed consent prior to enrolment. Approval was obtained from the local ethics committee (034309-006/2014/OTIG).

3.2 Image acquisition and analysis

3.2.1 Differentiation of pathological and physiological remodelling project

CMR imaging

CMR examinations were conducted on a 1.5 T MR scanner (Achieva, Philips Medical Systems, Best, The Netherlands) with a 5-channel cardiac coil. For the assessment of cardiac dimensions and functions, retrospectively-gated, balanced steady-state free precession (bSSFP) segmented cine images were acquired in 2-chamber, 4-chamber and LV and RV outflow tract views. Short-axis images with full coverage of the left and right ventricle were obtained. Late gadolinium enhancement (LGE) imaging was performed. During an inspiratory breath-hold, a bolus of gadobutrol (0.15 mmol/kg)

DOI:10.14753/SE.2020.2408

was injected at a rate of 2–3 ml/s through antecubital intravenous line. Contrast-enhanced images were acquired using a segmented inversion recovery sequence with additional phase sensitive reconstructions in the same views used for cine images 10–20 min after contrast administration.

Images were evaluated with Medis QMass 7.6 quantification software (Medis Medical Imaging Software, Leiden, The Netherlands). Endocardial and epicardial contour detection was performed by a blinded expert observer manually on short axis cine images. Quantification of the left ventricular ejection fraction (LVEF), volumes (LVESV, LVEDV, LVSV) and myocardial mass (LVM) were performed using conventional quantification method (CQ) (Medis QMass 7.6). Left ventricular volumes and masses were standardized to body surface area (BSA).

In nonathletic and athletic HCM patients and in a subgroup of athletes a threshold-based quantification method (TQ) (Medis QMass 7.6 MassK algorithm) was also performed **(Figure 13).** Using TQ the trabeculae and papillary muscles (TPM) were also quantified, the semi-automatic threshold-based algorithm allows us to estimate the spatially varying signal intensities of blood and muscle within an observer-provided epicardial contour. Voxels with signal intensities above the specified threshold are considered to be blood, voxels with signal intensities below the threshold are considered to be myocardium.

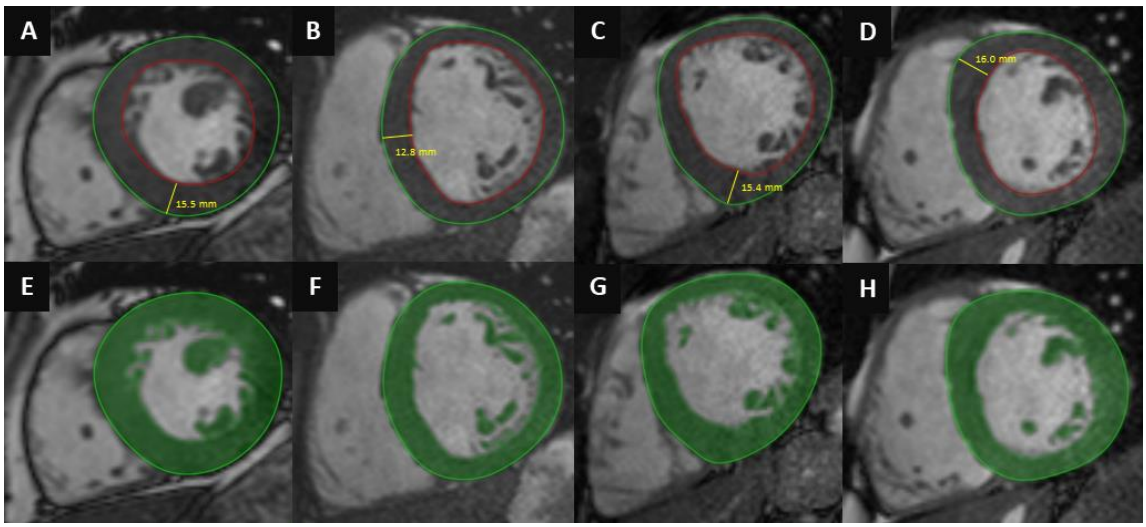

Figure 13: Conventional quantification (A,B,C,D) and threshold-based quantification method (E,F,G,H) in HCM (A,E), healthy athlete (B,F), healthy athlete with EDWT in the grey zone of hypertrophy (C,G) and athlete with HCM (D,H).

Maximal end-diastolic wall thickness (EDWT) measurements were performed in a short axis slice perpendicularly to the myocardial center line excluding right ventricular trabeculation. Minimal EDWT was measured in the same slice as the maximal EDWT. To further characterize the left ventricular hypertrophy and geometry, sport indices were derived using both conventional and threshold-based quantification method, such as left ventricular maximal diastolic wall thickness to end-diastolic volume index ratio (EDWT(mm)/LVEDVi(ml/m^2)) and left ventricular mass to end-diastolic volume ratio (LVM(g)/LVEDV(ml)). Using threshold-based quantification TPM% ((TPM(g)/LVM(g) *100) was also established.

In nonathletic and athletic ARVC patients and in a subgroup of healthy athletes additionally quantification of right ventricular ejection fraction (RVEF), volumes (RVESV, RVEDV, RVSV) and myocardial mass (RVM) were performed using conventional quantification method. Regional right ventricular akinesis, dyskinesis, dyssynchrony were qualitatively assessed. Global LV and RV strain analysis was performed based on cine images after manual contouring of the endocardial borders. Additionally, regional strain analysis for the right ventricular free wall was performed based on RV endocardial contours on 4CH-view, peak systolic longitudinal strain and strain rate values of the basal, midventricular and apical free wall were established **(Figure 14)**. Average and minimal values of the measured regional strain and strain rate values were also determined. Medical history, family history and 12-lead ECG were also obtained.

DOI:10.14753/SE.2020.2408

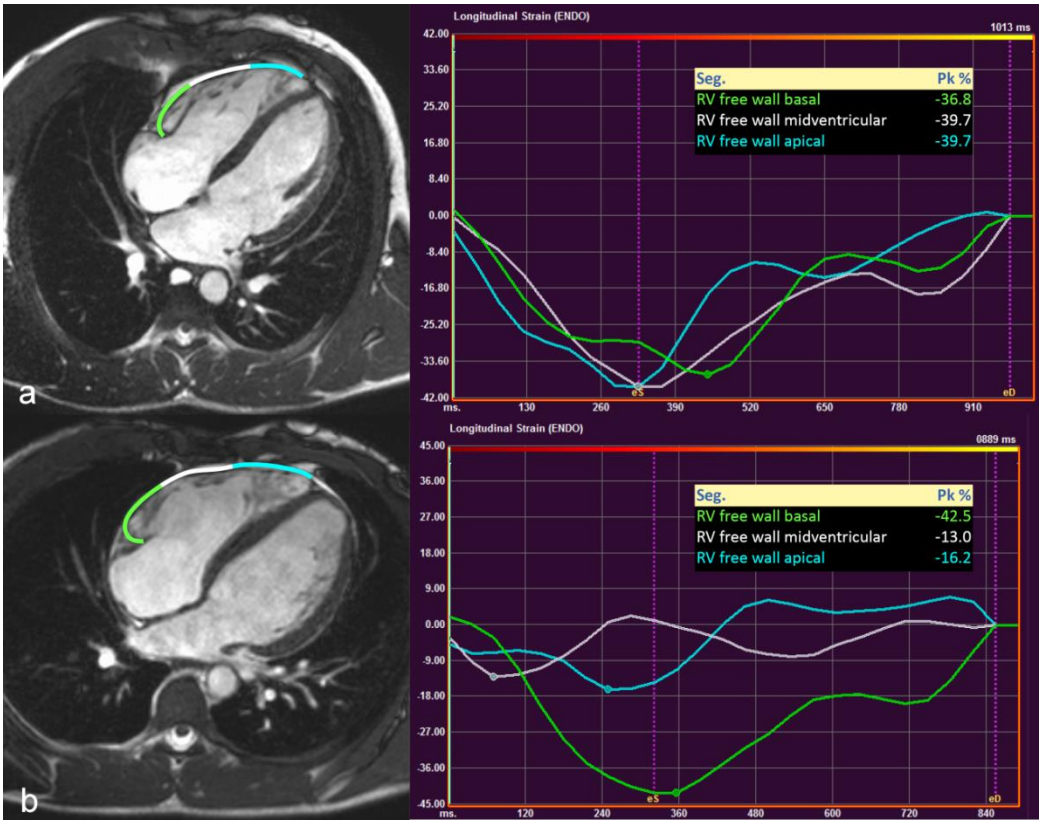

Figure 14. Regional free RV wall strain analysis of a healthy athlete (a) and a highly trained athlete with ARVC (b). Strain curves of the athlete with ARVC represent regional RV dyssynchrony and decreased longitudinal strain of the midventricular (white) and apical (blue) RV free wall. Segments of the RV free wall and regional strain values of these segments are presented with same colour. RV, right ventricular.

3.2.2 Electroanatomic and tissue characterization project

CMR imaging

CMR examinations were conducted on a 1.5 T MR scanner (Philips Ingenia, The Netherlands). Balanced steady-state free precession (bSSFP) segmented cine images were acquired as described before. Three-dimensional, high-resolution LGE-CMR imaging was performed more than 10 min after the application of intravenous contrast (gadolinium- DTPA, 0.2 mmol/kg). Two different protocols were used for patients with and without devices. For patients without devices, we performed a high-resolution,

three-dimensional LGE imaging: free breathing, navigator-gated image data acquisition, the measured in-plane spatial resolution was 1.4x1.4x4.0 mm which was reconstructed to 0.7x0.7x2.0 mm. For device patients, we used multi-slice two-dimensional LGE employing the wideband technique with a bandwidth of the pre-pulse of 3000 Hz and a frequency offset of +1000 Hz during breath holding. The scans were performed in single breath hold with a measured spatial resolution of 1.7x1.7x10 mm, and reconstructed to 1.3x1.3x10 mm. Image analysis was performed using IntelliSpace Portal 6, Philips Healthcare. LVEF, LVEDVi, LVESVi, LVSVi, and LVMi were evaluated based on short-axis images after manual contouring as described before. Images were evaluated qualitatively by an observer blinded to the electroanatomical map for the presence or absence, pattern (subendocardial, mid-myocardial, subepicardial, transmural) and regional distribution of LGE areas using standardized myocardial 17-segment model. Extent of the LGE and its volume were established, LGE positive areas were quantified by thresholding signal intensity using the full-width half maximum (FWHM) method that defines the enhanced area by using 50% of the maximum signal found within the enhanced area.

Electro-anatomical mapping and electro-anatomical map adjustment

Endo- and epicardial cardial detailed maps of the left ventricle were obtained during sinus rhythm or ventricular pacing using CARTO system (Biosense Webster Inc., Diamond Bar, CA) with a 3.5-mm open irrigated-tip catheter (Navistar Thermocool, Biosense Webster Inc.). Bipolar (bandpass filtered at 30 to 500 Hz) electrograms were recorded and displayed at 200 mm/s sweep speed. A detailed assessment of individual electrogram characteristics was made off-line. The perivalvular areas were excluded. The bipolar low-voltage areas were defined by the accepted thresholds for patients with ischaemic cardiomyopathy: 0.5–1.5 mV, dense scar area was defined as <0.5 mV. The distribution of the low-voltage areas was described based on the AHA (American Heart Association) 17-segment model **(Figure 15)**.

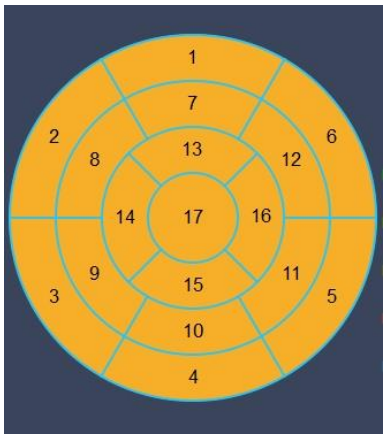

1. basal anterior
2. basal anteroseptal
3. basal inferoseptal
4. basal inferior
5. basal inferolateral
6. basal anterolateral
7. mid anterior
8. mid anteroseptal
9. mid inferoseptal
10. mid inferior
11. mid inferolateral
12. mid anterolateral
13. apical anterior
14. apical septal
15. apical inferior
16. apical lateral
17. apical

Figure 15: AHA 17-segment model of the left ventricule. Circumferential polar plot of the 17 myocardial segments and the nomenclature. AHA, American Heart Association.

The exits of the VTs were defined as sites showing the best best pace-mapping sites matching scores (based on 10 surface ECG channels) and S-QRS interval less than 80ms during pacing. First, we matched the CMR images with the EAM low-voltage areas defined using the standard bipolar threshold of 1.5mV. In terms of anatomical and electrical concordance, good agreement was defined if both EAM (<1.5mV) and CMR overlapped in all segments. Partially good agreement was defined as an overlap between LGE and EAM (<1.5mV) in at least one corresponding segment or in anatomically adjacent segments. As a second step, if no agreement between LGE and EAM was observed, a manual adjustment of the EAM cut-off limits was performed to match with LGE areas. Particular attention was paid on the abnormal potentials and the ablation lines to make sure that they fall within the borders of the newly defined low-voltage areas. Finally, the surface areas of the redefined low-voltage areas were measured and the maximal surface area on the endocardial or the epicardial surface was compared with the amount of the LGE mass and its distribution. The endpoint of acute success after ablation was non-inducibility of any sustained monomorphic VT with programmed ventricular stimulation with up to three extra beats down to the effective refractory period or 200 ms. For patients with VPB, successful catheter ablation was defined as complete elimination of VPB.

DOI:10.14753/SE.2020.2408

3.2.3 Reverse remodelling project

CMR imaging

CMR examinations were conducted on a 1.5 T MR scanner (Achieva, Philips Medical Systems, Best, The Netherlands) with a 5-channel cardiac coil. For the assessment of cardiac dimensions and functions, at baseline retrospectively-gated, balanced steady-state free precession (bSSFP) segmented cine images were acquired in 2-chamber, 4-chamber and LV outflow tract views. Short-axis images with full coverage of the left and right ventricle were obtained. At follow-up spoiled gradient echo (SGE) imaging was performed when the first acquired bSSFP cine images were found to be of suboptimal image quality. Additionally, high temporal resolution cine images with a temporal resolution of 50 phases per cardiac cycle were also acquired in 2-chamber, 4-chamber and LV outflow tract views and in three short-axis slices (basal, mid, apical) at baseline and follow-up. At the follow-up scan whole body specific absorption rate (SAR) was restricted according to the prescription of the implanted devices. At baseline, late gadolinium enhancement (LGE) imaging was performed as described in the first project. A CMR expert trained in cardiac life support and a physiologist with cardiac device expertise were present during the follow-up CMR examination. Cardiac rhythm, blood pressure and pulse oximetry were monitored from the time of device programming until reprogramming of baseline values using Invivo Precess 3160, Philips Medical Systems, Best, The Netherlands.

Image analysis was performed using Medis Suite 3.0 software (Medis Medical Imaging Systems, Leiden, The Netherlands). Assessment of cardiac dimensions and functions were performed on short-axis cine image as described earlier. Additionally, remodelling parameters, such as 2D sphericity index (end-diastolic SA/LA diameter), 3D sphericity index (ESV/(4/3x π*(end-diastolic LA diameter/2)3) and relative wall thickness were calculated (2xEDWT/end-diastolic LA diameter). Quantitative deformation assessment was performed based on the manually endocardially contoured cine images using dedicated feature tracking quantification software (Medis Suite 3.0 QStrain, Leiden, The Netherlands). Global longitudinal (GLS), circumferential (GCS) and radial (GRS) left ventricular strain parameters were measured. Global left ventricular dyssynchrony

was assessed by mechanical dispersion as the standard deviation of time to peak longitudinal (SD long TTP) and circumferential strain (SD circ TTP) in 16 LV segments. Regional left ventricular dyssynchrony was assessed by the maximum differences in time between peak septal and lateral transversal displacement based on regional strain analysis. Allowing comparisons between patients with different heart rates, regional LV dyssynchrony is expressed in ms adjusted to a standard cardiac cycle length of 1000 ms. The presence and localization of LGE was evaluated on baseline scans by an experienced reader.

Device interrogation and programming

Device interrogation was performed prior to CMR examination, in between different pacing modes and finally before patient discharge to record device parameters and verify system integrity. In order to achieve resynchronization therapy during image acquisition, the Medtronic devices were programmed manually according to Medtronic Field Technician's recommendations as these CRT devices are not able to perform biventricular pacing in MRI safe mode. DOO pacing was programmed with baseline paced atrioventricular delay (PAV), ventriculoventricular (V-V) delay and left ventricular pacing parameters. Right ventricular and right atrial pacing energy was programmed to high output (5.0 V/1.0 ms) and bipolar pacing while baseline left ventricular pacing was not modified to avoid phrenic nerve stimulation. Tachyarrhythmia detection and therapy was suspended in defibrillators and baseline pacing rate was programmed to 10 beats per minute above the patient's intrinsic sinus rate. SureScan mode OFF, the Medtronic Solara CRT-P device switches to magnet mode in the magnetic field. In magnet operation and pre-RRT battery status the device changes to asynchronous pacing with the programmed baseline ventricular pacing configuration and 85/min base rate. In order to obtain resynchronization, Solara CRT-P devices were programmed to 85/min DOO mode without any changes to the pacing intervals before CMR examination. Atrial pacing was performed by SureScan mode (AOO), and base rate was the same as in the DOO pacing configuration in both groups. Biotronik Intica 7 HF-T device was implanted in one patient. In this special case, MRI safe mode was able to maintain resynchronization during CMR imaging,

DOO MRI safe mode was programmed to obtain biventricular pacing (70/min base rate, 100 ms PAV, simultaneous V-V pacing). As MRI safe mode does not include AOO pacing as an option, pacing off option was used to mimic AOO mode.

3.3 Statistical analysis

3.3.1 Statistical analyses (Differentiation of pathological and physiological remodelling project)

All continuous variables are expressed as mean ± standard deviation, categorical variables are expressed as percentages. When comparing HCM patients and athletes, between-groups comparisons of CMR parameters and sport indices were based on least-squares linear regression if normality assumptions were satisfied and median regression otherwise. Models were stratified by HCM when comparing males versus females, and stratified for sex when comparing HCM patients versus athletes (i.e., practically, pairwise comparisons were made). Adjustment for age and heart frequency was applied by including these terms in the models as explanatory variables. When comparing ARVC patients and athletes, between-group comparisons were performed with the unpaired Student's t test or Mann–Whitney U-test where appropriate. For area under the curve (AUC), a value of 0.9–1.0 was considered excellent, 0.75–0.9 good, 0.6–0.75 moderate and 0.5–0.6 poor. Diagnostic accuracy of CMR parameters was evaluated using receiver operating characteristic (ROC) curve analysis. Cut-off values were set to maximize the proportion of subjects correctly classified. P-values <0.05 were considered to indicate statistical significance. Statistical analysis was performed using MedCalc software (version 17.9 Ostend, Belgium).

3.3.2 Statistical analyses (Electro-anatomic and tissue characterization project)

The data structure has been tested with Shapiro–Wilk test for normal distribution. Continuous variables with normal distribution are reported as mean ± standard deviation, whereas categorical variables are reported as absolute numbers and proportions. Dependent on its structure, groups were compared with test Student's t-test or Mann–Whitney U-test. Bivariate correlation analysis was performed using the correlation coefficient of Spearman. A double-sided $p \leq 0.05$ was considered statistically significant. Statistical analysis was performed using the software SPSS 20.0 (IBM, Armonk, NY, USA).

3.3.3 Statistical analyses (Reverse remodelling project)

Continuous variables were reported as mean and standard deviation, and categorical variables as frequency and percentages. Between–group comparisons were performed using paired Student's t-test or Wilcoxon test where appropriate. Pearson correlation coefficient was used to measure of the strength of the association between LV dyssynchrony and remodelling parameters. A p-value of ≤ 0.05 was considered statistically significant. Statistical analysis was performed using MedCalc software (version 17.9 Ostend, Belgium).

DOI:10.14753/SE.2020.2408

4. Results

4.1 Results of the Differentiation of pathological and physiological remodelling project

4.1.1 HCM and athlete's heart

4.1.1.1 Baseline characteristics

HCM patients

Twenty-eight percent and 30% of our HCM patients had positive family history for sudden cardiac death or HCM, respectively. Twenty-seven percent of HCM patients reported syncope and 32% palpitation. Only 55% had positive Sokolow or Cornell index, 82% showed T-wave inversion. Seventy-five percent (n=143) of HCM patients demonstrated LGE, mainly in the hypertrophic segments (80%) localized to the septum and anterior wall, in the right ventricular insertion points (55%), or only mild enhancement in the hypertrophic segments (19%). In our study population LGE showed excellent positive predictive value ($PPV = \frac{143}{143+0} * 100 = 100\%$) but low negative predictive value ($NPV = \frac{108}{108+47} * 100 = 70\%$).

Healthy athletes

None of our healthy athletes had positive family history of sudden cardiac death or HCM, all of them were asymptomatic. Seventy percent of athletes showed J-point elevation, 27% Sokolow or Cornell index positivity. Three athletes had T-wave inversion in more than one contiguous leads, all of them in V1-V3 leads without signs of left ventricular hypertrophy. None of the athletes showed pathological Q wave or ST-depression, and none of them showed any LGE (n=108).

Athletes with HCM

Ten additional athletes (31±10y; nine male, 14.4±6.5 training hours/week, football (n=3), basketball (n=2), snowboard (n=1), pentathlon (n=1), kayak (n=1), water-polo (n=1), wrestling (n=1)) were examined with CMR during training or competition period

because of the suspicion of HCM, where the comprehensive investigation including resting ECG, ambulatory ECG monitoring, echocardiography, CMR, medical and family history confirmed the diagnosis. No secondary cause of left ventricular hypertrophy was observed, and following 3-months training cessation only blunted or no deconditioning effect was observed: LVMi and EDWT remained in the pathological range. EDWT measured by CMR was 17.7±2.7 mm, five of them showed EDWT between 13-16 mm (**Table 2)**.

Table 2: Left ventricular CMR parameters of athletes with HCM assessed using conventional (CQ) and threshold-based (TQ) quantification. EDWT, maximal end-diastolic wall thickness; Max/min EDWT, maximal to minimal end-diastolic wall thickness ratio; LV, left ventricular; EF, ejection fraction; ESVi, end-systolic volume index; EDVi, end-diastolic volume index; SVi, stroke volume index; Mi, mass index; EDWT/LVEDVi, maximal end-diastolic wall thickness to left ventricular end-diastolic volume index ratio; LVM/LVEDV, left ventricular mass to left ventricular end-diastolic volume ratio, TPM, trabeculae and papillary muscles; TPMi, trabeculae and papillary muscles corrected to BSA; TPM% trabeculae and papillary muscles expressed as the percentage of total LV myocardial mass

	Athletes with HCM (n=10) mean ± SD
EDWT (mm)	17.7±2.7
Max/min EDWT	2.28±0.52
Conventional quantification	
$LVEF_{CQ}$ (%)	63.3±4.2
$LVESVi_{CQ}$ (ml/m^2)	37.3±5.1
$LVEDVi_{CQ}$ (ml/m^2)	101.3±7.8
$LVSVi_{CQ}$ (ml/m^2)	64.1±6.5
$LVMi_{CQ}$ (g/m^2)	94.8±15.0
max $EDWT/LVEDVi_{CQ}$ ($mm \times m^2 \times ml$)	0.18±0.03
$LVM_{TQ}/LVEDV_{CQ}$ (g/ml)	0.94±0. 13
Threshold-based quantification	
EF_{TQ} (%)	72.3±4.6
$LVESVi_{TQ}$ (ml/m^2)	21.1±4.3
$LVEDVi_{TQ}$ (ml/m^2)	75.8±7.7
$LVSVi_{TQ}$ (ml/m^2)	54.7±6.1
$LVMi_{TQ}$ (g/m^2)	121.3±16.9
max $EDWT/LVEDVi_{TQ}$ ($mm \times m^2 \times ml$)	0.24±0.05
$LVM_{TQ}/LVEDV_{TQ}$ (g/ml)	1.62±0.28
TPM (g)	41.1±12.6
TPMi (g/m^2)	21.4±6.3
TPM % (%)	17.4±4.4

DOI:10.14753/SE.2020.2408

All of the athletes with HCM showed at least one pathological ECG finding according to the 2014 ESC Guidelines on diagnosis and management of hypertrophic cardiomyopathy (15). Eight patients had positive Sokolow or Cornell index and nine patients showed T wave inversion on 12-lead ECG. Only two patients showed diastolic dysfunction on echocardiography. Apical HCM morphology was confirmed in four patients. Only four patients showed LGE in the hypertrophic regions and/or in the right ventricular insertion points **(Figure 17)**.

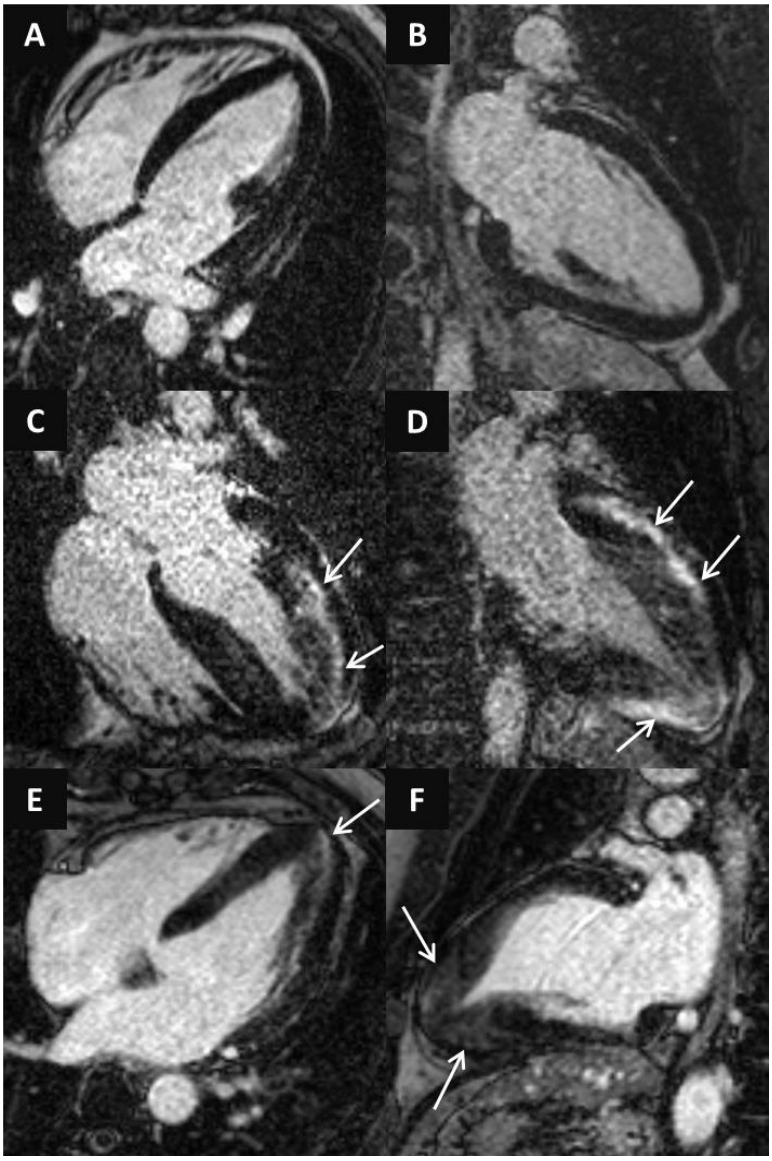

Figure 17: LGE images in 4-chamber (A,C,E) and 2-chamber views (B,D,F) of athletes with HCM. Concentric HCM with no LGE (A,B), asymmetric form with pronounced

midmyocardial patchy LGE (C,D) and apical HCM with mild LGE in the hypertrophic segments (D-F). White arrows show regions with high signal intensity representing late gadolinium enhancement. Heart and Vascular Center, Semmelweis University.

4.1.1.2 Comparison of left ventricular CMR parameters in healthy athletes and HCM patients evaluated using threshold-based and conventional quantification method

Both male and female HCM patients had higher EDWT compared to athletes (22.1 mm vs 12.6 mm; 19.7 vs 10.4, respectively), 14.8% of male HCM patients, 47.5% of male athletes, 19.8% of female HCM patients and 4.1% of female athletes were in the grey zone of borderline hypertrophy (EDWT 13-16 mm). Thirty-five percent of our male rowers, 52% of canoe and kayak paddlers and 54% of water-polo players showed EDWT between 13-16 mm.

Using conventional quantification sport indices EDWT/LVEDVi$_{CQ}$ and LVM$_{CQ}$/LVEDV$_{CQ}$ were significantly lower in athletes compared to HCM patients. Using threshold-based quantification method, LVMi$_{TQ}$ was lower in male athletes compared to HCM patients, TPM and TPM% were also lower in athletes than in HCM patients. Sport indices EDWT/LVEDVi$_{TQ}$ and LVM$_{TQ}$/LVEDV$_{TQ}$ were also lower in athletes compared to HCM patients**.** Compared to female athletes, male athletes showed significantly higher maximal EDWT, left ventricular volumes, mass and LVM/LVEDV using both conventional and threshold-based quantification method. TPMi was also higher and TPM% was lower in male athletes, and LVEF showed no significant difference between male and female athletes. **(Table 3)**

Table 3: Left ventricular CMR parameters in the four subgroups evaluated using conventional (CQ) and threshold-based (TQ) quantification. EDWT, maximal end-diastolic wall thickness; Max/min EDWT, maximal to minimal end-diastolic wall thickness ratio; LV, left ventricular; EF, ejection fraction; ESVi, end-systolic volume index; EDVi, end-diastolic volume index; SVi, stroke volume index; Mi, mass index; EDWT/LVEDVi, maximal end-diastolic wall thickness to left ventricular end-diastolic volume index ratio; LVM/LVEDV, left ventricular mass to left ventricular end-diastolic volume ratio evaluated using CQ and TQ.

*significantly different from male HCM, #significantly different from female HCM, ¥significantly different from female athletes.

	Male athlete (n=101) mean ± SD	**Male HCM (n=108)** mean ± SD	**Female athlete (n=49)** mean ± SD	**Female HCM (n=86)** mean ± SD
EDWT (mm)	12.6±1.3*¥	22.1±5.4#	10.4±1.2#	19.7±5.2
Max/min EDWT	1.93±0.30*¥	3.56±1.53	2.17±0.45#	3.86±1.63
Conventional quantification				
$LVEF_{CQ}$ (%)	57.4±4.36*	62.2±7.29#	58.4±4.51#	63.8±8.31
$LVESVi_{CQ}$ (ml/m^2)	52.6±9.60*¥	35.2±10.1#	44.7±7.72#	29.1±9.67
$LVEDVi_{CQ}$ (ml/m^2)	123±14.0*¥	91.6±16.7#	107±11.2#	79.9±13.8
$LVSVi_{CQ}$ (ml/m^2)	73.2±14.8*¥	57.5±11.1#	62.5±6.80	50.7±9.96
$LVMi_{CQ}$ (g/m^2)	90.3±14.7*¥	99.9±34.0#	65.9±10.7	76.9±22.9
Max $EDWT/LVEDVi_{CQ}$	0.10±0.02*	0.25±0.08	0.10±0.02#	0.25±0.07
$LVM_{CQ}/LVEDV_{CQ}$ (g/ml)	0.75±0.13*¥	1.08±0.30	0.62±0.10#	0.97±0.25
Threshold-based quantification				
$LVEF_{TQ}$ (%)	65.7±4.9*	71.9±9.0#	65.7±6.4#	74.4±8.6
$LVESVi_{TQ}$ (ml/m^2)	34.9±7.4*¥	18.6±6.5#	30.4±7.1#	14.5±6.3
$LVEDVi_{TQ}$ (ml/m^2)	101.0±12.1*¥	66.2±11.1#	89.3±10.1#	57.0±11.1
$LVSVi_{TQ}$ (ml/m^2)	66.3±7.6*¥	47.6±10.2#	58.8±7.1#	42.3±9.7
$LVMi_{TQ}$ (g/m^2)	113.0±16.8*¥	126.0±40.5#	84.3±12.1#	101.0±27.8
Max $EDWT/LVEDVi_{TQ}$	0.13±0.02*	0.34±0.10	0.12±0.02#	0.36±0.12
$LVM_{TQ}/LVEDV_{TQ}$ (g/ml)	1.13±0.16*¥	1.93±0.60	0.95±0.14#	1.83±0.56
TPM (g)	44.8±11.5*¥	55.6±17.5#	32.1±7.7	40.5±11.1
TPMi (g/m^2)	21.4±4.8*¥	27.4±8.6#	17.7±4.2	23.0±6.5
TPM% = $\frac{\text{TPM [g]}}{\text{LVM [g]}}$ x 100 (%)	19.0±3.7*¥	22.1±4.6	21.1±4.7	23.1±4.1

DOI:10.14753/SE.2020.2408

4.1.1.3 Diagnostic accuracy of sport indices to differentiate HCM and athlete's heart

We compared the efficiency of CMR based sport indices in differentiation of athlete's heart from HCM evaluated using conventional and threshold-based methods. Although efficiency of EDWT/LVEDVi evaluated using TQ and CQ showed no significant difference, LVM/LVEDV evaluated using TQ performed significantly better than CQ in both males and females **(Figure 18)**. Both sport indices established using TQ performed significantly better than max/min EDWT ($p < 0.05$). Cut-off value for max/min EDWT>2.4 (AUC 0.900) discriminated with a sensitivity of 81.4% and a specificity of 86.7 %.

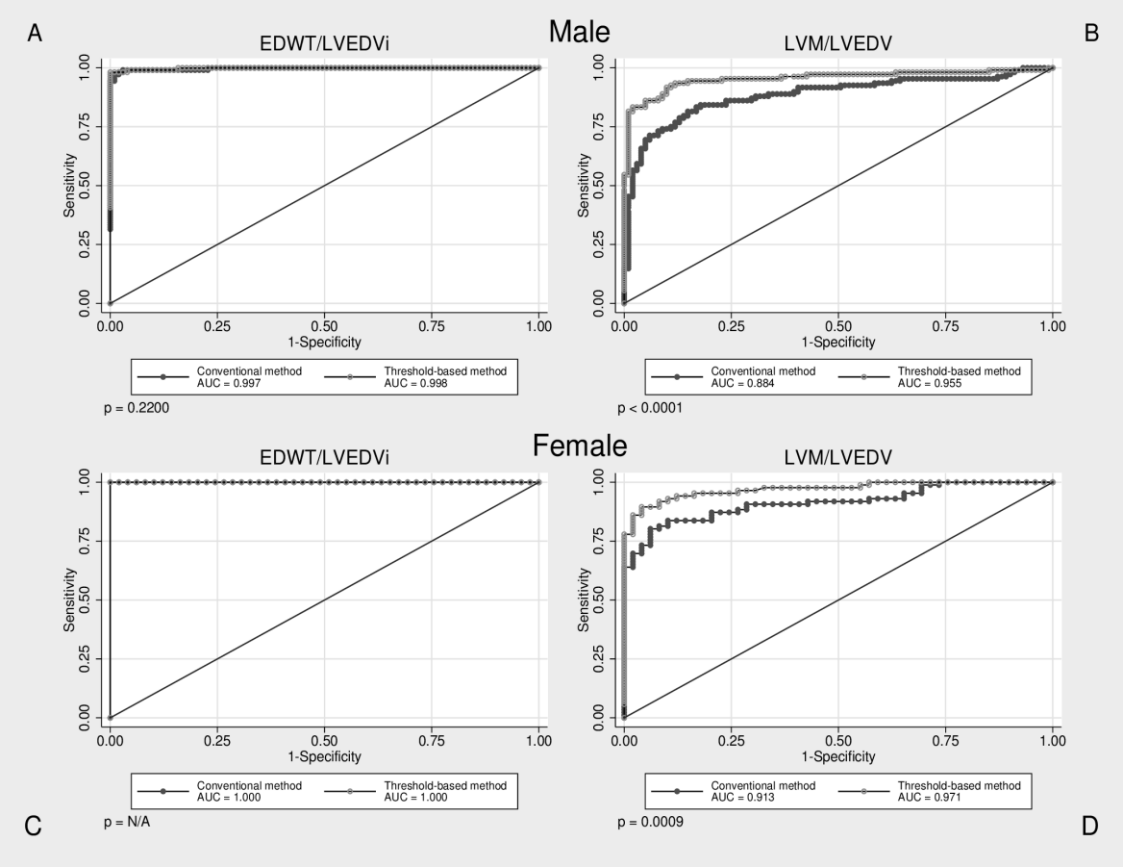

Figure 18: ROC curves visualizing correct identification of HCM among male and female subjects, p values represent the difference in diagnostic performance between conventional and threshold-based quantification methods. EDWT/LVEDVi, maximal

DOI:10.14753/SE.2020.2408

end-diastolic wall thickness to left ventricular end-diastolic volume index ratio; LVM/LVEDV, left ventricular mass to left ventricular end-diastolic volume ratio; AUC, area under the curve.

Sport indices showed also high diagnostic accuracy in the male subgroup with EDWT between 13-16 mm, LVM/LVEDV evaluated using TQ performed significantly better than CQ **(Figure 19).**

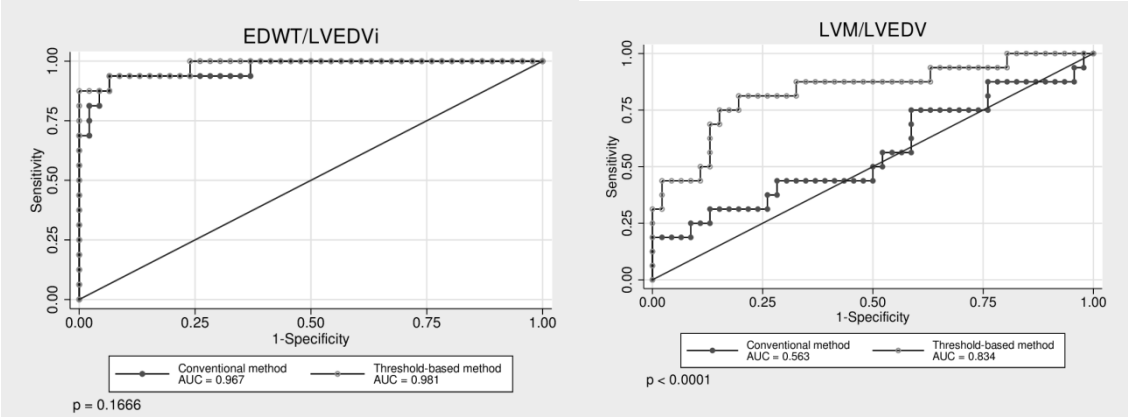

Figure 19: ROC curves visualizing correct identification of HCM among subgroup of individuals with EDWT between 13–16 mm, p values represent the difference in diagnostic performance between conventional and threshold based quantification methods. EDWT/LVEDVi, maximal end-diastolic wall thickness to left ventricular end-diastolic volume index ratio; LVM/LVEDV, left ventricular mass to left ventricular end-diastolic volume ratio; AUC, area under the curve.

Cut-off value for ratio of EDWT/LVEDVi$_{CQ}$ less than 0.14 mm×m^2/ml and cut-off value for EDWT/LVEDVi$_{TQ}$ less than 0.17 discriminated between physiological and pathological LV hypertrophy with a sensitivity of 99.5% and 99.0%, a specificity of 98% and 99.3%, respectively. Cut-off value for ratio of LVM/LVEDV$_{CQ}$ less than 0.82 mm×m^2/ml and cut-off value for LVM/LVEDV$_{TQ}$ less than 1.27 discriminated between physiological and pathological LV hypertrophy with a sensitivity of 77.8% and 89.2%, a specificity of 86.7% and 91.3%, respectively **(Table 4).** Despite the apparent gender-specific differences in cardiovascular sport adaptation, our cut-off values regarding sport indices are applicable in both males and females.

DOI:10.14753/SE.2020.2408

Table 4: Cut-off values for optimised sensitivity and specificity. EDWT/LVEDVi, maximal end-diastolic wall thickness to left ventricular end-diastolic volume index ratio; LVM/LVEDV, left ventricular mass to left ventricular end-diastolic volume ratio evaluated using conventional (CQ) and threshold based quantification (TQ), AUC, area under curve, sens, sensitivity; spec, specificity; PPV, positive predictive value; NPV, negative predictive value.

	Cut-off value	**AUC**	**Sens**	**Spec**	**PPV**	**NPV**	**Correctly classified instances**
Conventional quantification							
$EDWT/LVEDVi_{CQ}$ ($mm \times m^2/ml$)	>0.14	0.998	99.5	98.0	95.5	99.3	99.4
$LVM_{CQ}/LVEDV_{CQ}$ (g/ml)	>0.82	0.873	77.84	86.7	88.3	75.1	93.6
Threshold-based quantification							
$EDWT/LVEDVi_{TQ}$ ($mm \times m^2/ml$)	>0.17	0.999	99.0	99.3	99.5	98.7	99.4
$LVM_{TQ}/LVEDV_{TQ}$ (g/ml)	>1.27	0.948	89.2	91.3	93.0	86.7	94.4

According to our cut-off values $EDWT/LVEDVi_{CQ}$, $EDWT/LVEDVi_{TQ}$, $LVM_{CQ}/LVEDVi_{CQ}$ and $LVM_{TQ}/LVEDVi_{TQ}$ were in the pathological range in nine, nine, eight and 10 athletes with HCM, respectively **(Figure 20)**.

DOI:10.14753/SE.2020.2408

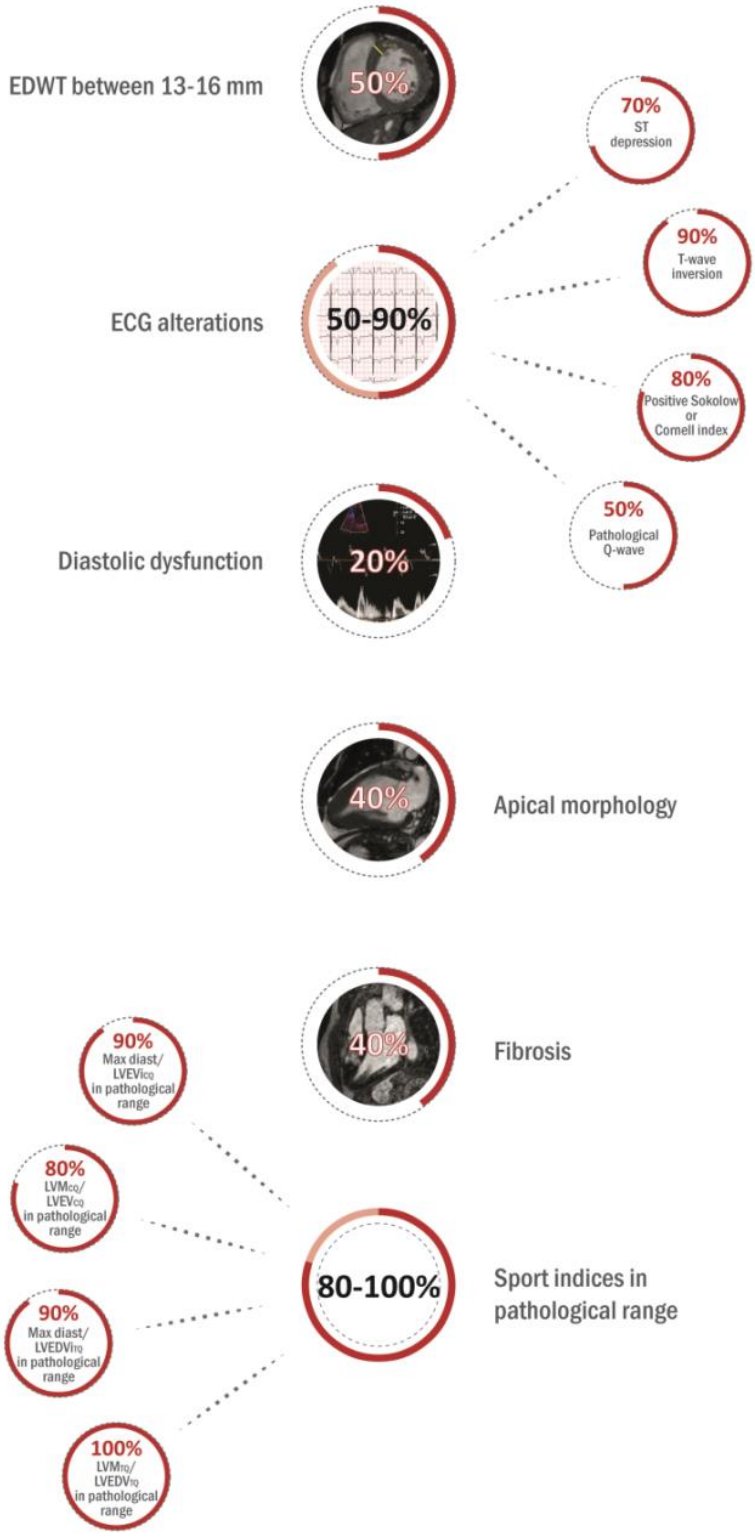

Figure 20: Clinical characteristics of athletes with HCM including pathological ECG findings, diastolic dysfunction evaluated using echocardiography and EDWT, morphology, fibrosis and sport indices evaluated using CMR.

DOI:10.14753/SE.2020.2408

4.1.2 ARVC and athlete's heart

4.1.2.1 Baseline characteristics

ARVC patients and healthy athletes

Thirty-four non-athlete ARVC patients were enrolled (40.5±13.4 years, 22 male). Diagnosis of ARVC was based on the current TFC. Positive family history for SCD or ARVC was present in 18% of the ARVC patients, 59% had recorded sustained ventricular tachycardia (VT) or ventricular fibrillation (VF), and aborted sudden cardiac death was reported in 12%. Average Task Force score (major = 2 points, minor = 1 point) was 4.9 points. Biventricular involvement was observed in 71%. LGE was present in 69%, in 14 patients only in the LV, in two patients only in the RV, and six patients demonstrated biventricular LGE **(Figure 16)**.

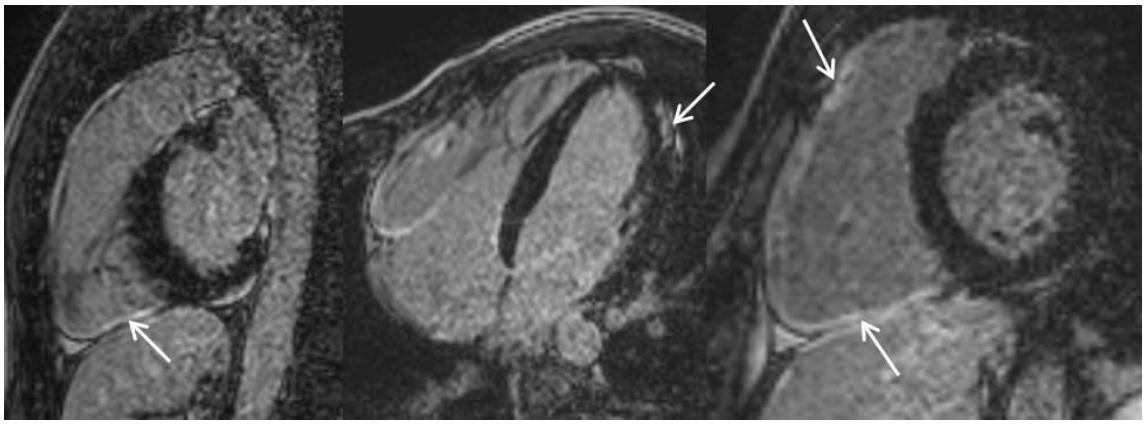

Figure 16: Biventricular LGE in ARVC presenting with biventricular involvement. White arrows show regions with high signal intensity representing late gadolinium enhancement. Heart and Vascular Center, Semmelweis University.

None of the healthy athletes had positive family history of sudden cardiac death or ARVC, all of them were asymptomatic. None of the healthy athletes had any ECG abnormality suggesting structural heart disease, none of them showed T-wave inversion in more than 1 continuous leads, Q wave inversion or ST-depression. 81% of athletes showed J-point elevation, 19% Sokolow or Cornell index positivity for left ventricular hypertrophy. None of them showed regional right ventricular wall motion abnormality

or late gadolinium enhancement (LGE). RVEDVi was in the proposed range of the major TFC (>110 ml/m^2 in males, >100 ml/m2 in females) in all healthy male athletes and 83.3% of healthy female athletes. RVEDVi of the remaining female athletes were in the proposed range of the minor TFC (>90 ml/m^2 in females). None of the athletes showed RVEF ≤45%, RVEF between 45 and 50% was observed in five cases (14.7%, three male and two female athletes).

Athletes with ARVC

In eight additional athletes (18.9±4.6 training h/week, triathletes n=3, cyclists n=2, swimmers n=2, football player n=1) the comprehensive investigation including resting ECG, ambulatory ECG monitoring, echocardiography, CMR and medical history confirmed the diagnosis. In three cases, CMR examination was repeated after training cessation for 2–3 months. Successful deconditioning effect was observed on LV values (LVEDVi: 127.4±5.4 ml/m^2 vs 109±10.6 ml/m^2; LVMi: 93.4±16.7 vs 73.5±9.4 g/m^2). However, only blunted deconditioning effect was observed on RV values, and RVEDVi remained in the pathological range (169.7±10.5 ml/m^2 vs 137.3±17.1 ml/m^2). Four athletes had documented sustained VT or VF, and aborted SCD was reported in two cases. None of them had positive family history for ARVC or SCD. Two athletes did not fulfil any repolarization or depolarization criteria, T-wave inversion (TWI) in lead V1–V2 and in V1–V3 leads was observed in one and four athletes, respectively. One patient had complete right bundle branch block. Epsilon wave was observed in 3 patients. Average Task Force score was 5.4 points. Biventricular involvement was confirmed in three patients (defined by left ventricular LGE and/or LVEF <50). Three patients showed LGE: two of them biventricular and one solely left ventricular LGE. All athletes with definite diagnosis of ARVC were disqualified from competitive sport.

DOI:10.14753/SE.2020.2408

4.1.2.2 Comparison of CMR parameters between healthy athletes and ARVC patients

Healthy athletes showed higher LVEDVi, LVSVi, LVMi, RVSVi and RVMi than non-athlete ARVC patients. No significant difference was found between athletes and non-athlete ARVC patients regarding the RVEDVi. Both RVEF and LVEF were significantly lower in ARVC patients compared to healthy athletes **(Table 5)**.

Table 5: Baseline characteristics and conventional left and right ventricular CMR parameters in healthy athletes, ARVC patients and athletes with ARVC. Values are expressed in mean ± SD. BSA, body surface area; LV, left ventricular; RV, right ventricular; EF, ejection fraction; ESVi, end-systolic volume index; EDVi, end-diastolic volume index; SVi, stroke volume index; Mi, mass index.
*significant difference between sedentary ARVC patients and healthy athletes
$^{*}p < 0.05$; $^{**}p < 0.01$; $^{***}p < 0.001$

	Athletes (n=34) mean ± SD	**ARVC (n=34)** mean ± SD		**Athletes with ARVC (n=8)** mean ± SD
Age (ys)	31.8±7.7	40.5±16.3*		27.6±3.3
BSA (m^2)	1.94±0.19	1.88±0.21		1.86±0.13
Male (%)	65	65		87.5
Heart rate (bpm)	55.0±7.6	63.0±7.4***		58.5±8.8
LVEF (%)	57.6±4.7	52.0±11.2*		60.1±3.1
LVESVi (ml/m^2)	50.3±10.9	50.9±20.0		50.2±8.3
LVEDVi (ml/m^2)	117.8±17.3	107.2±22.5*		121.1±17.4
LVSVi (ml/m^2)	67.6±9.4	54.0±13.1***		72.6±10.9
LVMi (g/m^2)	82.9±16.1	58.2±12.8***		87.2±16.3
RVEF (%)	55.7±4.6	40.5±13.6***		47.5±3.8
RVESVi (ml/m^2)	55.6±11.9	88.3±45.1***		76.2±10.8
RVEDVi (ml/m^2)	123.6±17.0	142.7±47.5		146.1±25.7
RVSVi (ml/m^2)	68.6±9.1	52.7±17.5***		70.0±15.1
RVMi (g/m^2)	21.8±6.2	18.7±4.8		22.3±2.3

Right ventricular global longitudinal strain (RV GLS) was decreased in the ARVC group compared to athletes. Regional longitudinal strain and strain rates of the RV free wall are presented in **Table 6.** Right ventricular mid strain, RV mid strain rate, and average and minimal values of the measured regional strain and strain rate values showed significant difference between the two groups.

Table 6: Global and regional strain and strain rate values of healthy athletes, ARVC patients and athletes with ARVC. Values are expressed in mean ± SD. GLS, global longitudinal strain; GCS, global circumferential strain; GRS, global regional strain; LV left ventriular.

*significant difference between sedentary ARVC patients and healthy athletes; $^{*}p < 0.05$; $^{**}p < 0.01$; $^{***}p < 0.001$

	Athletes (n=34) mean ± SD	**ARVC (n=34)** mean ± SD		**Athletes with ARVC (n=8)** mean ± SD
Global left and right ventricular strain				
LV GLS	-22.0±3.4	-20.4±5.0		-24.9±1.4
LV GCS	-30.5±6.0	-26.3±.8*		-35.6±5.7
LV GRS	57.6±14.5	49.8±49.9		71.4±11.2
RV GLS	-25.6±3.9	-20.4±7.6**		-21.3±3.9
Regional longitudinal strain and strain rate values of the RV free wall				
RV basal strain	-34.5±8.6	-30.9±11.8		-35.6±8.3
RV mid strain	-31.5±10.2	-20.0±13.4***		-21.5±4.9
RV apical strain	-30.9±8.0	-24.6±11.6**		-19.7±11.1
RV average strain	-32.3±5.0	-25.1±9.3**		-25.6±3.0
RV min strain	-24.0±7.2	-15.2±9.0***		-15.4±7.1
RV basal strain rate	-1.74±0.59	-1.52±0.97*		-1.61±0.63
RV mid strain rate	-1.37±0.56	-1.04±0.68**		-1.05±0.22
RV apical strain rate	-1.33±0.40	-1.17±0.56		-0.96±0.34
RV average strain rate	-1.48±0.38	-1.24±0.59 *		-1.21±0.28
RV min strain rate	-1.09±0.31	-0.79±0.32**		-0.80±0.24

DOI:10.14753/SE.2020.2408

4.1.2.3 Diagnostic accuracy of CMR parameters and feature tracking based deformation imaging to differentiate ARVC and athlete's heart

Establishing AUC values for the CMR parameters RVEF showed good accuracy (AUC =0.830), whereas RVEDVi failed as a discriminator between ARVC and athlete's heart (AUC =0.599). Cut-off value for RVEF ≤45.8 discriminates between ARVC and athlete's heart with a sensitivity of 68% and a specificity of 100%. RV mid strain, average and minimum of the measured regional strain values demonstrated good discrimination between athlete's heart and ARVC. We investigated whether establishing gender-specific cut-off values may influence the diagnostic accuracy, but comparing male and female ROC curves for CMR parameters with the highest diagnostic accuracy (RVEF, RV mid strain, RV average strain, RV min strain) showed no significant difference. These results suggest that gender-specific differences regarding these parameters are negligible, so we present cut-off values for both males and females. Cut-off values for global and regional strain values are presented in **Table 7.**

Table 7: Area under the ROC curves and cut-off values. Parameters showing good diagnostic accuracy appears in bold. EF, ejection fraction; EDVi, end-diastolic volume index; GLS, global longitudinal strain; GCS, global circumferential strain; GRS, global regional strain; LV, left ventricular; RV, right ventricular.

DOI:10.14753/SE.2020.2408

	Cut-off value	AUC	Sensitivity	Specificity	p
CMR Task Force criteria					
RVEF	≤45.8	**0.830**	67.65	100.00	0.0001
RVEDVi	>150.8	0.599	29.41	94.12	NS
Global left and right ventricular strain values					
LV GLS	>-17.7	0.596	32.35	94.12	NS
LV GCS	>-22.5	0.643	38.24	100.00	0.0386
LV GRS	≤41.8	0.607	41.18	94.12	NS
RV GLS	>-20.1	0.726	50.00	97.06	0.0004
Regional strain values of the RV free wall					
RV basal strain	<-35.8	0.634	70.59	58.82	NS
RV mid strain	>-25.6	**0.767**	70.59	82.35	0.0001
RV apical strain	>-23.9	0.694	55.88	85.29	0.0042
RV average strain	>-29.4	**0.772**	73.53	76.47	0.0001
RV min strain	>-18.1	**0.786**	70.59	85.29	0.0001
RV basal strain rate	>-1.3	0.665	58.82	85.29	0.0195
RV mid strain rate	>-1,4	0.686	82.35	50.00	0.0045
RV apical strain rate	>-0.9	0.606	38.24	91.18	NS
RV average strain rate	>-1.13	0.665	52.94	88.24	0.0175
RV min strain rate	>0.8	0.702	55.88	82.35	0.0014

We tested the established cut-off values for CMR parameters in the group of highly trained athletes with diagnosed ARVC. Applying these cut-off values, RVEF was in the pathological range in only three athletes with ARVC. Half of the athletes with ARVC showed normal RV GLS. Regional longitudinal strain and strain rate of the RV mid free wall were in the pathological range in all eight athletes with ARVC **(Figure 21)**.

DOI:10.14753/SE.2020.2408

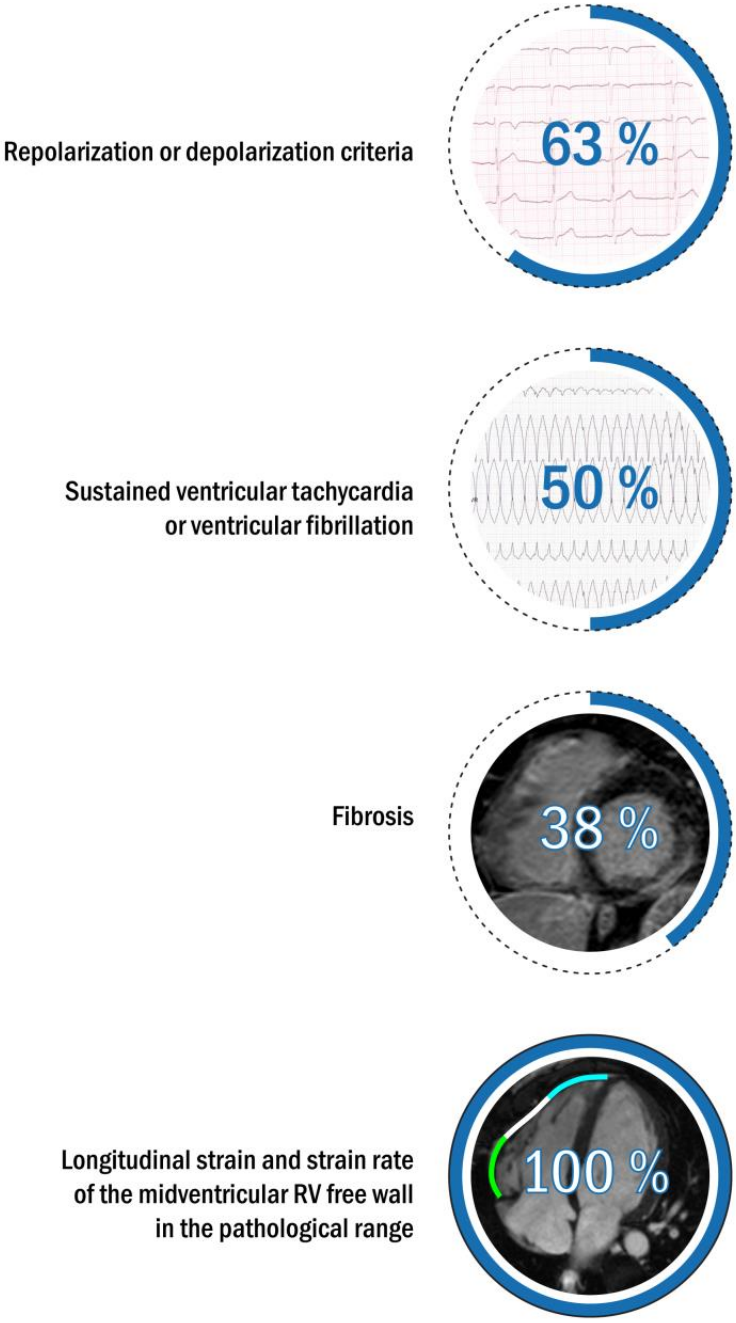

Figure 21: Clinical characteristics of athletes with ARVC including pathological ECG findings, arrhythmias and myocardial fibrosis. Midventricular RV longitudinal strain and strain rate were in the pathological range based on our cut-off values in all of the athletes with ARVC.

DOI:10.14753/SE.2020.2408

4.2 Results of the Electro-anatomic and tissue characterization project

4.2.1 Baseline characteristics

Out of 147 patients with a phenotype of DCM who received catheter ablation for VA, 50 suitable patients (age 58±15 y, 78% male) were identified. The mean LVEF was 35.5%±12% and the mean LVEDVi was 121± 43ml/m^2. Of them, 21 (44%) patients received RFCA for sustained VT, 22 (42%) for pleomorphic VPB and nsVT, and seven (14%) for VPB from the left ventricular outflow tract or aortic cusps. The median number of induced VTs (IQR) was two (1–3) VTs. Nine patients received at least 1 cardioversion during ablation. The median number of cardioversions during ablation was 1 (IQR 0–3). Eight patients received amiodarone before ablation which was continued thereafter. Mean fluoroscopy time was 24±16.6 min. No patients were lost to follow-up. The baseline clinical characteristics and CMR/EAM data are presented in **Table 8** and **Table 9**, respectively.

Table 8: Baseline characteristics. Values are expressed as mean ± SD, numbers and percentage. ACEI/ARB, angiotensin-converting-enzyme inhibitor/angiotensin receptor blockers; CMR, cardiac magnetic resonance; ICD, implantable cardioverter-defibrillator; nsVT, non-sustained ventricular tachycardia; VPB, ventricular premature beat; VT, ventricular tachycardia.

Baseline characteristics	All n=50
Age (at CMR), y	58±15
Female, n (%)	11 (22)
Cause, n (%)	
Familiar	2 (4)
Valvular	1 (2)
Myocarditis	10 (20)
Sarcoidosis	1 (2)
Idiopathic	36 (72)
Arterial hypertension, n (%)	34 (68)
Diabetes mellitus, n (%)	12 (24)
Atrial fibrillation, n (%)	10 (20)
Therapy	
ACEI/ARB, n (%)	42 (84)

Statin, n (%)	12 (24)
Antiarrhythmic drugs, n (%)	
Flecainide	12 (24)
Sotalol	1 (2)
Amiodarone	11 (22)
Other	3 (6)
Betablockers, n (%)	38 (76)
ICD, n (%)	19 (38)
Electrical storm, n (%)	9 (18)
ICD shocks, n (%)	12 (24)
Indication for ablation, n (%)	
Sustained VT	21 (44)
VPB or nsVT	29(56)

Table 9: CMR and EAMs characteristics. Values are expressed as mean ± SD or median, inter-quartile range (Q1–Q3). BSA, body surface area; CMR, cardiac magnetic resonance; EAM, electroanatomical maps; EDV, end-diastolic volume; EF, ejection fraction; ESV, end-systolic volume; FWHM, full-width half maximum; IVS, interventricular septum; LGE, late gadolinium enhancement; LV, left ventricle; LVA, low-voltage area; LVM, left ventricular mass; PW, posterior wall.

Procedural Data	All n=50
CMR	
EF, %	36±11.9
IVS, mm	10±1.95
PW, mm	9±1.85
LVEDV, ml	251±92
LVEDVi, ml/m^2	121±43
LVESV, ml	173±90
LVESVi, ml/m^2	84±43
LGE Volume (%)	2.79±5.1
LGE Mass (FWHM), g	3.1±5.9
LVM, g	135±45
EAM	
Minimal bipolar amplitude endo, mV	0.31±0.18
Maximal bipolar amplitude endo, mV	12.4±4.7
Minimal bipolar amplitude epi, mV	0.2±0.16
Maximal bipolar amplitude epi, mV	11.2±5
Bipolar LVA surface endo (< 1.5 mV), cm^2	24.8±20.7
Largest LVA (endo or epic) (<1.5 mV), cm^2	16.5 (6.8 - 47)
Largest LVA (endo or epic) (<0.5 mV), cm^2	4.4 (0.2 - 16.4)

DOI:10.14753/SE.2020.2408

4.2.2 Characteristics and distribution of the late gadolinium enhancement and electroanatomical substrate

Late gadolinium enhancement was observed in 16 (32%) patients (LGE+). Epicardial LGE spreading to the mid-myocardial layers was observed in eight patients, only mid-myocardial LGE was observed in five patients, and endocardial to mid-myocardial LGE in three patients. LGE was detected in 12 out of 19 (63%) patients with ICDs vs four out of 31 (13%) patients without ICD, which was a significant difference ($p< 0.001$). Furthermore, LGE was observed in 15 (71.4%) patients with sustained monomorphic VT, in one (4.8%) patient with pleomorphic nsVT and in none of the patients with VPB originating from the LV summit ($p <0.0001$). The most frequently enhancing segments were the basal inferolateral, inferior and inferoseptal segments: 2, 3, 4, 5, as well as segment 9. Furthermore, in the LGE+ patients, the best pace mapping sites with clinical VT were found in the basal anterior and anterolateral segments: 1 and 6. In 23 patients with low-voltage areas <1.5mV, 16 patients had sustained monomorphic VTs and the other seven patients had only VPB or nsVT. The most frequently affected segments in these patients were the basal anterior and anteroseptal (1 and 2) as well as the inferoseptal segments (3 and 4) at the endocardial surface. On the epicardial surface, the most frequently involved segments were 1, 5, 6, and 8.

4.2.3 Agreement between late gadolinium enhancement and electroanatomical maps

Among the 50 patients, 23 (46%) patients with low-voltage areas (LVA) (<1.5mV) and 16 (32%) patients with LGE were identified. Presence of low-voltage areas without any evidence of LGE was observed in seven (14%) patients. In 27 (54%) patients neither LGE nor low-voltage areas in EAM were detected. In the 16 LGE+ patients, a good agreement between LGE and LVA (<1.5 mV) was observed in four (25%) patients, partially good agreement in nine (56%), and no agreement in three (12%) cases.

DOI:10.14753/SE.2020.2408

Regarding VT exit sites, the best pace-mapping sites were observed in segments with LGE in 12 out of 16 patients. In two patients, the best pace-mapping sites were located in anatomically adjacent LGE segments, and in two patients—in segments without evidence of LGE in CMR. The mean LGE (FWHM) mass was 10.6±6.2 g and the mean LGE as a percentage of the LV was 8.73%±5.4%. The largest low-voltage area (endo- or epicardially) with amplitude <1.5 mV had median (Q1–Q3) of 16.5 (6.8–47) cm^2, whereas the largest dense scar area (endo- or epicardially) <0.5 mV had median (Q1–Q3) of 4.4 (0.2–16.4) cm^2. There was no significant correlation between the LGE extent and size of the low-voltage areas (<1.5 mV) in EAM (Pearson correlation: p=0.351).

4.2.4 Electroanatomical map adjustment based on the late gadolinium enhancement

In 16 patients with LGE (LGE+), the bipolar thresholds of low-voltage areas were individually adjusted in an attempt to match the localization and the size of the LGE. The median for the new bipolar threshold (Q1–Q3) was 1.5 (1.5–2.75) mV and the mean (SD) was 1.97±0.92 mV. Using the revised EAM thresholds, the mean size of the adjusted bipolar low voltage was 35.4± 27.6 cm^2 **(Table 10)**. Finally, the redefined bipolar EAM threshold showed a significant positive correlation with the LGE volume % (Pearson r=0.559).

Table 10: Adapted EAM characteristics after adjustments according to the LGE. EAM, electroanatomical maps; LVA, low voltage area.

Adapted EAM charactersitics	LGE (+); n=16
Adjusted bipolar endo LVA size, (mean ± SD), cm^2	35.4±27.6
Adjsuted bipolar threshold, (mean ± SD), mV	1.97±0.92
Adjusted bipolar threshold, (median, Q1-Q3), mV	1.5 (1.5 – 2.75)

DOI:10.14753/SE.2020.2408

4.2.5 Ablation outcomes and predictors for success

Acute success was achieved in 12 out of 16 patients (75%). Recurrence of VT was observed in seven (44%) patients during one year of follow-up. In patients with VT recurrence, the LGE volume was significantly larger than in those without VT recurrence: 12%±5.76% vs 6.9%±3.4%; p =0.049. The VT exits were found in areas with LGE in five out of seven patients with VT recurrence and in seven out of nine patients without VT recurrence. There was no difference in the surface of the low-voltage areas between patients with recurrence and without **(Table 11)**.

Table 11: EAM and CMR characteristics of the patients with VT recurrences after ablation. CMR, cardiac magnetic resonance; EAM, electroanatomical maps; EDV, end-diastolic volume; EF, ejection fraction; ESV, end-systolic volume; FWHM, full-width half maximum; IVS, interventricular septum; LGE, late gadolinium-enhancement; LV, left ventricle; LVA, low-voltage area; LVM, left ventricular mass; PW, posterior wall; VT, ventricular tachycardia.

Procedural data	VT recurrence, n=7	VT free, n=9	P
CMR characteristics			
EF, %	35±12.6	36±11.3	0.839
IVS, mm	10.9±2.3	10.9±2.1	0.937
PW, mm	10±1.6	9.7±1.56	0.605
LVEDV, ml	217±95	258±123	0.485
LVEDVi, ml/m^2	108±45	123±57	0.574
LVESV, ml	146±88	173±103	0.581
LVESVi, ml/m^2	72±42	83±50	0.651
LGE Volume (%)	12±5.76	6.9±3.47	0.049
LGE Mass (FWHM), g	14.1±6.13	8.7±5.7	0.126
LVM, g	115±33	147±48	0.204
EAM characteristics			
Adapted bipol EAM, cm^2	28±19	41±33	0.369
Adapted bipol threshold,mV	2±0.95	1.94±0.95	0.91
VT exits in LGE segments	5	7	0.771

DOI:10.14753/SE.2020.2408

4.3 Results of the Reverse remodelling project

4.3.1 Baseline characteristics

A total of 13 patients (mean age 64±7 years, 38% male) were enrolled. CRT-D was implanted in 62%. Ten patients (77%) had non-ischaemic, one patient (8%) ischaemic and two patients (15%) had mixed aetiology based on the invasive coronary angiography and LGE pattern on CMR. Only one patient had prior acute myocardial infarction and PCI according to medical history.

One patient showed no LGE, one patient had solely subendocardial LGE proving previous myocardial infarction, the two patients with mixed aetiology showed both subendocardial and midmyocardial LGE. Nine patients showed non-ischaemic LGE pattern: five of them had septal mid wall stripe pattern suggesting DCM, three patients showed focal patchy midmyocardial LGE in the insertion points suggesting the role of pressure overload, and one patient had subepicardial LGE suggesting prior myocarditis.

4.3.2 Safety and image quality

The follow-up scanning time including both AOO and biventricular pacing was 46±6 minutes. During the CMR scan no supraventricular or ventricular arrhythmias were noted. Atrial fibrillation started ten minutes after the CMR scan in one patient. On the same day pharmacological cardioversion using amiodarone was successful. Patient notification for atrial fibrillation or atrial tachycardia detection was switched on and Medtronic CareLink remote monitoring was initiated. Follow-up interrogation one month later showed no atrial fibrillation episode. None of the patients showed generator failure, lead failure, loss of capture, or electrical reset. Pre- and post-MRI device interrogation yielded no significant changes (mean change of battery voltage 0.0±0.0 V; pacing threshold: atrial: 0.0±0.1 V, right and left ventricular lead: 0.0±0.0 V; change in pacing impedance: atrial: -21.2±23.9 Ω, RV: -0.4±17.3 Ω, LV lead: -29.2±32.6 Ω, and change in shock impedance in CRT-D patients: -0.4±2.3 Ω).

Left sided implantation was performed in all patients. Banding artefacts were present on bSSFP images in all patients with CRT-D (n=8). Therefore in CRT-D patients SGE cine

DOI:10.14753/SE.2020.2408

images were also acquired achieving significant improvement of image quality. Precise analysis of SGE images was limited due to device artefacts in only two patients (three and two LV segments). Due to suboptimal image quality two patients were excluded from regional dyssynchrony analysis and one from global dyssynchrony and strain analysis. Device artefacts are presented on **Figure 22.**

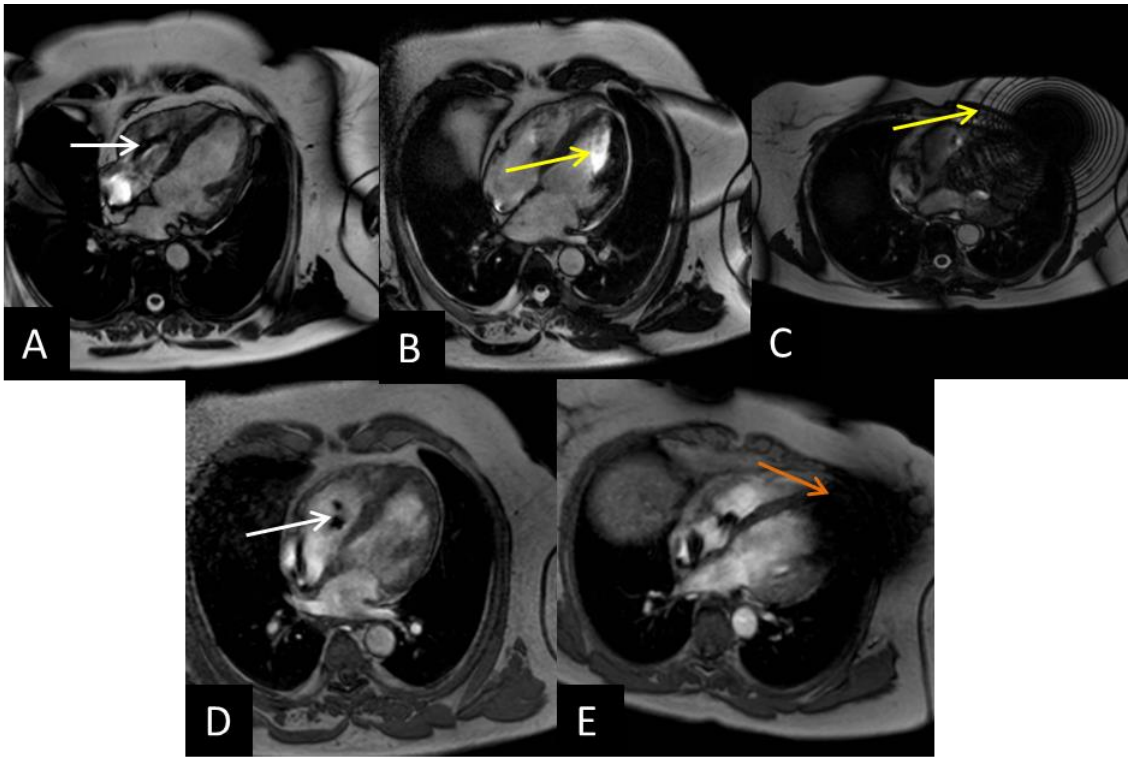

Figure 22: bSSFP (A-C) and SGE cine images (D,E) performed six months after CRT implantation. In case of CRT-P devices the generator related artefact on bSSFP images (yellow arrows) did not affect the heart, the lead related artefacts (white arrows) do not have any impact on the image analysis (A). In case of CRT-D devices generator related dark band off-resonance artefacts on bSSFP images are usually present (B,C). Therefore SGE images were obtained, which enables precise image analysis in majority of the cases (D), but two patients were excluded from the detailed analysis due to suboptimal image quality caused by generator related ferromagnetic susceptibility artefacts (orange arrows) (E). Heart and Vascular Center, Semmelweis University. bSSFP, balanced steady-state free precession; SGE, spoiled gradient echo.

DOI:10.14753/SE.2020.2408

4.3.3 Reverse remodelling (Baseline vs BIV pacing)

At 6-month follow-up two patients showed no symptomatic improvement (NYHA II), the conditions of 11 patients improved and were categorized in lower NYHA class **(Figure 23)**.

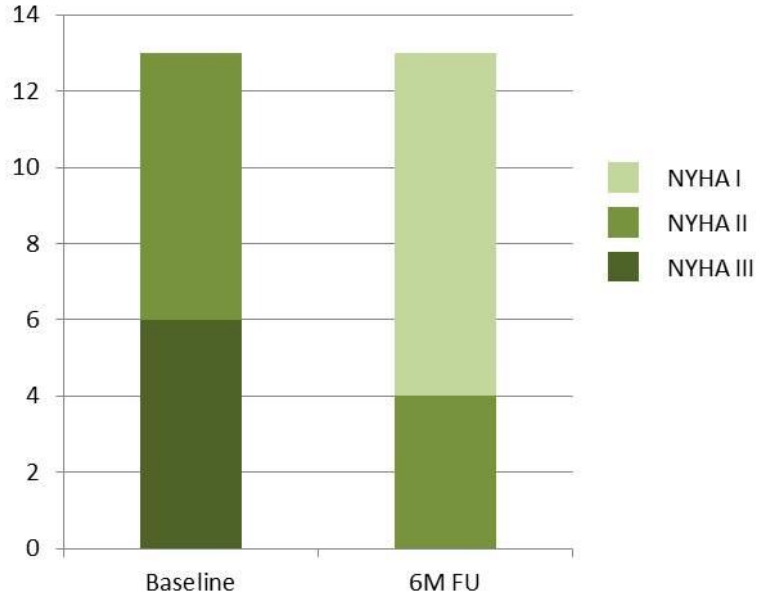

Figure 23: NYHA functional class at baseline and six months after CRT implantation. NYHA class improved in the vast majority of patients (85%) during the follow-up. NYHA, New York Heart Association Classification

ProBNP levels (1186±863 vs 323±271 pg/ml, $p<0.05$) and QRS width (165±9 vs 128±27, $p<0.01$) decreased. Based on the decrease of LVESVi, 11 patients were classified as super responders, one patient as responder and one did not reach the 15% LVESVi decrease (ΔLVESVi 9%).

Comparing baseline and follow-up CMR parameters measured during biventricular pacing significant differences were found; a marked increase in LVEF and a decrease in LVEDVi, LVESVi and RVEDVi was detected. Left ventricular remodelling parameters such as relative wall thickness, 2D and 3D sphericity indices showed a noticeable improvement **(Table 12)**.

Table 12: Characteristics and CMR parameters at baseline and at 6-month follow-up during biventricular pacing. HR, heart rate; BSA, body surface area; LV, left ventricular; EF, ejection fraction; EDVi, end-diastolic volume index; ESVi, end-systolic volume index; SVi, stroke volume index; COi, cardiac output index; HR, heart rate; Mi, mass index; RV, right ventricular; max EDWT, maximal end-diastolic wall thickness; 3D sphericity (ESV/(4/3x π∗(end-diastolic LA diameter/2)3); 2D sphericity (end-diastolic SA/LA diameter); RWT, relative wall thickness (2xEDWT/ end-diastolic LA diameter); GLS, global longitudinal strain; GCS, global circumferential strain; GRS, global radial strain, SD long TTP, mechanical dispersion as the standard deviation of time to peak longitudinal strain in 16 LV segments; SD circ TTP, mechanical dispersion as the standard deviation of time to peak circumferential strain in 16 LV segments; regional dyssynchrony, maximum differences in time between the peak septal and lateral transversal displacement.

	Baseline	**Follow-up BIV**	**p**
HR (bpm)	65±10	79±8	<0.001
BSA (m^2)	1.93±0.24	1.93±0.24	NS
QRS (ms)	165±9	128±27	<0.01
proBNP (pg/ml)	1186±863	323±271	<0.05
CMR parameters			
LVEF (%)	27.0±7.1	45.7±7.6	<0.001
LVEDVi (ml/m^2)	144.3±28.6	88.8±20.0	<0.001
LVESVi (ml/m^2)	104.1±31.2	49.0±15.5	<0.001
LVSVi (ml/m^2)	37.7±7.2	39.8±7.3	NS
LVCOi (ml/m^2)	2.4±0.5	3.1±0.7	<0.05
LVMi (g/m^2)	83.6±15.4	77.5±16.5	NS
RVEF (%)	62.2±5.4	62.0±4.1	NS
RVEDVi (ml/m^2)	64.4±12.2	58.2±10.7	<0.01
RVESVi (ml/m^2)	26.6±8.8	22.2±5.3	NS
RVSVi (ml/m^2)	39.6±7.0	36.0±6.4	NS
RVCOi (ml/m^2)	2.6±0.5	2.8±0.5	NS
RVMi (g/m^2)	15.0±2.3	12.2±2.9	NS
Remodelling parameters			
max EDWT (mm)	10.8±1.9	11.7±1.2	NS
3D sphericity	0.44±0.12	0.28±0.11	<0.01
2D sphericity	0.70±0.11	0.61±0.12	<0.001
RWT	0.33±0.08	0.45±0.09	<0.001

Quantitative deformation assessment			
GLS (%)	-13.4±4.7	-17.3±3.0	<0.05
GCS (%)	-10.8±4.5	-21.3±4.9	<0.001
GRS (%)	25.9±11.7	38.8±10.8	<0.01
SD long TTP (%)	17.6±2.9	15.8±4.1	NS
SD circ TTP (%)	20.5±5.5	13.4±3.4	<0.001
Regional dyssynchrony (ms)	362±96	104±66	<0.001

Global left ventricular longitudinal, circumferential and radial strain values also showed a significant improvement. The analysis of global dyssynchrony showed that circumferential mechanical dispersion decreased (20.5±5.5 vs 13.4±3.4, p <0.001), while the longitudinal mechanical dispersion did not show significant change. Comparing regional dyssynchrony (defined by the maximum difference in time to peak septal and lateral transversal displacement) at baseline and at follow-up during biventricular pacing, it improved significantly (362±96 vs 104±66 ms, p <0.001).

Decrease of regional dyssynchrony correlated with the decrease of LVESV (p <0.05, r =0.63) and with the increase of LVEF (p <0.05, r =0.66), and negative correlation between the decrease of regional dyssynchrony and RWT (p <0.05, r =-0.61) was found.

4.3.4 Switching off the biventricular pacing (BIV vs AOO pacing)

Analysing CMR parameters measured during biventricular pacing and with AOO pacing (BIV OFF), we found that after switching off the biventricular pacing LVEF (45.7±7.6 vs 37.9±7.4%, p <0.001) and LVSVi immediately decreased (39.8±7.3 vs 33.1±8.7 ml/m^2, p <0.001), and LVESVi immediately increased (49.0±15.5 vs 55.5±16.9 ml/m^2, p <0.001).

GCS deteriorated significantly (-21.3±4.9 vs -17.7±5.6, p <0.05). There was a deterioration in terms of GRS (38.8±10.8 vs 32.9±7.6, p =0.055), whereas GLS showed no remarkable change (-17.3±3.0 vs -15.9±3.5, p =0.118). Examining mechanical dispersion, SD circ TTP increased (13.4±3.4 vs 17.0±4.4, p <0.05), while SD long TTP did not change significantly (15.8±4.1 vs 16.8±5.2, p =0.559). Increased regional

dyssynchrony was detected after switching off biventricular pacing (98±66 vs 335±148 ms, p <0.001) **(Figure 24)**.

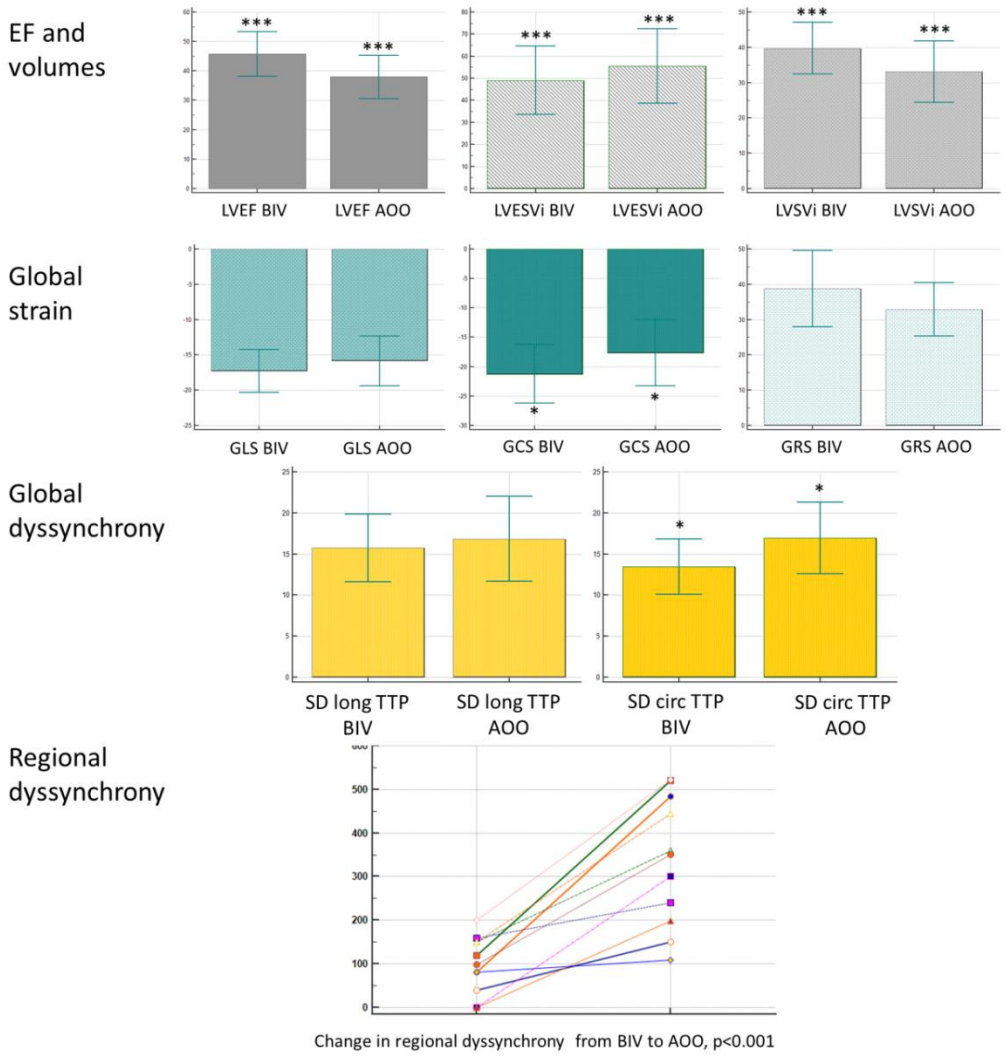

Figure 24: Comparison of CMR parameters at six months between biventricular and AOO pacing. LV, left ventricular; EF, ejection fraction (%); ESVi, end-systolic volume index (ml/m^2); SVi, stroke volume index (ml/m^2); GLS, global longitudinal strain (%); GCS, global circumferential strain(%); GRS, global radial strain(%), SD long TTP, mechanical dispersion as the SD of time to peak longitudinal strain in 16 LV segments (%); SD circ TTP, mechanical dispersion as the SD of time to peak circumferential strain in 16 LV segments (%); regional dyssynchrony, maximum differences in time between the peak septal and lateral transversal displacement (ms). Level of significance: * p <0.05, ** p <0.01, *** p <0.001.

DOI:10.14753/SE.2020.2408

5. Discussion

5.1 Physiological adaptation mimicking pathological remodelling – the role of CMR in the differential diagnosis

5.1.1 Overlapping features and differences between physiological and pathological remodelling

Regular and intensive physical training as well as cardiomyopathies trigger electrical, structural and functional cardiovascular changes. These alterations may cause difficulties in the differentiation of physiological and pathological remodelling.

Electrical alterations

J-point elevation is considered as the most common, benign, training related ECG finding (132); it was present in 70-81% in our healthy athletes. In our healthy athletic cohorts isolated voltage criteria for left ventricular hypertrophy were observed in 19-27%, while 55% of HCM patients showed positive Sokolow or Cornell index. Although ST-segment depression may be a finding on ECG even in athletes without any cardiac diseases, none of the athletes showed ST-depression and no pathological Q wave was present. T-wave inversion is considered to be a common ECG abnormality in athletes. According to the ESC recommendation T-wave inversion ≥2 mm in at least two adjacent leads is pathological, however the significance of T-wave inversion <2 mm is unclear (133). Only two percent of our healthy athletes had T-wave inversion in more than one contiguous leads, all of them in V1-V3 leads without signs of left ventricular hypertrophy. Eighty-two percent of HCM patients showed T-wave inversion.

Repolarization abnormalities fulfilling major and minor TFC were detected in 65% and 3% of sedentary ARVC patients, respectively. Depolarization abnormalities were less frequently present, 6% and 18% of sedentary ARVC patients showed depolarization abnormalities fulfilling major and minor TFC, respectively. All of the athletes with HCM showed at least one pathological ECG finding according to the 2014 ESC Guidelines on diagnosis and management of hypertrophic cardiomyopathy (15), 80%

had Sokolow or Cornell index positivity and 90% showed T wave inversion on 12-lead ECG. Athletes with ARVC showed epsilon wave in 38%, TWI in lead V1-V2 and in V1-V3 leads was observed in 13% and 50%, respectively. Two athletes did not fulfil any repolarization or depolarization criteria, one patient had complete right bundle branch block. ECG alterations are common in sedentary patients and athletes with cardiomyopathies. However, lack of pathological ECG finding does not necessarily indicate pure physiological remodelling.

Structural and functional alterations

The physiological upper limit for left ventricular hypertrophy is considered as maximal EDWT of 16mm, therefore athletes with a maximal EDWT >16 mm may be considered to have pathological left ventricular hypertrophy (17, 47). In contrast with prior – mainly two-dimensional echocardiographic – data referring 2-15% of male athletes in the grey zone of hypertrophy (4, 17), almost half of male athletes in our population reached EDWT of 13mm. According to previous observations, gender, age, BSA, level of dynamic and static component, training hours and intensity can also have a high impact on EDWT. Being members of the National or Olympic Team, our athletes represent an elite athlete population with extremely intensive and regular training. All of our athletes were performing high dynamic and at least moderate static sports. These characteristics of our athlete population and the fact that echocardiography may underestimate EDWT compared to CMR can be the explanation of the high rate of grey zone athletes (134, 135). Using echocardiography reliable delineation of LV wall significantly depends on the acoustic window, and EDWT could be underestimated because the epicardial border (especially in the LV free wall) is not visualized accurately. Moreover echocardiographic EDWT measurements are not always performed perfectly perpendicular to the myocardial center line. According to recent cardiac magnetic resonance (CMR) data phenotypic crossover between extreme forms of the athlete's heart and mild forms of pathological hypertrophy is much more common than former literature suggested – the number can reach 23% among healthy young army recruits (136). Petersen and his colleagues have shown on a small cohort that LV geometric indices determined by CMR can improve the sensitivity and specificity for

differentiating physiological left ventricular hypertrophy from HCM (137). Based on our large population, sport indices established using both conventional and threshold-based quantification method showed a good diagnostic accuracy even in the subgroup of athletes and HCM patients in the grey zone of hypertrophy.

Although LV and RV systolic function is usually within normal limits in professional athletes, functional changes due to regular intensive training may include decrease of LV and RVEF. In our population less than 2% of athletes had LVEF<50% and LVEF between 50% and 55% was observed in more than one fourth of all athletes. Although none of the athletes in our population showed RVEF ≤45%, almost 15% of our athletes showed RVEF between 45% and 50%. Based on literature data RVEF between 40% and 45% could be observed in 5% of elite athletes (138, 139). Preserved LV or RVEF was more common in male than in female athletes.

Beside electrical and functional changes, prolonged endurance exercise may lead to structural changes in the right ventricle as well. Although CMR is the gold standard non-invasive method to measure RV volumes and function, there are only few studies investigating the role of athletic performance using CMR (64, 140, 141). Although it is well known, that competitive athletes have significantly larger RV volumes than recreational athletes or sedentary patients, current TFC contain no athlete-specific criteria, therefore misdiagnosis of ARVC in healthy athletes may occur. The right ventricular cut-off values for CMR parameters differentiating ARVC and athlete's heart presented in our study could improve the diagnostic value of CMR in this special population.

5.1.2 Gender-specific differences

As in the last decades the number of women participating in competitive sport activities has been increased, the attention has been focused on the gender-specific differences in physiological remodelling. Electrical, structural and functional remodelling show significant differences between male and female athletes (142). The *importance* of gender-specific differences in athletes also confirms the fact, that the risk of SCD shows a male predominance Male athletes represent a 2.3-10-fold higher risk compared to

women (19, 20). Although the low number of athletes with HCM or ARVC in our studies does not allow us to draw powerful conclusions. Additionally, the representation of the female gender was modest, only 10% of our athletes with cardiomyopathies were female.

Several studies have proven that sex has a remarkable effect on electrical remodelling. Sokolow-Lyon voltage criteria for left ventricular hypertrophy and left axis deviation are less common in female athletes compared to males (143). TWI in the precordial leads is 2-3 fold more common in females than males (143, 144). J point elevation in combination with anterior TWI is a common ECG pattern in male athletes whereas is rarely observed in female athletes (145). These observations are in agreement with our results, J point elevation and criteria for left ventricular hypertrophy (Sokolow or Cornell index) were more common in male athletes, while no clear gender-specific difference was found regarding the presence of TWI.

Structural remodelling of the ventricles due to intensive exercise also shows differences between males and females. Based on a large cohort of athletes, Pelliccia and his colleagues observed that maximal EDWT is 23% lower in female athletes compared to male athletes. None of the females showed left ventricular hypertrophy ≥12mm confirming the observation that differentiation between HCM and athlete's heart there is a less common clinical conundrum in females (83). In accordance with this observation, in our highly trained athletic population almost 50% of male athletes reached the grey zone of hypertrophy, this pronounced hypertrophy was absent in female athletes. In our study the AUC value of one evaluated in EDWT/LVEDVi using both conventional and threshold-based methods among female patients characterized a perfect classification result in female individuals, suggesting that differentiation between HCM and athlete's heart in female individuals presents no remarkable difficulty. Recent echocardiographic data showed that absolute LV and RV dimensions are higher in males, but LV and RV diameters standardized to BSA are higher in females compared to males (143, 146). Although only limited CMR data are available about gender-specific normal left and right ventricular values for elite athletes (13, 18, 138), their results did not confirm these observations. Our study also showed higher LVEDVi in male athletes compared to female athletes.

Although it is well known, that gender-specific differences in normal EDWT or mass in non-athlete healthy controls are present, HCM diagnostic criteria does not include gender specific cut-off values. In the revised Task Force Criteria for RVEDVi we do have different cut-off values in both genders. The question arises whether our cut-off values established for the differentiation between cardiomoypathies and athlete's heart are applicable in both genders. Interestingly, despite the apparent gender-specific differences in cardiovascular sport adaptation our cut-off values for sport indices are applicable in both males and females. In the differentiation of athlete's heart and ARVC, comparing male and female ROC curves of CMR parameters with the highest diagnostic accuracy (RVEF, RV mid strain, RV average strain, RV min strain) showed no significant difference. These results suggest that gender-specific differences regarding these parameters are negligible, so the presented right ventricular cut-off values are also applicable in both males and females.

5.1.3 Role of novel CMR techniques in the differential diagnosis

Threshold-based quantification method

Previous studies already confirmed that threshold-based quantification in CMR provides an improved accuracy regarding left ventricular volumes and mass with an excellent intra- and interobserver variability. Moreover, it also contributes to a significant reduction in time required for post-processing (109, 147). As HCM patients show more pronounced left ventricular trabeculation and papillary muscles than healthy controls (148). Quantification methods enabling precise evaluation of trabeculae and papillary muscles may have a significant importance in this patient population. Literature data imply that as evaluation of trabeculae and papillary muscles can fundamentally change left ventricular parameters due to the large papillary muscles and pronounced trabeculation, in HCM patients analysis, which excludes papillary muscles and trabeculae from LV volume, is preferred (149, 150). Although it is also known that approximately one fifth of trained athletes represent left ventricular hypertrabeculation

(151), earlier we lacked data regarding left ventricular normal values using quantification excluding trabeculae and papillary muscles from the blood pool.

Our results confirmed the hypothesis that threshold-based method significantly alters left ventricular volumes and mass, moreover for sport index LVM/LVEDVi threshold-based quantification provides significantly better diagnostic accuracy than the conventional method even in subjects in the grey zone of hypertrophy. In the small group of athletes with HCM in our study sport, indices were in the pathological range in a bigger proportion when we applied sport indices using threshold-based quantification method.

Feature tracking analysis

Myocardial strain analysis demonstrated a clear significance in both early diagnosis and risk stratification in cardiomyopathy patients (152, 153).

Several CMR techniques were developed to estimate myocardial deformation. Myocardial tagging was the first method to achieve CMR based myocardial strain measurement. Cardiac magnetic resonance based strain assessment underwent a significant evolution in order to develop the clinical significance of the technique (154). Although myocardial tagging is a well validated technique with high reproducibility and also served as a gold standard method for validation, other strain measurement techniques including speckle-tracking echocardiography, the acquisition of additional images and the time consuming post processing has limited the widespread use of myocardial tagging in the everyday clinical routine (110). In the last decade, feature tracking has become a widely available technique to assess myocardial deformation without requiring further images. Left and right ventricular strain parameters can be established using the standard bSSFP images. The technique is based on the excellent blood-myocardium contrast on CMR images which enables the precise tracking of the endocardial contour (110).

Right ventricular strain has become a popular technique both in diagnosis and risk stratification in RV pathologies such as right heart failure, pulmonary arterial hypertension and congenital heart diseases (155-157). However, because of the complex anatomy of the right ventricle, strain analysis is still a challenging technique (158). As

CMR enables perfect visualisation of the right ventricle, CMR based strain imaging may have an added value in RV pathologies.

Although CMR is the gold standard method to evaluate RV function and volumes, subjective assessment of right ventricular wall thinning and wall motion abnormalities in the clinical routine represents the Achilles' heel of CMR. As feature tracking technique provides quantitative assessment of right ventricular function, it may have an added value in diagnosing ARVC. Based on recent literature data, global and regional right ventricular strain values of overt ARVC patients are decreased compared to healthy subjects, suggesting that feature tracking analysis may have an important added value in the diagnostic workup of ARVC patients (159-162).

To best of our knowledge we are the first to report feature tracking based CMR strain values of highly trained athletes and report cut-off values to differentiate ARVC and athlete's heart. Our results suggest that regional strain and strain rate of the right ventricular mid free wall are valuable discriminators even in patients with preserved RVEF and normal RV GLS. This fact highlights the significance of reporting CMR based strain parameters for differentiating athlete's heart and ARVC. Although the moderate sensitivity of our cut-off values confirms that CMR is not an appropriate first line screening method. The good or excellent specificity enhances its role to prevent unnecessary disqualification because of overdiagnosing ARVC.

Additional CMR techniques

With the help of gadolinium based contrast administration CMR enables to detect fibrosis/scar which may be pathognomic for certain cardiomyopathies, moreover it tends to have significance in predicting sudden cardiac death. Prevalence of LGE in HCM patients is approximately 60%, myocardial fibrosis is most commonly present in the hypertrophic segments and in the right ventricular insertion points (163). Our sedentary HCM cohort presented a higher prevalence of LGE in the same localizations, while the presence of LGE was lower in athletes with HCM, and none of the athletes showed LGE. Detection of LGE in the hypertrophic segments or in the insertion points may help the diagnosis of HCM in athletes, but the lack of myocardial fibrosis does not rule out the possibility of the disease. Based on our findings LGE has an excellent

positive predictive value, but low negative predictive value; in athletes with HCM even lower than in sedentary HCM patients.

Although fibro-fatty replacement is a hallmark of ARVC and LGE can be present in approximately 30% of the patients (164), the current Task Force Criteria does not include presence of LGE as a criterion. Assessment of LGE especially in the thin right ventricular myocardium is challenging, additionally, the presence of left ventricular LGE is not specific as varying pathologies including sarcoidosis, myocarditis or DCM may mimic ARVC. Therefore, we have reason to believe that detection of LGE in suspected ARVC may have an important role, as it has been proved that VTs and VPBs often originates from the scarred regions indicating a relation between electrophysiological and structural abnormalities (165). In our ARVC cohort the prevalence of LGE was higher, two third of the patients showed LGE mainly in the left ventricle or in biventricular location, while only three of the eight athletes with ARVC showed LGE. Given the small sample size it might be misleading to draw definitive conclusions about the true prevalence of LGE in ARVC patients.

LGE technique is a gold standard non-invasive method for assessing focal fibrosis. However, diffuse fibrosis may be underdetected on LGE images. Tissue characterization with the use of parametric mapping is an appropriate method to detect both focal and diffuse myocardial fibrosis. Native T1 mapping is feasible to tissue characterization even without the use of contrast agent. Post-contrast T1 mapping enables the quantification of extracellular volume. These techniques may play an important role in the differentiation of physiological and pathological remodelling.

5.2 Electroanatomic and tissue characterization in patients with DCM

5.2.1 Tissue characterization in patients with DCM using CMR

Besides the visualization of fibrotic tissue, CMR enables quantification of LGE mass or volume using different techniques. The full-width at half maximum (FWHM) method defines scar core as signal intensity >50% of maximum signal intensity in the

hyperenhanced region, while different SD thresholds techniques defines scar tissue based on the mean signal intensity in the remote myocardium. Because of the high prevalence of diffuse interstitial fibrosis in the remote myocardium in DCM patients, SD threshold techniques may underestimate LGE volume. Based on this fact and the better reproducibility of FWHM method in our current study we applied FWHM quantification technique.

Up to one third of DCM patients may show LGE mainly in the basal septum or the lateral wall and various LGE pattern such as linear mid-wall, subepicardial, focal patchy and diffuse pattern could be observed in DCM patients (115). In our current study 32% of DCM patients showed LGE most frequently in basal inferolateral, inferior and inferoseptal segments. Our results regarding the prevalence of LGE in patients with different ventricular arrhythmias (71% with VT, 5% with nsVT and none of the patients with VPBs showed LGE) emphasize the importance of LGE presence in VT prediction.

It is well known that the presence of myocardial fibrosis correlates with functional parameters and clinical markers of heart failure in DCM patients. Moreover, large clinical trials have shown the predictive value of LGE pattern in DCM patients. Septal LGE is associated with increased risk of death and SCD in DCM patients even when the extent of LGE is small. Greatest risk may be present in case of concomitant septal and free-wall LGE (115).

Besides all advantages, LGE technique has its limitations as diffuse interstitial fibrosis, which may contribute to arrhythmogenic substrate in DCM cannot be identified using traditional LGE technique. T1 mapping technique enables us to evaluate diffuse fibrosis. Furthermore, extracellular volume values closely correlate with collagen volume fraction quantified histologically from endomyocardial biopsies in DCM patients (166). Performing quantitative tissue characterization using T1 mapping may play an important role in the future as native T1 values are an independent predictor for ventricular arrhythmias (167).

5.2.2 Electroanatomic characterization in patients with DCM

Areas of fibrosis in DCM can be visualized indirectly using bipolar and unipolar electroanatomic voltage mapping. It has been proven that homogenization of low-voltage areas and elimination of the abnormal signals in patients with scar related VT is associated with better short- and long-term success rates in comparison to ablation targeting only clinical and stable VTs in patients with ischaemic aetiology with tolerated VT (168).

In DCM patients, low-voltage areas are less frequently observed compared to patients with ischaemic aetiology. In DCM patients the scar is usually located midmyocardial or epicardial. Therefore scar may remain undetected during endocardial bipolar voltage mapping. Its visualization may require epicardial voltage mapping. The bipolar electroanatomic mapping has a narrower field of view and proved insensitive to delineate scars away from the endocardium (169). Data regarding optimal low-amplitude definition in nonischaemic aetiologies are still controversial.

The agreement between the identified bipolar low-voltage areas and LGE remained suboptimal. In order to improve the agreement between LGE and EAM, we adjusted the bipolar thresholds to match the EAM to the LGE areas. The newly defined median thresholds for the bipolar low-voltage maps were 1.5 mV, which are close to those observed in a large multicenter study (168). Because the adjusted bipolar thresholds showed significant correlation with LGE volume, it is possible that thresholds for the bipolar EAM should be adjusted in each patient depending on LGE volume. Higher thresholds should be used in patients with larger LGE volume and lower thresholds in patients with small LGE.

5.2.3 The role of CMR imaging in patients with ventricular arrhythmias

Diagnostic role

Accurate characterization of the underlying aetiology is crucial in patients with ventricular arrhythmias as it may have serious prognostic and therapeutic significance. Identifying CMR-based scar pattern enables to distinguish between ischaemic and non-ischaemic aetiologies or differentiate between specific non-ischaemic aetiologies. A

recent study showed that CMR modifies the clinical diagnosis in approximately one third of patients with ventricular arrhythmias (170).

Risk stratification

As already mentioned earlier, the presence and extent of LGE may have an independent prognostic value in patients with DCM. In our current study patients with VT recurrence showed more extensive LGE compared to patients without VT recurrence, while no difference was found in the surface of LVAs in patients with or without VT recurrence. More detailed analysis of LGE images may provide more specific scar characteristics including extent and pattern of the scar tissue, scar transmurality and heterogeneity, size of the scar core and border zone, presence of conducting channels within the scar leading to more precise risk stratification (171-174).

CMR to improve VT ablation success

The role of CMR in patients undergoing VT ablation has been increased in the last decades. CMR imaging may play a role in preprocedural assessment of cardiac anatomy and myocardial scar tissue. LGE imaging enables to identify left ventricular regions that may be responsible for VT. In our study VT exits were presence in areas with LGE in 75% of our patients. Previous studies have been demonstrated that critical VT isthmuses are located within LGE areas, suggesting the importance of CMR based ablation strategies. Siontis et al. have been proven that CMR performed before VT ablation in DCM patients showed a significantly higher rate of acute complete procedural success in comparison with patients without CMR (63% vs 24 %). After a median follow-up of 7.6 months, 27% vs 60% of patients in the CMR and non-CMR group achieved the composite end-point of VT-recurrence, heart transplantation or death, respectively (175). Performing preprocedural CMR in order to establish the transmurality and pattern of LGE may help to identify the optimal access route. Patients with epicardial substrates show higher success rates in case of epicardial ablation. Identification of patients who may benefit from first-line epicardial ablation using LGE assessment has been reported to improve outcomes (176). Preprocedural CMR may minimize procedural complications and contribute to a reduction in fluoroscopy and procedure time.

DOI:10.14753/SE.2020.2408

Recently, as increased interest has noticed regarding pre- or intraprocedural integration of structural and electroanatomical substrate in order to guide ablation procedures. By integrating CMR images into the electroanatomic systems may facilitate a more targeted VT ablation approach especially in nonischaemic aetiology with epicardial or midmyocardial scar (173, 177).

Due to providing excellent tissue-specific information CMR enables postprocedural assessment of the ablation's effect by direct visualization of the ablation lesion in detail. Ablation lesions are characterized by presenting oedema, LGE and microvascular obstruction. It is possible to accurately assess the size and transmurality of the lesion. Real-time CMR-based assessment of ablation lesion formation (based on myocardial oedema, intramural haematoma or tissue temperature rise) could be a potential strategy to guide VT ablation (178). However, significant technological challenges (i.e. MR compatibility of electrophysiology catheters, appropriate processing of electrophysiology signals and improvements to simplify cardioversion in an MR environment etc.) impede the use of real-time MR-guided electrophysiological suite in the clinical routine.

DOI:10.14753/SE.2020.2408

5.3 The role of CMR in the detailed assessment of reverse remodelling after CRT implantation

5.3.1 Assessment of the reverse remodelling using CMR

In the clinical routine, assessment of the reverse remodelling achieved by CRT is performed using echocardiography. Although the many advantages of this imaging technique (cost-efficiency, low acquisition time, availability) have already been recognized, some disadvantages such as high inter and intraobserver variability and suboptimal image quality (especially in patients with poor echocardiographic window) still limits its applicability. Cardiac magnetic resonance is the gold standard method to evaluate ventricular volumes, masses and ejection fraction, and it enables a precise functional, mechanical and morphological assessment even in patients with suboptimal image quality on echocardiography. Owing to the low intra- and inter-observer variability, CMR enables optimal patient monitoring, and it may be used as part of a routine after CRT implantation and it may facilitate precise identification of patients in different "responder groups". Despite the numerous advantages of CMR, potential disadvantage of CMR in CRT patient population that device related artefacts may hamper image analysis. Moreover, we have to deal with the fact that certain CRT manufacturers' MRI safe mode does not include biventricular pacing as an option (179). Applying AOO or DOO RV only pacing during CMR examination may lead to unreliable measurements regarding LV function and mechanics.

The metallic content of a PM or ICD generator in the magnet may lead to serious artefacts on bSSFP images. Dark band off-resonance and generator related ferromagnetic susceptibility artefacts may hamper image analysis. Recent literature data suggest that applying device-dependent imaging strategy using specific sequences (i.e. cine spoiled gradient echo) can eliminate or minimize the presence of device-related artefacts (180). The use of SGE technique eliminates the dark band off-resonance artefacts, and the remaining ferromagnetic susceptibility artefact usually does not affects the heart allowing detailed image analysis even in patients after left-sided CRT-D implantation. In our study all patients with CRT-P showed excellent image quality

even when acquiring bSSFP images. Although banding artefacts were present on bSSFP images in all patients with CRT-D, applying SGE sequence appropriate image quality was reached. In CRT-D patients, only 2% of the LV segments were affected by serious banding artefacts on SGE, making dyssynchrony assessment more difficult, but not affecting volumetric and functional assessment despite the fact that all of our patients had left sided CRT-D. The relatively good image quality might be also explained by the size reduction of the generators during the last decades, because our study included devices implanted in the last few years only.

In our study, CMR examination performed before CRT implantation and six months thereafter has proven that CMR is a valuable tool to monitor reverse remodelling in patients with CRT. Based on the decrease of LVESVi assessed using CMR, 11 patients were classified as super responders, one patient as responder and only one did not reach the 15% LVESVi decrease. Comparing baseline and follow-up CMR parameters during biventricular pacing, significant improvement was found in terms of LVEF, LVEDVi, LVESVi, RVEDVi and LV geometry. As CMR based deformation imaging also enables the assessment of global and regional strain values, it may also provide additional information besides standard volumetric and functional response. In our patient population a significant improvement in GLS, GCS and GRS, moreover global dyssynchrony expressed in circumferential mechanical dispersion decreased significantly. Regional dyssynchrony defined by the maximum difference in time to peak septal and lateral transversal displacement also decreased significantly. Proving that biventricular pacing during CMR is safe and feasible, we can conclude that CMR is an optimal method to precisely estimate reverse remodelling after CRT and may also open future perspectives in identifying optimal CRT settings.

Prompt changes in LV function and mechanics

High biventricular pacing rate is essential in CRT patients, because decreased LV pacing rate may lead to rapid deterioration of LV function. In our patients switching off the biventricular pacing and applying AOO pacing a prompt significant deterioration of LV mechanics and function was observed. Not to our surprise, no differences in LVEDVi or LV geometry were observed in biventricular vs AOO pacing, as volumetric

remodelling is a long-term process. Although significant changes in the LVEF, LVSVi, LVESVi, GCS, mechanical dispersion and regional dyssynchrony were observed, parameters measured during AOO pacing did not reach the baseline values suggesting an existing memory.

Based on these finding we can conclude that in order to utilize the advantages of CMR and measure the effect of CRT, avoiding asynchronous AOO or D00 RV pacing and applying biventricular pacing during CMR imaging is essential.

5.3.2 The current role and future perspectives of CMR in CRT therapy

CMR is a non-invasive modality, which enables precise quantification of function, structure and mechanics by assessment of LVEF, LV volumes, geometry, necrosis/fibrosis, global myocardial strain and dyssynchrony. Therefore, besides monitoring response to CRT, CMR may play an important role in optimal patient selection for CRT, risk stratification and CMR guided lead positioning.

5.4. Limitations

The single-center nature and the relatively limited number of patients are the major limitations of our studies.

Additional potential limitation of our project entitled “Differentiation of pathological and physiological remodelling” may be the age differences. Our cardiomyopathy cohort represents an older population compared to the athletes, although age differences may not necessarily influence our results. There have been contradictory data originating from the studies on the effect of aging on strain values (181, 182). To eliminate the potential confounding effect of differences in age between HCM patients and athletes we made an effort to adjust our estimates for age. As physiological remodelling significantly depends on factors such as intensity of exercise, sport type and race, our findings should be interpreted with caution. Our athletic cohort exclusively comprised

of Caucasian athletes and mainly of sports with high static and dynamic components. Feature-tracking technique has its limitation including variability across different vendor software platforms. Standardization of the feature tracking technique remains an important challange in order to achieve the opportunity to the widespread use of feature tracking analysis in the clinical routine. Genetic mutation screening was not routinely performed in our cardiomyopathy patients.

Potential limitation of our project entitled “Electroanatomical and tissue characterization” can be the applied scar quantification technique. Traditional methods to delineate LGE on CMR images depend on either the maximum signal intensity within the scar region, the mean signal intensity in remote regions and/or the standard deviation of signal intensity in remote regions. The extent of the scar quantified using the FWHM method in patients with non-ischaemic aetiology may be more variable than in patients with an ischaemic scar. Due to the fact that the reproducibility of FWHM seems to be better than scar signal intensity threshold based techniques. Furthermore, artefacts from the ICD devices can lead to false positive LGE findings, however, with the use of the wideband sequences, we were able to successfully distinguish between true LGE and false hyperenhancement. In terms of substrate visualization, T1 mapping can be more sensitive for the detection of diffuse fibrosis in patients with DCM than the LGE method.

DOI:10.14753/SE.2020.2408

6. Conclusions

Intensive and regular training can lead to physiological cardiac remodelling including LV hypertrophy and ventricular dilation, which may mimic pathological conditions causing differential diagnostic dilemmas. Based on our results half of elite healthy male athletes with very intensive and regular training may reach the grey zone hypertrophy, which may mimic HCM and cause diagnostic challenges in the everyday clinical routine. However, only minority of highly trained female athletes reached EDWT of 13 mm suggesting that differentiation between HCM and athlete's heart is a less common clinical conundrum in females. CMR based sport indices provide an important tool to diagnose HCM and distinguish it from athlete's heart. Not only EDWT/LVEDVi$_{CQ}$ but also our new indices determined using TQ (EDWT/LVEDVi$_{TQ}$ and LVMTQ/LVEDVi$_{TQ}$) showed high diagnostic accuracy both in the whole cohort and in the male subgroup with an EDWT 13–16 mm. In our athletes with HCM, the only parameter falling into the pathological range was the LVMTQ/LVEDV$_{TQ}$ ratio. Our results highlight that RV dilatation in healthy endurance athletes may reach the proposed Task Force criteria in almost 95%. Therefore, elevated RVEDVi is an insufficient criterion for morphological diagnosis of ARVC. Besides establishing RVEF using CMR, RV strain analysis can provide an important tool to diagnose ARVC and distinguish it from athlete's heart. CMR based regional strain and strain rate values may help to identify ARVC even in highly trained athletes with preserved RVEF and normal RV GLS.

The link between structural and electrophysiological remodelling in cardiomyopathies is not yet fully understood. Assessing tissue and electroanatomic characteristics of DCM patients using CMR and electroanatomic mapping, we found that LGE was observed in approximately one third of the DCM patients with VA. Late gadolinium enhancement was seen mainly in patients with sustained VT. Comparing tissue and electroanatomic characteristics showed a fairly poor agreement between the distribution and the size of the LGE and bipolar low-voltage areas. No certain cut-off values for EAM could be identified. On the other hand, most VT exits were found in areas of LGE in patients with sustained VT. The outcomes were related only to the extent of LGE.

DOI:10.14753/SE.2020.2408

As a result of successful cardiac resynchronization therapy, reverse remodelling may be detected in symptomatic heart failure patients with broad QRS and LBBB morphology. In our study, we proved that CMR imaging is feasible and safe in CRT patients with resynchronization on. Compared to baseline measurements, left ventricular reverse remodelling, improvement of systolic function, global strain, global and regional dyssynchrony were detected. Applying AOO pacing, we discovered an immediate deterioration of LVEF, LVESVi, LV strain and dyssynchrony. Biventricular pacing during CMR enables a more precise quantification of LV function, morphology and mechanics. Therefore, CMR imaging may contribute to a better understanding of the effects of resynchronization therapy and could help to improve responder rate in the future.

DOI:10.14753/SE.2020.2408

7. Summary

Cardiac remodelling is a compensatory process leading to functional and structural changes of the heart including scar formation, left ventricular dilation and geometrical changes with increasing spherical geometry. Similar changes may be present in cardiomyopathies or in athletes with marked physiological remodelling.

As HCM and ARVC are leading causes of sudden cardiac death in young athletes, diagnosing these conditions in highly trained athletes is crucial. Novel CMR techniques may further improve the diagnostic accuracy and contribute to distinguish cardiomyopathies from marked physiological remodelling. We have first proven that sport indices such as EDWT/LVEDVi and LVM/LVEDV established using threshold based quantification may improve the diagnostic accuracy in athletes with suspected HCM. Our study has described first in the literature that CMR-based strain analysis is a useful tool to distinguish ARVC from athlete's heart. CMR-based right ventricular regional strain values may help to identify ARVC even in highly trained athletes with preserved right ventricular ejection fraction. Although it is known, that structural and electrophysiological remodelling are strongly related, to describe detailed information regarding tissue and electroanatomic characteristics of cardiomyopathy patients has been warranted. Based on our results, although only sub-optimal agreement could be found between the LGE and low-voltage areas, most VT exits were found in LGE areas in patients with sustained VT. Moreover, VT recurrence was influenced only by the LGE volume and none of the electroanatomic parameters. We have first proven that CMR imaging is a feasible and safe technique in CRT patients with resynchronization on, therefore precise assessment of reverse remodelling has become a clinical reality using biventricular pacing during CMR imaging. We have shown that in the absence of biventricular pacing (AOO pacing) immediate deterioration of function and mechanics occurs, therefore scanning with resynchronization on is crucial in this clinical setting.

Based on our results using different novel CMR techniques may improve the diagnostic accuracy in athletes with suspected cardiomyopathies. Moreover, it may contribute to our better understanding of structural and electrophysiological changes in cardiac remodelling and reverse remodelling as well.

DOI:10.14753/SE.2020.2408

8. Összefoglaló

A kardiális remodelling a szívben funkcionális és strukturális változásokat (hegképződés, bal kamra tágulat és spherikus átalakulás) eredményező kompenzatorikus mechanizmus. Hasonló eltérések figyelhetők meg különböző cardiomyopathiákban, valamint az intenzív sporttevékenység hatására kialakuló sportszívben is.

A fiatalkori sportolói hirtelen szívhalál hátterében leggyakrabban ARVC vagy HCM áll, ezért ezen állapotok diagnosztizálása élsportolók körében nagy jelentőségű. Vizsgálataink igazolták, hogy egyes új CMR technikák alkalmazása segítheti a cardiomyopathiák egészséges sportszívtől való elkülönítését. Elsőként igazoltuk, hogy a trabekulakvantifikációval meghatározott spotindexek (EDWT/LVEDVi és LVM/LVEDV) alklamazásával javítható a diagnosztikus pontosság HCM gyanús sportolók esetén. Vizsgálatunkban elsőként igazoltuk, hogy a CMR alapú strain analízis segítheti az ARVC és sportszív elkülönítését. A regionális jobb kamrai strain paraméterek alkalmazása megtartott jobb kamrai ejekciós frakciójú élsportolókban is segítheti az ARVC diagnózisának felállítását.

Habár közismert, hogy a strukturális és eletrofiziológiai remodelling szorosan összefügg, a cardiomyopathiák strukturális és elektroanatómiai jellegzetességeiről szóló ismereteink hiányosak. Habár jelen vizsgálatunkban csak gyenge egyezést találtunk az alacsony feszültségű területek és a LGE-t mutató területek között, a legtöbb VT exit a LGE-t mutató területekre lokalizálódott. Továbbá kiemelendő, hogy a VT rekurrenciát egyedül a LGE kiterjedése befolyásolta, míg egyik elektroanatómiai paraméterrel sem mutatott összefüggést. Elsőként bizonyítottuk, hogy a CMR vizsgálat CRT implantációt követően biventikurális ingerlés alatt is biztonságosan kivitelezhető, és kiválóan alkalmas a reverz remodelling pontos megítélésére. Igazoltuk, hogy AOO ingerlésre váltva azonnali romlás mérhető a bal kamra funkcióban és mechanikában, igazolva a biventricularis ingerlés jelentőségét a CMR vizsgálat során.

Eredményeink alapján megállapítható, hogy a különböző új CMR technikák alkalmazása nagyban segítheti a cardiomyopathiák és egészséges sportszív elkülönítését, továbbá hozzájárulhat a remodelling és reverz remodelling során végbemenő sturkturális és elektrofiziológiai változások pontosabb megértéséhez is.

9. References

1. Heusch G, Libby P, Gersh B, Yellon D, Bohm M, Lopaschuk G, & Opie L (2014) Cardiovascular remodelling in coronary artery disease and heart failure. *Lancet* 383(9932):1933-1943.
2. Koitabashi N & Kass DA (2011) Reverse remodeling in heart failure--mechanisms and therapeutic opportunities. *Nat Rev Cardiol* 9(3):147-157.
3. Roberts CS, Maclean D, Maroko P, & Kloner RA (1984) Early and late remodeling of the left ventricle after acute myocardial infarction. *Am J Cardiol* 54(3):407-410.
4. Spirito P, Pelliccia A, Proschan MA, Granata M, Spataro A, Bellone P, Caselli G, Biffi A, Vecchio C, & Maron BJ (1994) Morphology of the "athlete's heart" assessed by echocardiography in 947 elite athletes representing 27 sports. *Am J Cardiol* 74(8):802-806.
5. Burchfield JS, Xie M, & Hill JA (2013) Pathological ventricular remodeling: mechanisms: part 1 of 2. *Circulation* 128(4):388-400.
6. Sekaran NK, Crowley AL, de Souza FR, Resende ES, & Rao SV (2017) The Role for Cardiovascular Remodeling in Cardiovascular Outcomes. *Curr Atheroscler Rep* 19(5):23.
7. Henschen S (1899) Eine medizinische sportstudie. *Mitt. Med. Klin. Upsala.* 2::15–18.
8. Darling MD (1899) The effects of training. A study of the harvard university crews. . *Boston Med. Surg. J.*:229–233.
9. Morganroth J, Maron BJ, Henry WL, & Epstein SE (1975) Comparative left ventricular dimensions in trained athletes. *Ann Intern Med* 82(4):521-524.
10. Spence AL, Naylor LH, Carter HH, Buck CL, Dembo L, Murray CP, Watson P, Oxborough D, George KP, & Green DJ (2011) A prospective randomised longitudinal MRI study of left ventricular adaptation to endurance and resistance exercise training in humans. *The Journal of physiology* 589(Pt 22):5443-5452.
11. É. M (2005) Sportorvosi szemle. . *Országos Sportegészségügyi Intézet (OSEI) és a Magyar Sportorvos Társaság.*
12. Mitchell JH, Haskell W, Snell P, & Van Camp SP (2005) Task Force 8: classification of sports. *J Am Coll Cardiol* 45(8):1364-1367.
13. Petersen SE, Hudsmith LE, Robson MD, Doll HA, Francis JM, Wiesmann F, Jung BA, Hennig J, Watkins H, & Neubauer S (2006) Sex-specific characteristics of cardiac

function, geometry, and mass in young adult elite athletes. *J Magn Reson Imaging* 24(2):297-303.

14. Basavarajaiah S, Boraita A, Whyte G, Wilson M, Carby L, Shah A, & Sharma S (2008) Ethnic differences in left ventricular remodeling in highly-trained athletes relevance to differentiating physiologic left ventricular hypertrophy from hypertrophic cardiomyopathy. *J Am Coll Cardiol* 51(23):2256-2262.
15. Pelliccia A, Culasso F, Di Paolo FM, & Maron BJ (1999) Physiologic left ventricular cavity dilatation in elite athletes. *Ann Intern Med* 130(1):23-31.
16. Pelliccia A, Maron BJ, Di Paolo FM, Biffi A, Quattrini FM, Pisicchio C, Roselli A, Caselli S, & Culasso F (2005) Prevalence and clinical significance of left atrial remodeling in competitive athletes. *J Am Coll Cardiol* 46(4):690-696.
17. Pelliccia A, Maron BJ, Spataro A, Proschan MA, & Spirito P (1991) The upper limit of physiologic cardiac hypertrophy in highly trained elite athletes. *N Engl J Med* 324(5):295-301.
18. Csecs I, Czimbalmos C, Toth A, Dohy Z, Suhai IF, Szabo L, Kovacs A, Lakatos B, Sydo N, Kheirkhahan M, Peritz D, Kiss O, Merkely B, & Vago H (2019) The impact of sex, age and training on biventricular cardiac adaptation in healthy adult and adolescent athletes: Cardiac magnetic resonance imaging study. *Eur J Prev Cardiol*:2047487319866019.
19. Corrado D, Basso C, Rizzoli G, Schiavon M, & Thiene G (2003) Does sports activity enhance the risk of sudden death in adolescents and young adults? *J Am Coll Cardiol* 42(11):1959-1963.
20. Harmon KG, Asif IM, Klossner D, & Drezner JA (2011) Incidence of sudden cardiac death in National Collegiate Athletic Association athletes. *Circulation* 123(15):1594-1600.
21. Maron BJ, Haas TS, Ahluwalia A, Murphy CJ, & Garberich RF (2016) Demographics and Epidemiology of Sudden Deaths in Young Competitive Athletes: From the United States National Registry. *Am J Med* 129(11):1170-1177.
22. Maron BJ, Shirani J, Poliac LC, Mathenge R, Roberts WC, & Mueller FO (1996) Sudden death in young competitive athletes. Clinical, demographic, and pathological profiles. *JAMA* 276(3):199-204.
23. Thompson PD, Funk EJ, Carleton RA, & Sturner WQ (1982) Incidence of death during jogging in Rhode Island from 1975 through 1980. *JAMA* 247(18):2535-2538.

24. Siscovick DS, Weiss NS, Fletcher RH, & Lasky T (1984) The incidence of primary cardiac arrest during vigorous exercise. *N Engl J Med* 311(14):874-877.
25. Maron BJ (2003) Sudden death in young athletes. *N Engl J Med* 349(11):1064-1075.
26. Eckart RE, Scoville SL, Campbell CL, Shry EA, Stajduhar KC, Potter RN, Pearse LA, & Virmani R (2004) Sudden death in young adults: a 25-year review of autopsies in military recruits. *Ann Intern Med* 141(11):829-834.
27. Eckart RE, Scoville SL, Shry EA, Potter RN, & Tedrow U (2006) Causes of sudden death in young female military recruits. *Am J Cardiol* 97(12):1756-1758.
28. Meyer L, Stubbs B, Fahrenbruch C, Maeda C, Harmon K, Eisenberg M, & Drezner J (2012) Incidence, causes, and survival trends from cardiovascular-related sudden cardiac arrest in children and young adults 0 to 35 years of age: a 30-year review. *Circulation* 126(11):1363-1372.
29. Corrado D, Basso C, Pavei A, Michieli P, Schiavon M, & Thiene G (2006) Trends in sudden cardiovascular death in young competitive athletes after implementation of a preparticipation screening program. *JAMA* 296(13):1593-1601.
30. Csecs I, Czimbalmos, C., Toth A., Kiss O., Komka Z., Barczi G., Kovats T., Suhai F.i., Sydo N., Simor T., Geller L., Becker D., Merkely B., Vago H. (2017) Structural myocardial disease or athlete's heart? The diagnostic role of cardiac magnetic resonance (CMR) imaging in athletes with the suspicion of structural heart disease. *Cardiologia Hungarica* 47(1):10-17.
31. Sharma S, Drezner JA, Baggish A, Papadakis M, Wilson MG, Prutkin JM, La Gerche A, Ackerman MJ, Borjesson M, Salerno JC, Asif IM, Owens DS, Chung EH, Emery MS, Froelicher VF, Heidbuchel H, Adamuz C, Asplund CA, Cohen G, Harmon KG, Marek JC, Molossi S, Niebauer J, Pelto HF, Perez MV, Riding NR, Saarel T, Schmied CM, Shipon DM, Stein R, Vetter VL, Pelliccia A, & Corrado D (2017) International recommendations for electrocardiographic interpretation in athletes. *European heart journal*.
32. Sharma S, Merghani A, & Mont L (2015) Exercise and the heart: the good, the bad, and the ugly. *Eur Heart J* 36(23):1445-1453.
33. Maron BJ, Gardin JM, Flack JM, Gidding SS, Kurosaki TT, & Bild DE (1995) Prevalence of hypertrophic cardiomyopathy in a general population of young adults. Echocardiographic analysis of 4111 subjects in the CARDIA Study. Coronary Artery Risk Development in (Young) Adults. *Circulation* 92(4):785-789.

34. Semsarian C, Ingles J, Maron MS, & Maron BJ (2015) New perspectives on the prevalence of hypertrophic cardiomyopathy. *J Am Coll Cardiol* 65(12):1249-1254.

35. Zou Y, Song L, Wang Z, Ma A, Liu T, Gu H, Lu S, Wu P, Zhang dagger Y, Shen dagger L, Cai Y, Zhen double dagger Y, Liu Y, & Hui R (2004) Prevalence of idiopathic hypertrophic cardiomyopathy in China: a population-based echocardiographic analysis of 8080 adults. *Am J Med* 116(1):14-18.

36. Hada Y, Sakamoto T, Amano K, Yamaguchi T, Takenaka K, Takahashi H, Takikawa R, Hasegawa I, Takahashi T, Suzuki J, & et al. (1987) Prevalence of hypertrophic cardiomyopathy in a population of adult Japanese workers as detected by echocardiographic screening. *Am J Cardiol* 59(1):183-184.

37. Maron BJ, Mathenge R, Casey SA, Poliac LC, & Longe TF (1999) Clinical profile of hypertrophic cardiomyopathy identified de novo in rural communities. *J Am Coll Cardiol* 33(6):1590-1595.

38. Hartmannova H, Kubanek M, Sramko M, Piherova L, Noskova L, Hodanova K, Stranecky V, Pristoupilova A, Sovova J, Marek T, Maluskova J, Ridzon P, Kautzner J, Hulkova H, & Kmoch S (2013) Isolated X-linked hypertrophic cardiomyopathy caused by a novel mutation of the four-and-a-half LIM domain 1 gene. *Circ Cardiovasc Genet* 6(6):543-551.

39. Branzi A, Romeo G, Specchia S, Lolli C, Binetti G, Devoto M, Bacchi M, & Magnani B (1985) Genetic heterogeneity of hypertrophic cardiomyopathy. *Int J Cardiol* 7(2):129-138.

40. Authors/Task Force m, Elliott PM, Anastasakis A, Borger MA, Borggrefe M, Cecchi F, Charron P, Hagege AA, Lafont A, Limongelli G, Mahrholdt H, McKenna WJ, Mogensen J, Nihoyannopoulos P, Nistri S, Pieper PG, Pieske B, Rapezzi C, Rutten FH, Tillmanns C, & Watkins H (2014) 2014 ESC Guidelines on diagnosis and management of hypertrophic cardiomyopathy: the Task Force for the Diagnosis and Management of Hypertrophic Cardiomyopathy of the European Society of Cardiology (ESC). *Eur Heart J* 35(39):2733-2779.

41. Marian AJ & Braunwald E (2017) Hypertrophic Cardiomyopathy: Genetics, Pathogenesis, Clinical Manifestations, Diagnosis, and Therapy. *Circ Res* 121(7):749-770.

42. Spirito P, Autore C, Formisano F, Assenza GE, Biagini E, Haas TS, Bongioanni S, Semsarian C, Devoto E, Musumeci B, Lai F, Yeates L, Conte MR, Rapezzi C, Boni L, & Maron BJ (2014) Risk of sudden death and outcome in patients with hypertrophic

cardiomyopathy with benign presentation and without risk factors. *Am J Cardiol* 113(9):1550-1555.

43. Elliott PM, Poloniecki J, Dickie S, Sharma S, Monserrat L, Varnava A, Mahon NG, & McKenna WJ (2000) Sudden death in hypertrophic cardiomyopathy: identification of high risk patients. *J Am Coll Cardiol* 36(7):2212-2218.

44. Pelliccia A, Fagard R, Bjornstad HH, Anastassakis A, Arbustini E, Assanelli D, Biffi A, Borjesson M, Carre F, Corrado D, Delise P, Dorwarth U, Hirth A, Heidbuchel H, Hoffmann E, Mellwig KP, Panhuyzen-Goedkoop N, Pisani A, Solberg EE, van-Buuren F, Vanhees L, Blomstrom-Lundqvist C, Deligiannis A, Dugmore D, Glikson M, Hoff PI, Hoffmann A, Hoffmann E, Horstkotte D, Nordrehaug JE, Oudhof J, McKenna WJ, Penco M, Priori S, Reybrouck T, Senden J, Spataro A, Thiene G, Study Group of Sports Cardiology of the Working Group of Cardiac R, Exercise P, Working Group of M, & Pericardial Diseases of the European Society of C (2005) Recommendations for competitive sports participation in athletes with cardiovascular disease: a consensus document from the Study Group of Sports Cardiology of the Working Group of Cardiac Rehabilitation and Exercise Physiology and the Working Group of Myocardial and Pericardial Diseases of the European Society of Cardiology. *Eur Heart J* 26(14):1422-1445.

45. Maron BJ, Udelson JE, Bonow RO, Nishimura RA, Ackerman MJ, Estes NAM, 3rd, Cooper LT, Jr., Link MS, & Maron MS (2015) Eligibility and Disqualification Recommendations for Competitive Athletes With Cardiovascular Abnormalities: Task Force 3: Hypertrophic Cardiomyopathy, Arrhythmogenic Right Ventricular Cardiomyopathy and Other Cardiomyopathies, and Myocarditis: A Scientific Statement From the American Heart Association and American College of Cardiology. *J Am Coll Cardiol* 66(21):2362-2371.

46. Pelliccia A, Lemme E, Maestrini V, Di Paolo FM, Pisicchio C, Di Gioia G, & Caselli S (2018) Does Sport Participation Worsen the Clinical Course of Hypertrophic Cardiomyopathy? Clinical Outcome of Hypertrophic Cardiomyopathy in Athletes. *Circulation* 137(5):531-533.

47. Maron BJ, Pelliccia A, & Spirito P (1995) Cardiac disease in young trained athletes. Insights into methods for distinguishing athlete's heart from structural heart disease, with particular emphasis on hypertrophic cardiomyopathy. *Circulation* 91(5):1596-1601.

48. Sheikh N, Papadakis M, Schnell F, Panoulas V, Malhotra A, Wilson M, Carre F, & Sharma S (2015) Clinical Profile of Athletes With Hypertrophic Cardiomyopathy. *Circ Cardiovasc Imaging* 8(7):e003454.
49. Basso C, Corrado D, Marcus FI, Nava A, & Thiene G (2009) Arrhythmogenic right ventricular cardiomyopathy. *Lancet* 373(9671):1289-1300.
50. El Ghannudi S, Nghiem A, Germain P, Jeung MY, Gangi A, & Roy C (2014) Left ventricular involvement in arrhythmogenic right ventricular cardiomyopathy - a cardiac magnetic resonance imaging study. *Clin Med Insights Cardiol* 8(Suppl 4):27-36.
51. Mast TP, Teske AJ, vd Heijden JF, Groeneweg JA, Te Riele AS, Velthuis BK, Hauer RN, Doevendans PA, & Cramer MJ (2015) Left Ventricular Involvement in Arrhythmogenic Right Ventricular Dysplasia/Cardiomyopathy Assessed by Echocardiography Predicts Adverse Clinical Outcome. *J Am Soc Echocardiogr* 28(9):1103-1113 e1109.
52. Berte B, Denis A, Amraoui S, Yamashita S, Komatsu Y, Pillois X, Sacher F, Mahida S, Wielandts JY, Sellal JM, Frontera A, Al Jefairi N, Derval N, Montaudon M, Laurent F, Hocini M, Haissaguerre M, Jais P, & Cochet H (2015) Characterization of the Left-Sided Substrate in Arrhythmogenic Right Ventricular Cardiomyopathy. *Circ Arrhythm Electrophysiol* 8(6):1403-1412.
53. Marcus FI, McKenna WJ, Sherrill D, Basso C, Bauce B, Bluemke DA, Calkins H, Corrado D, Cox MG, Daubert JP, Fontaine G, Gear K, Hauer R, Nava A, Picard MH, Protonotarios N, Saffitz JE, Sanborn DM, Steinberg JS, Tandri H, Thiene G, Towbin JA, Tsatsopoulou A, Wichter T, & Zareba W (2010) Diagnosis of arrhythmogenic right ventricular cardiomyopathy/dysplasia: proposed modification of the Task Force Criteria. *Eur Heart J* 31(7):806-814.
54. Bhonsale A, James CA, Tichnell C, Murray B, Gagarin D, Philips B, Dalal D, Tedford R, Russell SD, Abraham T, Tandri H, Judge DP, & Calkins H (2011) Incidence and predictors of implantable cardioverter-defibrillator therapy in patients with arrhythmogenic right ventricular dysplasia/cardiomyopathy undergoing implantable cardioverter-defibrillator implantation for primary prevention. *J Am Coll Cardiol* 58(14):1485-1496.
55. Orgeron GM, James CA, Te Riele A, Tichnell C, Murray B, Bhonsale A, Kamel IR, Zimmerman SL, Judge DP, Crosson J, Tandri H, & Calkins H (2017) Implantable Cardioverter-Defibrillator Therapy in Arrhythmogenic Right Ventricular

Dysplasia/Cardiomyopathy: Predictors of Appropriate Therapy, Outcomes, and Complications. *J Am Heart Assoc* 6(6).

56. Corrado D, Wichter T, Link MS, Hauer R, Marchlinski F, Anastasakis A, Bauce B, Basso C, Brunckhorst C, Tsatsopoulou A, Tandri H, Paul M, Schmied C, Pelliccia A, Duru F, Protonotarios N, Estes NA, 3rd, McKenna WJ, Thiene G, Marcus FI, & Calkins H (2015) Treatment of arrhythmogenic right ventricular cardiomyopathy/dysplasia: an international task force consensus statement. *Eur Heart J* 36(46):3227-3237.
57. Wichter T, Borggrefe M, Haverkamp W, Chen X, & Breithardt G (1992) Efficacy of antiarrhythmic drugs in patients with arrhythmogenic right ventricular disease. Results in patients with inducible and noninducible ventricular tachycardia. *Circulation* 86(1):29-37.
58. Wichter T, Paul TM, Eckardt L, Gerdes P, Kirchhof P, Bocker D, & Breithardt G (2005) Arrhythmogenic right ventricular cardiomyopathy. Antiarrhythmic drugs, catheter ablation, or ICD? *Herz* 30(2):91-101.
59. Marcus GM, Glidden DV, Polonsky B, Zareba W, Smith LM, Cannom DS, Estes NA, 3rd, Marcus F, Scheinman MM, & Multidisciplinary Study of Right Ventricular Dysplasia I (2009) Efficacy of antiarrhythmic drugs in arrhythmogenic right ventricular cardiomyopathy: a report from the North American ARVC Registry. *J Am Coll Cardiol* 54(7):609-615.
60. Sawant AC, Bhonsale A, te Riele AS, Tichnell C, Murray B, Russell SD, Tandri H, Tedford RJ, Judge DP, Calkins H, & James CA (2014) Exercise has a disproportionate role in the pathogenesis of arrhythmogenic right ventricular dysplasia/cardiomyopathy in patients without desmosomal mutations. *J Am Heart Assoc* 3(6):e001471.
61. Sawant AC, Te Riele AS, Tichnell C, Murray B, Bhonsale A, Tandri H, Judge DP, Calkins H, & James CA (2016) Safety of American Heart Association-recommended minimum exercise for desmosomal mutation carriers. *Heart Rhythm* 13(1):199-207.
62. James CA, Bhonsale A, Tichnell C, Murray B, Russell SD, Tandri H, Tedford RJ, Judge DP, & Calkins H (2013) Exercise increases age-related penetrance and arrhythmic risk in arrhythmogenic right ventricular dysplasia/cardiomyopathy-associated desmosomal mutation carriers. *J Am Coll Cardiol* 62(14):1290-1297.
63. Rojas A & Calkins H (2015) Present understanding of the relationship between exercise and arrhythmogenic right ventricular dysplasia/cardiomyopathy. *Trends Cardiovasc Med* 25(3):181-188.

64. Ruwald AC, Marcus F, Estes NA, 3rd, Link M, McNitt S, Polonsky B, Calkins H, Towbin JA, Moss AJ, & Zareba W (2015) Association of competitive and recreational sport participation with cardiac events in patients with arrhythmogenic right ventricular cardiomyopathy: results from the North American multidisciplinary study of arrhythmogenic right ventricular cardiomyopathy. *Eur Heart J* 36(27):1735-1743.

65. Mussigbrodt A, Czimbalmos C, Stauber A, Bertagnolli L, Bode K, Dagres N, Doring M, Richter S, Sommer P, Husser D, Bollmann A, Hindricks G, & Arya A (2019) Effect of Exercise on Outcome after Ventricular Tachycardia Ablation in Arrhythmogenic Right Ventricular Dysplasia/Cardiomyopathy. *Int J Sports Med*.

66. La Gerche A, Burns AT, Mooney DJ, Inder WJ, Taylor AJ, Bogaert J, Macisaac AI, Heidbuchel H, & Prior DL (2012) Exercise-induced right ventricular dysfunction and structural remodelling in endurance athletes. *Eur Heart J* 33(8):998-1006.

67. La Gerche A, Claessen G, Dymarkowski S, Voigt JU, De Buck F, Vanhees L, Droogne W, Van Cleemput J, Claus P, & Heidbuchel H (2015) Exercise-induced right ventricular dysfunction is associated with ventricular arrhythmias in endurance athletes. *Eur Heart J* 36(30):1998-2010.

68. La Gerche A, Heidbuchel H, Burns AT, Mooney DJ, Taylor AJ, Pfluger HB, Inder WJ, Macisaac AI, & Prior DL (2011) Disproportionate exercise load and remodeling of the athlete's right ventricle. *Med Sci Sports Exerc* 43(6):974-981.

69. La Gerche A, Roberts T, & Claessen G (2014) The response of the pulmonary circulation and right ventricle to exercise: exercise-induced right ventricular dysfunction and structural remodeling in endurance athletes (2013 Grover Conference series). *Pulm Circ* 4(3):407-416.

70. La Gerche A, Robberecht C, Kuiperi C, Nuyens D, Willems R, de Ravel T, Matthijs G, & Heidbuchel H (2010) Lower than expected desmosomal gene mutation prevalence in endurance athletes with complex ventricular arrhythmias of right ventricular origin. *Heart* 96(16):1268-1274.

71. Wasfy MM, DeLuca J, Wang F, Berkstresser B, Ackerman KE, Eisman A, Lewis GD, Hutter AM, Weiner RB, & Baggish AL (2015) ECG findings in competitive rowers: normative data and the prevalence of abnormalities using contemporary screening recommendations. *Br J Sports Med* 49(3):200-206.

72. Pinto YM, Elliott PM, Arbustini E, Adler Y, Anastasakis A, Bohm M, Duboc D, Gimeno J, de Groote P, Imazio M, Heymans S, Klingel K, Komajda M, Limongelli G, Linhart A, Mogensen J, Moon J, Pieper PG, Seferovic PM, Schueler S, Zamorano JL,

Caforio AL, & Charron P (2016) Proposal for a revised definition of dilated cardiomyopathy, hypokinetic non-dilated cardiomyopathy, and its implications for clinical practice: a position statement of the ESC working group on myocardial and pericardial diseases. *Eur Heart J* 37(23):1850-1858.

73. Elliott P, Andersson B, Arbustini E, Bilinska Z, Cecchi F, Charron P, Dubourg O, Kuhl U, Maisch B, McKenna WJ, Monserrat L, Pankuweit S, Rapezzi C, Seferovic P, Tavazzi L, & Keren A (2008) Classification of the cardiomyopathies: a position statement from the European Society Of Cardiology Working Group on Myocardial and Pericardial Diseases. *Eur Heart J* 29(2):270-276.
74. Codd MB, Sugrue DD, Gersh BJ, & Melton LJ, 3rd (1989) Epidemiology of idiopathic dilated and hypertrophic cardiomyopathy. A population-based study in Olmsted County, Minnesota, 1975-1984. *Circulation* 80(3):564-572.
75. Hershberger RE, Hedges DJ, & Morales A (2013) Dilated cardiomyopathy: the complexity of a diverse genetic architecture. *Nat Rev Cardiol* 10(9):531-547.
76. Weintraub RG, Semsarian C, & Macdonald P (2017) Dilated cardiomyopathy. *Lancet* 390(10092):400-414.
77. Mestroni L, Maisch B, McKenna WJ, Schwartz K, Charron P, Rocco C, Tesson F, Richter A, Wilke A, & Komajda M (1999) Guidelines for the study of familial dilated cardiomyopathies. Collaborative Research Group of the European Human and Capital Mobility Project on Familial Dilated Cardiomyopathy. *Eur Heart J* 20(2):93-102.
78. Japp AG, Gulati A, Cook SA, Cowie MR, & Prasad SK (2016) The Diagnosis and Evaluation of Dilated Cardiomyopathy. *J Am Coll Cardiol* 67(25):2996-3010.
79. Brignole M, Auricchio A, Baron-Esquivias G, Bordachar P, Boriani G, Breithardt OA, Cleland J, Deharo JC, Delgado V, Elliott PM, Gorenek B, Israel CW, Leclercq C, Linde C, Mont L, Padeletti L, Sutton R, Vardas PE, Guidelines ESCCfP, Zamorano JL, Achenbach S, Baumgartner H, Bax JJ, Bueno H, Dean V, Deaton C, Erol C, Fagard R, Ferrari R, Hasdai D, Hoes AW, Kirchhof P, Knuuti J, Kolh P, Lancellotti P, Linhart A, Nihoyannopoulos P, Piepoli MF, Ponikowski P, Sirnes PA, Tamargo JL, Tendera M, Torbicki A, Wijns W, Windecker S, Document R, Kirchhof P, Blomstrom-Lundqvist C, Badano LP, Aliyev F, Bansch D, Baumgartner H, Bsata W, Buser P, Charron P, Daubert JC, Dobreanu D, Faerestrand S, Hasdai D, Hoes AW, Le Heuzey JY, Mavrakis H, McDonagh T, Merino JL, Nawar MM, Nielsen JC, Pieske B, Poposka L, Ruschitzka F, Tendera M, Van Gelder IC, & Wilson CM (2013) 2013 ESC Guidelines on cardiac pacing and cardiac resynchronization therapy: the Task Force on cardiac pacing and

resynchronization therapy of the European Society of Cardiology (ESC). Developed in collaboration with the European Heart Rhythm Association (EHRA). *Eur Heart J* 34(29):2281-2329.

80. Priori SG, Blomstrom-Lundqvist C, Mazzanti A, Blom N, Borggrefe M, Camm J, Elliott PM, Fitzsimons D, Hatala R, Hindricks G, Kirchhof P, Kjeldsen K, Kuck KH, Hernandez-Madrid A, Nikolaou N, Norekval TM, Spaulding C, Van Veldhuisen DJ, Task Force for the Management of Patients with Ventricular A, & the Prevention of Sudden Cardiac Death of the European Society of C (2015) 2015 ESC Guidelines for the management of patients with ventricular arrhythmias and the prevention of sudden cardiac death: The Task Force for the Management of Patients with Ventricular Arrhythmias and the Prevention of Sudden Cardiac Death of the European Society of Cardiology (ESC)Endorsed by: Association for European Paediatric and Congenital Cardiology (AEPC). *Europace* 17(11):1601-1687.
81. Spezzacatene A, Sinagra G, Merlo M, Barbati G, Graw SL, Brun F, Slavov D, Di Lenarda A, Salcedo EE, Towbin JA, Saffitz JE, Marcus FI, Zareba W, Taylor MR, Mestroni L, & Familial Cardiomyopathy R (2015) Arrhythmogenic Phenotype in Dilated Cardiomyopathy: Natural History and Predictors of Life-Threatening Arrhythmias. *J Am Heart Assoc* 4(10):e002149.
82. Halliday BP, Gulati A, Ali A, Guha K, Newsome S, Arzanauskaite M, Vassiliou VS, Lota A, Izgi C, Tayal U, Khalique Z, Stirrat C, Auger D, Pareek N, Ismail TF, Rosen SD, Vazir A, Alpendurada F, Gregson J, Frenneaux MP, Cowie MR, Cleland JGF, Cook SA, Pennell DJ, & Prasad SK (2017) Association Between Midwall Late Gadolinium Enhancement and Sudden Cardiac Death in Patients With Dilated Cardiomyopathy and Mild and Moderate Left Ventricular Systolic Dysfunction. *Circulation* 135(22):2106-2115.
83. Pelliccia A, Maron BJ, Culasso F, Spataro A, & Caselli G (1996) Athlete's heart in women. Echocardiographic characterization of highly trained elite female athletes. *JAMA* 276(3):211-215.
84. Pelliccia A, Maron BJ, De Luca R, Di Paolo FM, Spataro A, & Culasso F (2002) Remodeling of left ventricular hypertrophy in elite athletes after long-term deconditioning. *Circulation* 105(8):944-949.
85. Pelliccia A, Maron MS, & Maron BJ (2012) Assessment of left ventricular hypertrophy in a trained athlete: differential diagnosis of physiologic athlete's heart from pathologic hypertrophy. *Progress in cardiovascular diseases* 54(5):387-396.

86. Mitchell AR, MacLachlan HI, & Le Page P (2013) Deconditioning the athletic heart. *BMJ Case Rep* 2013.

87. Biffi A, Maron BJ, Verdile L, Fernando F, Spataro A, Marcello G, Ciardo R, Ammirati F, Colivicchi F, & Pelliccia A (2004) Impact of physical deconditioning on ventricular tachyarrhythmias in trained athletes. *J Am Coll Cardiol* 44(5):1053-1058.

88. Maron BJ & Pelliccia A (2006) The heart of trained athletes: cardiac remodeling and the risks of sports, including sudden death. *Circulation* 114(15):1633-1644.

89. Tayal U & Prasad SK (2017) Myocardial remodelling and recovery in dilated cardiomyopathy. *JRSM Cardiovasc Dis* 6:2048004017734476.

90. Breathett K, Allen LA, Udelson J, Davis G, & Bristow M (2016) Changes in Left Ventricular Ejection Fraction Predict Survival and Hospitalization in Heart Failure With Reduced Ejection Fraction. *Circ Heart Fail* 9(10).

91. Kramer DG, Trikalinos TA, Kent DM, Antonopoulos GV, Konstam MA, & Udelson JE (2010) Quantitative evaluation of drug or device effects on ventricular remodeling as predictors of therapeutic effects on mortality in patients with heart failure and reduced ejection fraction: a meta-analytic approach. *J Am Coll Cardiol* 56(5):392-406.

92. Cintron G, Johnson G, Francis G, Cobb F, & Cohn JN (1993) Prognostic significance of serial changes in left ventricular ejection fraction in patients with congestive heart failure. The V-HeFT VA Cooperative Studies Group. *Circulation* 87(6 Suppl):VI17-23.

93. Merlo M, Pyxaras SA, Pinamonti B, Barbati G, Di Lenarda A, & Sinagra G (2011) Prevalence and prognostic significance of left ventricular reverse remodeling in dilated cardiomyopathy receiving tailored medical treatment. *J Am Coll Cardiol* 57(13):1468-1476.

94. Amorim S, Campelo M, Martins E, Moura B, Sousa A, Pinho T, Silva-Cardoso J, & Maciel MJ (2016) Prevalence, predictors and prognosis of ventricular reverse remodeling in idiopathic dilated cardiomyopathy. *Rev Port Cardiol* 35(5):253-260.

95. McNamara DM, Starling RC, Cooper LT, Boehmer JP, Mather PJ, Janosko KM, Gorcsan J, 3rd, Kip KE, Dec GW, & Investigators I (2011) Clinical and demographic predictors of outcomes in recent onset dilated cardiomyopathy: results of the IMAC (Intervention in Myocarditis and Acute Cardiomyopathy)-2 study. *J Am Coll Cardiol* 58(11):1112-1118.

96. Moon J, Shim CY, Kim YJ, Park S, Kang SM, Chung N, & Ha JW (2016) Left Atrial Volume as a Predictor of Left Ventricular Functional Recovery in Patients With Dilated

Cardiomyopathy and Absence of Delayed Enhancement in Cardiac Magnetic Resonance. *J Card Fail* 22(4):265-271.

97. Blauwet LA, Delgado-Montero A, Ryo K, Marek JJ, Alharethi R, Mather PJ, Modi K, Sheppard R, Thohan V, Pisarcik J, McNamara DM, Gorcsan J, 3rd, & Investigators* I (2016) Right Ventricular Function in Peripartum Cardiomyopathy at Presentation Is Associated With Subsequent Left Ventricular Recovery and Clinical Outcomes. *Circ Heart Fail* 9(5).
98. Kubanek M, Sramko M, Maluskova J, Kautznerova D, Weichet J, Lupinek P, Vrbska J, Malek I, & Kautzner J (2013) Novel predictors of left ventricular reverse remodeling in individuals with recent-onset dilated cardiomyopathy. *J Am Coll Cardiol* 61(1):54-63.
99. Leong DP, Chakrabarty A, Shipp N, Molaee P, Madsen PL, Joerg L, Sullivan T, Worthley SG, De Pasquale CG, Sanders P, & Selvanayagam JB (2012) Effects of myocardial fibrosis and ventricular dyssynchrony on response to therapy in new-presentation idiopathic dilated cardiomyopathy: insights from cardiovascular magnetic resonance and echocardiography. *Eur Heart J* 33(5):640-648.
100. Birnie DH & Tang AS (2006) The problem of non-response to cardiac resynchronization therapy. *Curr Opin Cardiol* 21(1):20-26.
101. Rickard J, Michtalik H, Sharma R, Berger Z, Iyoha E, Green AR, Haq N, & Robinson KA (2016) Predictors of response to cardiac resynchronization therapy: A systematic review. *Int J Cardiol* 225:345-352.
102. Sogaard P, Egeblad H, Kim WY, Jensen HK, Pedersen AK, Kristensen BO, & Mortensen PT (2002) Tissue Doppler imaging predicts improved systolic performance and reversed left ventricular remodeling during long-term cardiac resynchronization therapy. *J Am Coll Cardiol* 40(4):723-730.
103. Bax JJ, Bleeker GB, Marwick TH, Molhoek SG, Boersma E, Steendijk P, van der Wall EE, & Schalij MJ (2004) Left ventricular dyssynchrony predicts response and prognosis after cardiac resynchronization therapy. *J Am Coll Cardiol* 44(9):1834-1840.
104. Bax JJ, Marwick TH, Molhoek SG, Bleeker GB, van Erven L, Boersma E, Steendijk P, van der Wall EE, & Schalij MJ (2003) Left ventricular dyssynchrony predicts benefit of cardiac resynchronization therapy in patients with end-stage heart failure before pacemaker implantation. *Am J Cardiol* 92(10):1238-1240.
105. Notabartolo D, Merlino JD, Smith AL, DeLurgio DB, Vera FV, Easley KA, Martin RP, & Leon AR (2004) Usefulness of the peak velocity difference by tissue Doppler

imaging technique as an effective predictor of response to cardiac resynchronization therapy. *Am J Cardiol* 94(6):817-820.

106. Chung ES, Leon AR, Tavazzi L, Sun JP, Nihoyannopoulos P, Merlino J, Abraham WT, Ghio S, Leclercq C, Bax JJ, Yu CM, Gorcsan J, 3rd, St John Sutton M, De Sutter J, & Murillo J (2008) Results of the Predictors of Response to CRT (PROSPECT) trial. *Circulation* 117(20):2608-2616.
107. Donal E, Delgado V, Magne J, Bucciarelli-Ducci C, Leclercq C, Cosyns B, Sitges M, Edvardsen T, Sade E, Stankovic I, Agricola E, Galderisi M, Lancellotti P, Hernandez A, Plein S, Muraru D, Schwammenthal E, Hindricks G, Popescu BA, & Habib G (2017) Rational and design of EuroCRT: an international observational study on multi-modality imaging and cardiac resynchronization therapy. *Eur Heart J Cardiovasc Imaging* 18(10):1120-1127.
108. Mann DL, Barger PM, & Burkhoff D (2012) Myocardial recovery and the failing heart: myth, magic, or molecular target? *J Am Coll Cardiol* 60(24):2465-2472.
109. Varga-Szemes A, Muscogiuri G, Schoepf UJ, Wichmann JL, Suranyi P, De Cecco CN, Cannao PM, Renker M, Mangold S, Fox MA, & Ruzsics B (2016) Clinical feasibility of a myocardial signal intensity threshold-based semi-automated cardiac magnetic resonance segmentation method. *Eur Radiol* 26(5):1503-1511.
110. Salerno M (2018) Feature Tracking by CMR: A "Double Feature"? *JACC Cardiovasc Imaging* 11(2 Pt 1):206-208.
111. Wesbey GE, Higgins CB, McNamara MT, Engelstad BL, Lipton MJ, Sievers R, Ehman RL, Lovin J, & Brasch RC (1984) Effect of gadolinium-DTPA on the magnetic relaxation times of normal and infarcted myocardium. *Radiology* 153(1):165-169.
112. Karamitsos TD, Francis JM, Myerson S, Selvanayagam JB, & Neubauer S (2009) The role of cardiovascular magnetic resonance imaging in heart failure. *J Am Coll Cardiol* 54(15):1407-1424.
113. Almaas VM, Haugaa KH, Strom EH, Scott H, Dahl CP, Leren TP, Geiran OR, Endresen K, Edvardsen T, Aakhus S, & Amlie JP (2013) Increased amount of interstitial fibrosis predicts ventricular arrhythmias, and is associated with reduced myocardial septal function in patients with obstructive hypertrophic cardiomyopathy. *Europace* 15(9):1319-1327.
114. Mc LA, Ellims AH, Prabhu S, Voskoboinik A, Iles LM, Hare JL, Kaye DM, Macciocca I, Mariani JA, Kalman JM, Taylor AJ, & Kistler PM (2016) Diffuse Ventricular Fibrosis on Cardiac Magnetic Resonance Imaging Associates With Ventricular

Tachycardia in Patients With Hypertrophic Cardiomyopathy. *J Cardiovasc Electrophysiol* 27(5):571-580.

115. Halliday BP, Baksi AJ, Gulati A, Ali A, Newsome S, Izgi C, Arzanauskaite M, Lota A, Tayal U, Vassiliou VS, Gregson J, Alpendurada F, Frenneaux MP, Cook SA, Cleland JGF, Pennell DJ, & Prasad SK (2018) Outcome in Dilated Cardiomyopathy Related to the Extent, Location, and Pattern of Late Gadolinium Enhancement. *JACC Cardiovasc Imaging.*
116. Kuruvilla S, Adenaw N, Katwal AB, Lipinski MJ, Kramer CM, & Salerno M (2014) Late gadolinium enhancement on cardiac magnetic resonance predicts adverse cardiovascular outcomes in nonischemic cardiomyopathy: a systematic review and meta-analysis. *Circ Cardiovasc Imaging* 7(2):250-258.
117. McLenachan JM & Dargie HJ (1990) Ventricular arrhythmias in hypertensive left ventricular hypertrophy. Relationship to coronary artery disease, left ventricular dysfunction, and myocardial fibrosis. *Am J Hypertens* 3(10):735-740.
118. Kwong RY, Sattar H, Wu H, Vorobiof G, Gandla V, Steel K, Siu S, & Brown KA (2008) Incidence and prognostic implication of unrecognized myocardial scar characterized by cardiac magnetic resonance in diabetic patients without clinical evidence of myocardial infarction. *Circulation* 118(10):1011-1020.
119. Diez J (2007) Mechanisms of cardiac fibrosis in hypertension. *J Clin Hypertens (Greenwich)* 9(7):546-550.
120. van de Schoor FR, Aengevaeren VL, Hopman MT, Oxborough DL, George KP, Thompson PD, & Eijsvogels TM (2016) Myocardial Fibrosis in Athletes. *Mayo Clin Proc* 91(11):1617-1631.
121. McDiarmid AK, Swoboda PP, Erhayiem B, Lancaster RE, Lyall GK, Broadbent DA, Dobson LE, Musa TA, Ripley DP, Garg P, Greenwood JP, Ferguson C, & Plein S (2016) Athletic Cardiac Adaptation in Males Is a Consequence of Elevated Myocyte Mass. *Circ Cardiovasc Imaging* 9(4):e003579.
122. Mordi i. CD, Bezerra H., Tzemos N. (2015) Utility of Native T1 mapping to differentiate between athlete's heart and non-ischemic dilated cardiomyopathy. *J Cardiovasc Magn Reson* 17:379.
123. Wilkoff BL, Bello D, Taborsky M, Vymazal J, Kanal E, Heuer H, Hecking K, Johnson WB, Young W, Ramza B, Akhtar N, Kuepper B, Hunold P, Luechinger R, Puererfellner H, Duru F, Gotte MJ, Sutton R, Sommer T, & EnRhythm MRISPSSI (2011) Magnetic

resonance imaging in patients with a pacemaker system designed for the magnetic resonance environment. *Heart Rhythm* 8(1):65-73.

124. Nazarian S, Hansford R, Rahsepar AA, Weltin V, McVeigh D, Gucuk Ipek E, Kwan A, Berger RD, Calkins H, Lardo AC, Kraut MA, Kamel IR, Zimmerman SL, & Halperin HR (2017) Safety of Magnetic Resonance Imaging in Patients with Cardiac Devices. *N Engl J Med* 377(26):2555-2564.
125. Nazarian S, Hansford R, Roguin A, Goldsher D, Zviman MM, Lardo AC, Caffo BS, Frick KD, Kraut MA, Kamel IR, Calkins H, Berger RD, Bluemke DA, & Halperin HR (2011) A prospective evaluation of a protocol for magnetic resonance imaging of patients with implanted cardiac devices. *Ann Intern Med* 155(7):415-424.
126. Duru F (2002) CARTO three-dimensional non-fluoroscopic electroanatomic mapping for catheter ablation of arrhythmias: a useful tool or an expensive toy for the electrophysiologist? *Anadolu Kardiyol Derg* 2(4):330-337.
127. Hsia HH, Callans DJ, & Marchlinski FE (2003) Characterization of endocardial electrophysiological substrate in patients with nonischemic cardiomyopathy and monomorphic ventricular tachycardia. *Circulation* 108(6):704-710.
128. Saguner AM & Tandri H (2018) Electroanatomical voltage mapping and what to consider abnormal in non-ischaemic cardiomyopathy: when one size does not fit all. *Eur Heart J* 39(31):2876-2878.
129. Oduneye SO, Pop M, Biswas L, Ghate S, Flor R, Ramanan V, Barry J, Celik H, Crystal E, & Wright GA (2013) Postinfarction ventricular tachycardia substrate characterization: a comparison between late enhancement magnetic resonance imaging and voltage mapping using an MR-guided electrophysiology system. *IEEE Trans Biomed Eng* 60(9):2442-2449.
130. Glashan CA, Androulakis AFA, Tao Q, Glashan RN, Wisse LJ, Ebert M, de Ruiter MC, van Meer BJ, Brouwer C, Dekkers OM, Pijnappels DA, de Bakker JMT, de Riva M, Piers SRD, & Zeppenfeld K (2018) Whole human heart histology to validate electroanatomical voltage mapping in patients with non-ischaemic cardiomyopathy and ventricular tachycardia. *Eur Heart J* 39(31):2867-2875.
131. Chuang ML, Gona P, Hautvast GL, Salton CJ, Breeuwer M, O'Donnell CJ, & Manning WJ (2014) CMR reference values for left ventricular volumes, mass, and ejection fraction using computer-aided analysis: the Framingham Heart Study. *J Magn Reson Imaging* 39(4):895-900.

132. Tanguturi VK, Noseworthy PA, Newton-Cheh C, & Baggish AL (2012) The electrocardiographic early repolarization pattern in athletes: normal variant or sudden death risk factor? *Sports medicine (Auckland, N.Z.)* 42(5):359-366.

133. Corrado D, Pelliccia A, Heidbuchel H, Sharma S, Link M, Basso C, Biffi A, Buja G, Delise P, Gussac I, Anastasakis A, Borjesson M, Bjornstad HH, Carre F, Deligiannis A, Dugmore D, Fagard R, Hoogsteen J, Mellwig KP, Panhuyzen-Goedkoop N, Solberg E, Vanhees L, Drezner J, Estes NA, 3rd, Iliceto S, Maron BJ, Peidro R, Schwartz PJ, Stein R, Thiene G, Zeppilli P, & McKenna WJ (2010) Recommendations for interpretation of 12-lead electrocardiogram in the athlete. *European heart journal* 31(2):243-259.

134. Rickers C, Wilke NM, Jerosch-Herold M, Casey SA, Panse P, Panse N, Weil J, Zenovich AG, & Maron BJ (2005) Utility of cardiac magnetic resonance imaging in the diagnosis of hypertrophic cardiomyopathy. *Circulation* 112(6):855-861.

135. Maron MS, Maron BJ, Harrigan C, Buros J, Gibson CM, Olivotto I, Biller L, Lesser JR, Udelson JE, Manning WJ, & Appelbaum E (2009) Hypertrophic cardiomyopathy phenotype revisited after 50 years with cardiovascular magnetic resonance. *J Am Coll Cardiol* 54(3):220-228.

136. Lee PT, Dweck MR, Prasher S, Shah A, Humphries SE, Pennell DJ, Montgomery HE, & Payne JR (2013) Left ventricular wall thickness and the presence of asymmetric hypertrophy in healthy young army recruits: data from the LARGE heart study. *Circ Cardiovasc Imaging* 6(2):262-267.

137. Petersen SE, Selvanayagam JB, Francis JM, Myerson SG, Wiesmann F, Robson MD, Ostman-Smith I, Casadei B, Watkins H, & Neubauer S (2005) Differentiation of athlete's heart from pathological forms of cardiac hypertrophy by means of geometric indices derived from cardiovascular magnetic resonance. *J Cardiovasc Magn Reson* 7(3):551-558.

138. Prakken NH, Velthuis BK, Teske AJ, Mosterd A, Mali WP, & Cramer MJ (2010) Cardiac MRI reference values for athletes and nonathletes corrected for body surface area, training hours/week and sex. *Eur J Cardiovasc Prev Rehabil* 17(2):198-203.

139. Bohm P, Schneider G, Linneweber L, Rentzsch A, Kramer N, Abdul-Khaliq H, Kindermann W, Meyer T, & Scharhag J (2016) Right and Left Ventricular Function and Mass in Male Elite Master Athletes: A Controlled Contrast-Enhanced Cardiovascular Magnetic Resonance Study. *Circulation* 133(20):1927-1935.

140. Saberniak J, Hasselberg NE, Borgquist R, Platonov PG, Sarvari SI, Smith HJ, Ribe M, Holst AG, Edvardsen T, & Haugaa KH (2014) Vigorous physical activity impairs

myocardial function in patients with arrhythmogenic right ventricular cardiomyopathy and in mutation positive family members. *Eur J Heart Fail* 16(12):1337-1344.

141. Luijkx T, Velthuis BK, Prakken NH, Cox MG, Bots ML, Mali WP, Hauer RN, & Cramer MJ (2012) Impact of revised Task Force Criteria: distinguishing the athlete's heart from ARVC/D using cardiac magnetic resonance imaging. *Eur J Prev Cardiol* 19(4):885-891.
142. Colombo C & Finocchiaro G (2018) The Female Athlete's Heart: Facts and Fallacies. *Curr Treat Options Cardiovasc Med* 20(12):101.
143. Finocchiaro G, Dhutia H, D'Silva A, Malhotra A, Steriotis A, Millar L, Prakash K, Narain R, Papadakis M, Sharma R, & Sharma S (2017) Effect of Sex and Sporting Discipline on LV Adaptation to Exercise. *JACC Cardiovasc Imaging* 10(9):965-972.
144. Malhotra A, Dhutia H, Gati S, Yeo TJ, Dores H, Bastiaenen R, Narain R, Merghani A, Finocchiaro G, Sheikh N, Steriotis A, Zaidi A, Millar L, Behr E, Tome M, Papadakis M, & Sharma S (2017) Anterior T-Wave Inversion in Young White Athletes and Nonathletes: Prevalence and Significance. *J Am Coll Cardiol* 69(1):1-9.
145. Finocchiaro G, Papadakis M, Dhutia H, Zaidi A, Malhotra A, Fabi E, Cappelletto C, Brook J, Papatheodorou E, Ensam B, Miles CJ, Bastiaenen R, Attard V, Homfray T, Sharma R, Tome M, Carr-White G, Merlo M, Behr ER, Sinagra G, & Sharma S (2019) Electrocardiographic differentiation between 'benign T-wave inversion' and arrhythmogenic right ventricular cardiomyopathy. *Europace* 21(2):332-338.
146. D'Ascenzi F, Pisicchio C, Caselli S, Di Paolo FM, Spataro A, & Pelliccia A (2017) RV Remodeling in Olympic Athletes. *JACC Cardiovasc Imaging* 10(4):385-393.
147. Csecs I, Czimbalmos C, Suhai FI, Mikle R, Mirzahosseini A, Dohy Z, Szucs A, Kiss AR, Simor T, Toth A, Merkely B, & Vago H (2018) Left and right ventricular parameters corrected with threshold-based quantification method in a normal cohort analyzed by three independent observers with various training-degree. *Int J Cardiovasc Imaging* 34(7):1127-1133.
148. Haland TF, Saberniak J, Leren IS, Edvardsen T, & Haugaa KH (2017) Echocardiographic comparison between left ventricular non-compaction and hypertrophic cardiomyopathy. *Int J Cardiol* 228:900-905.
149. Han Y, Osborn EA, Maron MS, Manning WJ, & Yeon SB (2009) Impact of papillary and trabecular muscles on quantitative analyses of cardiac function in hypertrophic cardiomyopathy. *J Magn Reson Imaging* 30(5):1197-1202.

150. Gommans DH, Bakker J, Cramer GE, Verheugt FW, Brouwer MA, & Kofflard MJ (2016) Impact of the papillary muscles on cardiac magnetic resonance image analysis of important left ventricular parameters in hypertrophic cardiomyopathy. *Neth Heart J* 24(5):326-331.

151. Gati S, Chandra N, Bennett RL, Reed M, Kervio G, Panoulas VF, Ghani S, Sheikh N, Zaidi A, Wilson M, Papadakis M, Carre F, & Sharma S (2013) Increased left ventricular trabeculation in highly trained athletes: do we need more stringent criteria for the diagnosis of left ventricular non-compaction in athletes? *Heart* 99(6):401-408.

152. Hiemstra YL, Debonnaire P, Bootsma M, van Zwet EW, Delgado V, Schalij MJ, Atsma DE, Bax JJ, & Marsan NA (2017) Global Longitudinal Strain and Left Atrial Volume Index Provide Incremental Prognostic Value in Patients With Hypertrophic Cardiomyopathy. *Circ Cardiovasc Imaging* 10(7).

153. Smiseth OA, Torp H, Opdahl A, Haugaa KH, & Urheim S (2016) Myocardial strain imaging: how useful is it in clinical decision making? *Eur Heart J* 37(15):1196-1207.

154. Zerhouni EA, Parish DM, Rogers WJ, Yang A, & Shapiro EP (1988) Human heart: tagging with MR imaging--a method for noninvasive assessment of myocardial motion. *Radiology* 169(1):59-63.

155. Cameli M, Righini FM, Lisi M, Bennati E, Navarri R, Lunghetti S, Padeletti M, Cameli P, Tsioulpas C, Bernazzali S, Maccherini M, Sani G, Henein M, & Mondillo S (2013) Comparison of right versus left ventricular strain analysis as a predictor of outcome in patients with systolic heart failure referred for heart transplantation. *Am J Cardiol* 112(11):1778-1784.

156. Calcutteea A, Lindqvist P, Soderberg S, & Henein MY (2014) Global and regional right ventricular dysfunction in pulmonary hypertension. *Echocardiography* 31(2):164-171.

157. Alghamdi MH, Mertens L, Lee W, Yoo SJ, & Grosse-Wortmann L (2013) Longitudinal right ventricular function is a better predictor of right ventricular contribution to exercise performance than global or outflow tract ejection fraction in tetralogy of Fallot: a combined echocardiography and magnetic resonance study. *Eur Heart J Cardiovasc Imaging* 14(3):235-239.

158. Badano LP, Kolias TJ, Muraru D, Abraham TP, Aurigemma G, Edvardsen T, D'Hooge J, Donal E, Fraser AG, Marwick T, Mertens L, Popescu BA, Sengupta PP, Lancellotti P, Thomas JD, Voigt JU, Industry r, & Reviewers: This document was reviewed by members of the ESDC (2018) Standardization of left atrial, right ventricular, and right atrial deformation imaging using two-dimensional speckle tracking echocardiography: a

consensus document of the EACVI/ASE/Industry Task Force to standardize deformation imaging. *Eur Heart J Cardiovasc Imaging* 19(6):591-600.

159. Bourfiss M, Vigneault DM, Aliyari Ghasebeh M, Murray B, James CA, Tichnell C, Mohamed Hoesein FA, Zimmerman SL, Kamel IR, Calkins H, Tandri H, Velthuis BK, Bluemke DA, & Te Riele A (2017) Feature tracking CMR reveals abnormal strain in preclinical arrhythmogenic right ventricular dysplasia/ cardiomyopathy: a multisoftware feasibility and clinical implementation study. *J Cardiovasc Magn Reson* 19(1):66.
160. Vigneault DM, te Riele AS, James CA, Zimmerman SL, Selwaness M, Murray B, Tichnell C, Tee M, Noble JA, Calkins H, Tandri H, & Bluemke DA (2016) Right ventricular strain by MR quantitatively identifies regional dysfunction in patients with arrhythmogenic right ventricular cardiomyopathy. *J Magn Reson Imaging* 43(5):1132-1139.
161. Heermann P, Hedderich DM, Paul M, Schulke C, Kroeger JR, Baessler B, Wichter T, Maintz D, Waltenberger J, Heindel W, & Bunck AC (2014) Biventricular myocardial strain analysis in patients with arrhythmogenic right ventricular cardiomyopathy (ARVC) using cardiovascular magnetic resonance feature tracking. *J Cardiovasc Magn Reson* 16:75.
162. Prati G, Vitrella G, Allocca G, Muser D, Buttignoni SC, Piccoli G, Morocutti G, Delise P, Pinamonti B, Proclemer A, Sinagra G, & Nucifora G (2015) Right Ventricular Strain and Dyssynchrony Assessment in Arrhythmogenic Right Ventricular Cardiomyopathy: Cardiac Magnetic Resonance Feature-Tracking Study. *Circ Cardiovasc Imaging* 8(11):e003647; discussion e003647.
163. Green JJ, Berger JS, Kramer CM, & Salerno M (2012) Prognostic value of late gadolinium enhancement in clinical outcomes for hypertrophic cardiomyopathy. *JACC Cardiovasc Imaging* 5(4):370-377.
164. Rastegar N, Te Riele AS, James CA, Bhonsale A, Murray B, Tichnell C, Calkins H, Tandri H, Bluemke DA, Kamel IR, & Zimmerman SL (2016) Fibrofatty Changes: Incidence at Cardiac MR Imaging in Patients with Arrhythmogenic Right Ventricular Dysplasia/Cardiomyopathy. *Radiology* 280(2):405-412.
165. Andrews CM, Srinivasan NT, Rosmini S, Bulluck H, Orini M, Jenkins S, Pantazis A, McKenna WJ, Moon JC, Lambiase PD, & Rudy Y (2017) Electrical and Structural Substrate of Arrhythmogenic Right Ventricular Cardiomyopathy Determined Using Noninvasive Electrocardiographic Imaging and Late Gadolinium Magnetic Resonance Imaging. *Circ Arrhythm Electrophysiol* 10(7).

166. aus dem Siepen F, Buss SJ, Messroghli D, Andre F, Lossnitzer D, Seitz S, Keller M, Schnabel PA, Giannitsis E, Korosoglou G, Katus HA, & Steen H (2015) T1 mapping in dilated cardiomyopathy with cardiac magnetic resonance: quantification of diffuse myocardial fibrosis and comparison with endomyocardial biopsy. *Eur Heart J Cardiovasc Imaging* 16(2):210-216.

167. Chen Z, Sohal M, Voigt T, Sammut E, Tobon-Gomez C, Child N, Jackson T, Shetty A, Bostock J, Cooklin M, O'Neill M, Wright M, Murgatroyd F, Gill J, Carr-White G, Chiribiri A, Schaeffter T, Razavi R, & Rinaldi CA (2015) Myocardial tissue characterization by cardiac magnetic resonance imaging using T1 mapping predicts ventricular arrhythmia in ischemic and non-ischemic cardiomyopathy patients with implantable cardioverter-defibrillators. *Heart Rhythm* 12(4):792-801.

168. Di Biase L, Burkhardt JD, Lakkireddy D, Carbucicchio C, Mohanty S, Mohanty P, Trivedi C, Santangeli P, Bai R, Forleo G, Horton R, Bailey S, Sanchez J, Al-Ahmad A, Hranitzky P, Gallinghouse GJ, Pelargonio G, Hongo RH, Beheiry S, Hao SC, Reddy M, Rossillo A, Themistoclakis S, Dello Russo A, Casella M, Tondo C, & Natale A (2015) Ablation of Stable VTs Versus Substrate Ablation in Ischemic Cardiomyopathy: The VISTA Randomized Multicenter Trial. *J Am Coll Cardiol* 66(25):2872-2882.

169. Piers SR, Tao Q, van Huls van Taxis CF, Schalij MJ, van der Geest RJ, & Zeppenfeld K (2013) Contrast-enhanced MRI-derived scar patterns and associated ventricular tachycardias in nonischemic cardiomyopathy: implications for the ablation strategy. *Circ Arrhythm Electrophysiol* 6(5):875-883.

170. Hennig A, Salel M, Sacher F, Camaioni C, Sridi S, Denis A, Montaudon M, Laurent F, Jais P, & Cochet H (2018) High-resolution three-dimensional late gadolinium-enhanced cardiac magnetic resonance imaging to identify the underlying substrate of ventricular arrhythmia. *Europace* 20(FI2):f179-f191.

171. de Haan S, Meijers TA, Knaapen P, Beek AM, van Rossum AC, & Allaart CP (2011) Scar size and characteristics assessed by CMR predict ventricular arrhythmias in ischaemic cardiomyopathy: comparison of previously validated models. *Heart* 97(23):1951-1956.

172. Dawson DK, Hawlisch K, Prescott G, Roussin I, Di Pietro E, Deac M, Wong J, Frenneaux MP, Pennell DJ, & Prasad SK (2013) Prognostic role of CMR in patients presenting with ventricular arrhythmias. *JACC Cardiovasc Imaging* 6(3):335-344.

173. Mahida S, Sacher F, Dubois R, Sermesant M, Bogun F, Haissaguerre M, Jais P, & Cochet H (2017) Cardiac Imaging in Patients With Ventricular Tachycardia. *Circulation* 136(25):2491-2507.

174. Acosta J, Fernandez-Armenta J, Borras R, Anguera I, Bisbal F, Marti-Almor J, Tolosana JM, Penela D, Andreu D, Soto-Iglesias D, Evertz R, Matiello M, Alonso C, Villuendas R, de Caralt TM, Perea RJ, Ortiz JT, Bosch X, Serra L, Planes X, Greiser A, Ekinci O, Lasalvia L, Mont L, & Berruezo A (2018) Scar Characterization to Predict Life-Threatening Arrhythmic Events and Sudden Cardiac Death in Patients With Cardiac Resynchronization Therapy: The GAUDI-CRT Study. *JACC Cardiovasc Imaging* 11(4):561-572.

175. Siontis KC, Kim HM, Sharaf Dabbagh G, Latchamsetty R, Stojanovska J, Jongnarangsin K, Morady F, & Bogun FM (2017) Association of preprocedural cardiac magnetic resonance imaging with outcomes of ventricular tachycardia ablation in patients with idiopathic dilated cardiomyopathy. *Heart Rhythm* 14(10):1487-1493.

176. Bogun FM, Desjardins B, Good E, Gupta S, Crawford T, Oral H, Ebinger M, Pelosi F, Chugh A, Jongnarangsin K, & Morady F (2009) Delayed-enhanced magnetic resonance imaging in nonischemic cardiomyopathy: utility for identifying the ventricular arrhythmia substrate. *J Am Coll Cardiol* 53(13):1138-1145.

177. Njeim M, Desjardins B, & Bogun F (2016) Multimodality Imaging for Guiding EP Ablation Procedures. *JACC Cardiovasc Imaging* 9(7):873-886.

178. Bisbal F, Fernandez-Armenta J, Berruezo A, Mont L, & Brugada J (2014) Use of MRI to guide electrophysiology procedures. *Heart* 100(24):1975-1984.

179. Koshy AO, Swoboda PPP, Gierula J, & Witte KK (2019) Cardiac magnetic resonance in patients with cardiac resynchronization therapy: is it time to scan with resynchronization on? *Europace*.

180. Hilbert S, Jahnke C, Loebe S, Oebel S, Weber A, Spampinato R, Richter S, Doering M, Bollmann A, Sommer P, Hindricks G, & Paetsch I (2018) Cardiovascular magnetic resonance imaging in patients with cardiac implantable electronic devices: a device-dependent imaging strategy for improved image quality. *Eur Heart J Cardiovasc Imaging* 19(9):1051-1061.

181. Liu B, Dardeer AM, Moody WE, Edwards NC, Hudsmith LE, & Steeds RP (2018) Normal values for myocardial deformation within the right heart measured by feature-tracking cardiovascular magnetic resonance imaging. *Int J Cardiol* 252:220-223.

DOI:10.14753/SE.2020.2408

182. Taylor RJ, Moody WE, Umar F, Edwards NC, Taylor TJ, Stegemann B, Townend JN, Hor KN, Steeds RP, Mazur W, & Leyva F (2015) Myocardial strain measurement with feature-tracking cardiovascular magnetic resonance: normal values. *Eur Heart J Cardiovasc Imaging* 16(8):871-881.

DOI:10.14753/SE.2020.2408

Publications related to dissertation

1. **C Czimbalmos**, I Csecs, Z Dohy, A Toth, FI Suhai, A Müssigbrodt, O Kiss, L Geller,·B Merkely*,·H Vago*: Cardiac magnetic resonance based deformation imaging: role of feature tracking in athletes with suspected arrhythmogenic right ventricular cardiomyopathy. Int J Cardiovasc Imaging. 2019, 35(3):529-538

* B Merkely and H Vago contributed equally in this work.

IF: 1.860

2. **C Czimbalmos,** I Csecs, A Toth, O Kiss, FI Suhai, N Sydo, Dohy Z, A Apor, B Merkely*, H Vago*: The demanding grey zone: Sport indices by cardiac magnetic resonance imaging differentiate hypertrophic cardiomyopathy from athlete's heart. 2019, PLoS One 14(2):e0211624.

*B Merkely and H Vago contributed equally in this work.

IF: 2.766

3. F Torri, **C Czimbalmos**, L Bertagnolli, S Oebel, A Bollmann, I Paetsch, C Jahnke, A Arya, B Merkely, B Dinov. (2019) Agreement between gadolinium-enhanced cardiac magnetic resonance and electroanatomical maps in patients with non-ischaemic dilated cardiomyopathy and ventricular arrhythmias. 2019, Europace 21(9):1392-1399.

IF: 5.047

4. H Vago*, **C Czimbamos***, R Papp, L Szabo, AToth, Z Dohy, I Csecs, FI Suhai, A Kosztin, L Molnar, L Geller, B Merkely. Biventricular Pacing during Cardiac Magnetic Resonance Imaging. 2020, Europace 22(1):117-124.

*H Vago and C Czimbalmos contributed equally in this work.

IF: 5.047

Publications not related to dissertation

I Csecs, T Yamaguchi, M Kheirkhahan, C Czimbalmos, F Fochler, EG Kholmovski, AK Morris, G Kaur, H Vago, B Merkely, MG Chelu, NF Marrouche, BD Wilson: Left atrial functional and structural changes associated with ablation of atrial fibrillation - Cardiac magnetic resonance study., 2020 Int J Cardiol. In press.
IF 3.471

I Csecs, **C Czimbalmos**, A Toth A, Z Dohy, FI Suhai, LE Szabo, A Kovacs, B Lakatos, N Sydo, M Kheirkhahan, D Peritz, O Kiss, B Merkely, H Vago. The impact of sex, age and training on biventricular cardiac adaptation in healthy adult and adolescent athletes: Cardiac magnetic resonance imaging study. Eur J Prev Cardiol. 2019 Aug 1:2047487319866019. doi: 10.1177/2047487319866019.
IF: 5.64

A Müssigbrodt, **C Czimbalmos,** A Stauber, L Bertagnolli, K Bode, N Dagres, M Doering, S Richter, P Sommer, D Husser, A Bollmann, G Hindricks, A Arya: Effect of Exercise on Outcome after Ventricular Tachycardia Ablation in Arrhythmogenic Right Ventricular Dysplasia/Cardiomyopathy. Int J Sports Med. 2019 Sep;40(10):657-662. doi: 10.1055/a-0962-1325. Epub 2019 Jul 23.
IF: 2.132

A Szucs, AR Kiss, FI Suhai, A Tóth, Z Gregor, M Horváth, C Czimbalmos, I Csécs, Z Dohy, LE Szabó, B Merkely, H Vágó: The effect of contrast agents on left ventricular parameters calculated by a threshold-based software module: does it truly matter? Int J Cardiovasc Imaging. 2019 Sep;35(9):1683-1689.
IF: 1.860

A Fábián, BK Lakatos, O Kiss, N Sydó, H Vágó, C Czimbalmos, M Tokodi, Z Kántor, C Bognár, D Major, A Kovács, B Merkely: A jobb kamrai kontrakciós mintázat változása élsportolókban: háromdimenziós echokardiográfiás vizsgálat Cardiol Hung 2019; 49 (1) 17-23

A Müssigbrodt, H Knopp, **C Czimbalmos**, C Jahnke, S Richter, D Husser, T Gradistanac, G Hindricks: Exercise-related sudden cardiac death of an American football player with arrhythmogenic right ventricular dysplasia/cardiomyopathy AND sarcoidosis. Clin Case Rep. 2019 Feb 19;7(4):686-688.

C Czimbalmos, I Csecs, A Toth, FI Suhai, Z Dohy, L Szabo, G Barczi, E Zima, D Becker, B Merkely*,·H Vago*: Cardiac magnetic resonance characteristics of ST-segment elevation myocardial infarction in the acute period and during long-term follow up – prognostic role of microvascular obstruction. Cardiol Hung 2018; 48(5): 308-316

Z Dohy, I Csécs, **C Czimbalmos**, FI Suhai, A Tóth, LE Szabó, Z Pozsonyi, T Simor, B Merkely, H Vágó: Cardiac magnetic resonance „fingerprints" of cardiomyopathies with myocardial hypertrophy or increased left ventricular wall thickness. Cardiol Hung 2018; 48: 390–396

I Csecs, **C Czimbalmos**, FI Suhai, R Mikle, Z Dohy, A Szucs, AR Kiss, T Simor, B Merkely, H Vago: Left and right ventricular parameters corrected with threshold-based quantification method in a normal cohort analyzed by three independent observers with various training-degree. Int J Cardiovasc Imaging. 2018 Jul;34(7):1127-1133. **IF: 1.860**

FI Suhai, B Sax, A Assabiny, A Kiraly, **C Czimbalmos**, I Csecs, A Kovacs, B Lakatos, E Nemeth, Z Szabolcs, M Hubay, B Merkely, H Vago: The role of CMR in the evaluation of acute mixed cardiac allograft rejection. Cardiol Hung 2018; 48:44-51

R Skoda, D Becker, B Merkely, E Dinya, Z Ruzsa, I Édes, **C Czimbalmos**, H Vágó, G Bárczi, K Doan Nang: Epidemiologic research of mortality rates in women surviving acut myocardial infarction. 2018; 48: C61

C Czimbalmos, I Csecs, M Polos, E Bartha, N Szucs, A Toth, P Maurovich-Horvat, D Becker, Z Sapi, Z Szabolcs, B Merkely*, H Vago*: Uncommon presentation of a rare tumour-incidental finding in an asymptomatic patient: case report and comprehensive review of the literature on intrapericardial solitary fibrous tumours. BMC Cancer. 2017 Sep 2;17(1):612.
IF: 3.288

T Baranyai, Z Giricz, ZV Varga, G Koncsos, D Lukovic, A Makkos, M Sárközy, N Pávó, A Jakab, **C Czimbalmos**, H Vágó, Z Ruzsa, L Tóth, R Garamvölgyi, B Merkely, R Schulz, M Gyöngyösi, P Ferinandy: In vivo MRI and ex vivo histological assessment of the cardioprotection induced by ischemic preconditioning, postconditioning and remote conditioning in a closed-chest porcine model of reperfused acute myocardial infarction: importance of microvasculature. J Transl Med. 2017 Apr 1;15(1):67.
IF: 4.197

H Vago, **C Czimbalmos**: Stressz-kardiomiopátia Orvostovábbképző Szemle 2013; 23:10 pp. 308-316.

I Csecs, **C Czimbalmos**, A Toth, O Kiss, Z Komka, G Barczi, T Kovacs, FI Suhai, N Sydo, T Simor, L Geler, D Becker, B Merkely, H Vago: Structural myocardial disease or athlete's heart? The diagnostic role of cardiac magnetic resonance (CMR) imaging in athletes with the suspicion of structural heart disease. Cardiol Hung 2017; 47(1): 10-17

P Maurovich-Horvat, FI Suhai, **C Czimbalmos**, A Tóth, D Becker, E Kiss, M Ferencik, U Hoffmann, H Vago, B Merkely: Coronary Artery Manifestation of Ormond Disease: The "Mistletoe Sign". Radiology 2017 Feb;282(2):356-360
IF: 7.469

G Barczi, I Csecs, **C Czimbalmos**, R Jakus, D Becker, Z Szelenyi, G Szeplaki, H Vago, B Merkely. Much Ado About Nothing? – Young Female Cyclist Presented with Syncope – A Case Report. Cardiol Hung 2016; 46 : 301–304

LE Szabo, Z Pozsonyi, G Pesko, Z Dohy, **C Czimbalmos**, K Heltai, D Becker, B Merkely, H Vago: Abortált hirtelen szívhalál egy 39 éves biztonsági őrnél – Aborted sudden cardiac death on a 39-year-old security guard. Cardiol Hung 2018; 48(6): 397-400

O Kiss*, N Sydo N*, P Vargha, H Vago, **C Czimbalmos**, E Edes, E Zima, G Apponyi, G Merkely, T Sydo, D Becker, TG Allison, B Merkely: Detailed heart rate variability analysis in athletes. Clin Auton Res 2016; 26(4): 245-252. **IF: 1.276**

H Vago, A Toth, **C Czimbalmos**, FI Suhai, K Kecskes, K Heltai, E Zima, G Barczi, T Simor, D Becker, B Merkely: Differential diagnosis of ST-elevation myocardial infarction without culprit lesion using cardiac magnetic resonance imaging. Cardiol Hung 2014; 2014; 44(5): 300-305

DOI:10.14753/SE.2020.2408

10. Acknowledgement

Throughout conducting my research I have received a great support and assistance. I would like to extend thanks to many people, who contributed to the work presented in my thesis.

I would like to express my sincere gratitude to my supervisors, **Dr. Hajnalka Vágó** and **Prof. Dr. Béla Merkely** for their continuous support from the very beginning.

I would like to express my gratefulness to **Dr. Hajnalka Vágó** for her valuable advices and constant feedback on my research and for always being supportive of my work as a medical and later as a graduate student. Her mentorship was unparalleled in the field of cardiac magnetic resonance imaging as well as in clinical research. Undertaking this PhD would not have been possible without the support and guidance that I received from her.

I would like to express my special appreciation and thanks to **Prof. Dr. Béla Merkely** for his extraordinary support from day one, for giving me so many opportunities to participate in scientific projects and to brighten my knowledge in the field of cardiology. I could not imagine having a better advisor and mentor. I doubt that I shall ever be able to convey my appreciation fully, but I owe him my eternal gratitude.

Special thanks to my colleague and best friend **Dr. Ibolya Csécs,** who motivated and inspired me during the last eight years. I hugely appreciate her presence in the most difficult moments and her advice on research, career and private life as well. Thanks for all the wonderful memories and for this outstanding friendship.

I am also very grateful to **Dr. Attila Tóth,** who helped me to improve my knowledge in the field of cardiac magnetic resonance imaging. As a mentor and as a friend he inspired and motivated me. I truly appreciate the time and energy he put into my professional development.

I am also very grateful to my colleagues in the Cardiac Magnetic Resonance Research Group at Semmelweis University Heart and Vascular Center, especially to **Dr. Ferenc Imre Suhai, Dr. Liliána Szabó, Dr. Zsófia Dohy, Dr. Andrea Szűcs, Dr. Anna Réka**

DOI:10.14753/SE.2020.2408

Kiss, Dr. Zsófia Gregor, Dr. Márton Horváth and to all the student researchers and radiology assistants for their help and support.

I gratefully acknowledge the support and assistance received from my colleagues in the Sports Cardiology Research Group at Semmelweis University Heart and Vascular Center, especially to **Dr. Orsolya Kiss, Dr. Nóra Sydó, Dr. Emese Csulak,** who all have helped me to carry out my research.

I would like to acknowledge my colleagues in the Pacemaker Working Group at Semmelweis University Heart and Vascular Center, especially to **Dr. Roland Papp, Dr. Zoltán Tarjányi, Dr. Annamária Kosztin, Dr. Levente Molnár, Prof. Dr. László Gellér.** I would like to thank you for your excellent cooperation during our common scientific projects.

I gratefully acknowledge the support received from **Dr. Dávid Becker**, who helped me to brighten my knowledge in the field of cardiology and provided valuable advices during these years.

I am also very grateful to **Dr. Violetta Kékesi** for the helpful guidance during my learning curve and for her help in organizing my PhD studies.

Apart from my colleagues in the Semmelweis University, I would like to express the gratitude to **Prof. Dr. Gerhard Hindricks** giving me an opportunity to become a part of their team. I greatly appreciate the support received through the collaborative work with the Department of Electrophysiology in Heart Center University of Leipzig. I would like to thank the electrophysiology and CMR team in Leipzig, especially **Dr. Andreas Müssigbrodt, Dr. Federica Torri, Dr. Borislav Dinov, Dr. Cosima Jahnke and Dr. Ingo Paetsch**. It would not have been possible to conduct our research without their precious support.

Lastly but not least, I would like to thank my parents, my husband, my family and friends for all their love, patience and encouragement.